

AWARD NUMBER: **W81XWH-14-1-0442**

TITLE: **Reinnervation of Paralyzed Muscle by Nerve-Muscle-Endplate Band Grafting**

PRINCIPAL INVESTIGATOR: **Liancai Mu, M.D., Ph.D.,**

CONTRACTING ORGANIZATION: **Hackensack University Medical Center,  
Hackensack, NJ 07610**

REPORT DATE: **December 2018**

TYPE OF REPORT: **Final**

PREPARED FOR: U.S. Army Medical Research and Materiel Command  
Fort Detrick, Maryland 21702-5012

DISTRIBUTION STATEMENT: Approved for Public Release;  
Unlimited Distribution

The views, opinions and/or findings contained in this report are those of the author(s) and should not be construed as an official Department of the Army position, policy or decision unless so designated by other documentation.

**REPORT DOCUMENTATION PAGE**Form Approved  
OMB No. 0704-0188

Public reporting burden for this collection of information is estimated to average 1 hour per response, including the time for reviewing instructions, searching existing data sources, gathering and maintaining the data needed, and completing and reviewing this collection of information. Send comments regarding this burden estimate or any other aspect of this collection of information, including suggestions for reducing this burden to Department of Defense, Washington Headquarters Services, Directorate for Information Operations and Reports (0704-0188), 1215 Jefferson Davis Highway, Suite 1204, Arlington, VA 22202-4302. Respondents should be aware that notwithstanding any other provision of law, no person shall be subject to any penalty for failing to comply with a collection of information if it does not display a currently valid OMB control number. **PLEASE DO NOT RETURN YOUR FORM TO THE ABOVE ADDRESS.**

<b>1. REPORT DATE</b> December 2018		<b>2. REPORT TYPE</b> Final		<b>3. DATES COVERED</b> 15 Sep 2014 - 14 Sep 2018	
<b>4. TITLE AND SUBTITLE</b> Reinnervation of Paralyzed Muscle by Nerve-Muscle-Endplate Band Grafting				<b>5a. CONTRACT NUMBER</b>	
				<b>5b. GRANT NUMBER</b> W81XWH-14-1-0442	
				<b>5c. PROGRAM ELEMENT NUMBER</b>	
<b>6. AUTHOR(S)</b> Liancai Mu, M.D., Ph.D. Stanislaw Sobotka, Ph.D. Jingming Chen, M.D. Themba Nyirenda, Ph.D. <a href="mailto:Liancai.Mu@hackensackmeridian.org">Liancai.Mu@hackensackmeridian.org</a>				<b>5d. PROJECT NUMBER</b>	
				<b>5e. TASK NUMBER</b>	
				<b>5f. WORK UNIT NUMBER</b>	
<b>7. PERFORMING ORGANIZATION NAME(S) AND ADDRESS(ES)</b>  Hackensack University Medical Center, 30 Prospect Avenue, Hackensack, NJ 07601-1914				<b>8. PERFORMING ORGANIZATION REPORT NUMBER</b>	
<b>9. SPONSORING / MONITORING AGENCY NAME(S) AND ADDRESS(ES)</b>  U.S. Army Medical Research and Materiel Command Fort Detrick, Maryland 21702-5012				<b>10. SPONSOR/MONITOR'S ACRONYM(S)</b>	
				<b>11. SPONSOR/MONITOR'S REPORT NUMBER(S)</b>	
<b>12. DISTRIBUTION / AVAILABILITY STATEMENT</b>  Approved for Public Release; Distribution Unlimited					
<b>13. SUPPLEMENTARY NOTES</b>					
<b>14. ABSTRACT</b> This research aimed to assess the efficacy of our recently developed a new surgical technique called nerve-muscle-endplate grafting (NMEG) in the native motor zone (NMZ) for muscle reinnervation in a rat neck muscle model. An NMEG harvested from a donor muscle was implanted into the NMZ of the experimentally denervated muscle. Our experiments showed that NMEG-NMZ technique yielded optimal functional recovery (82% of the control) of the target muscle. Importantly, the outcome of the NMEG-NMZ was further improved by additional use of exogenous neurotrophic factors (ENF) and intraoperative brief electrical stimulation (ES). Specifically, the combination of NMEG-NMZ with ENF and ES resulted in more optimal functional recovery (91% and 90% of the control, respectively) as compared with NMEG-NMZ surgery alone. Our studies have demonstrated that NMEG-NMZ procedure physically facilitates rapid axon-endplate connections and that focal administration of the ENF and intraoperative brief ES result in extensive nerve regeneration and muscle reinnervation.					
<b>15. SUBJECT TERMS</b> Peripheral nerve injury, muscle reinnervation, nerve-muscle-endplate band grafting, nerve regeneration, motor endplate band, native motor zone, muscle force measurement, functional recovery					
<b>16. SECURITY CLASSIFICATION OF:</b>			<b>17. LIMITATION OF ABSTRACT</b>	<b>18. NUMBER OF PAGES</b>	<b>19a. NAME OF RESPONSIBLE PERSON</b>
<b>a. REPORT</b>	<b>b. ABSTRACT</b>	<b>c. THIS PAGE</b>			USAMRMC
U	U	U	UU	99	<b>19b. TELEPHONE NUMBER</b> (include area code)

## Table of Contents

	<u>Page</u>
Introduction.....	4
Keywords.....	4
Accomplishments.....	4-14
Impact.....	14-15
Changes/Problems.....	15
Products.....	15-16
Supporting Data.....	17-42
Appendices (publications).....	43-99

## 1. Introduction

Traumatic peripheral nerve injury (PNI) represents a significant cause of morbidity and disability in both military and civilian populations, and poses a major healthcare/rehabilitation problem. There are 200,000 cases of PNIs in the United States annually. There is a pressing need to seek new approaches for restoration of paralyzed muscles as the presently used methods result in poor functional recovery.

We developed a novel surgical technique called “nerve-muscle-endplate grafting (NMEG) in the native motor zone (NMZ)”. The idea is that an intact motor endplate (MEP) band with a nerve branch and terminals, that innervates a noncritical muscle, can be implanted into the NMZ of a denervated critical muscle to restore its function. The NMZ is located in the middle of the muscle that contains a MEP band and intramuscular axons. Increasing evidence indicates that poor motor recovery after PNIs and nerve repair is caused primarily by insufficient axonal regeneration and failure of reinnervation of the denervated MEPs in the target muscle. The NMEG-NMZ technique is based on the rationale that denervated MEPs in the NMZ are preferential sites for reinnervation. Transplantation of a NMEG to the NMZ of the target muscle physically shortens regeneration distances and favors rapid axon-MEP connections and functional recovery.

In this research, the efficacy of the NMEG-NMZ technique in muscle reinnervation was assessed in a rat neck muscle model. In addition, two promising approaches, including intraoperative 1 hour of low-frequency (20 Hz) continuous electrical stimulation (ES) developed by Dr. Gordon group and local application of a fibrin sealant containing nerve growth factor (NGF) and basic fibroblast growth factor (FGF-2) were also used to enhance axonal regeneration for improving the outcomes of NMEG-NMZ surgery. For comparison, direct nerve implantation into the NMZ (DNI-NMZ) and denervation were used as controls. After a 3-month recovery period, the animals underwent postoperative evaluations to determine the extent of functional recovery, axonal regeneration, MEP reinnervation, and muscle recovery using electrophysiological, histomorphological and immunohistochemical techniques. Our results indicate that the NMEG-NMZ is an option for restoring motor function of the denervated muscle following PNIs.

## 2. Keywords

Peripheral nerve injury, muscle reinnervation, nerve-muscle-endplate band grafting, nerve regeneration, motor endplate band, native motor zone, muscle force measurement, functional recovery.

## 3. Accomplishments

### Major Objectives of the Project

**Objective 1 – Evaluate functional recovery of the paralyzed muscles treated by the NMEG-NMZ technique with/without intraoperative 1-hour electrical stimulation (ES) and focal administration of exogenous neurotrophic factors.**

*Task 1.1. Regulatory approvals for the use of rats in this research were obtained from both the Hackensack IACUC (protocol #: 227.00) on 1/31/2014 and ACURO approval on 7/10/2014.*

### ***Task 1.2. Perform reinnervation surgeries and supplemental therapies (Months 1-32)***

A total of 150 adult female Sprague-Dawley rats underwent multiple survival surgeries, commencing on 10/06/2014 and completed on 06/03/2017.

#### ■ *NMEG-NMZ procedures*

The effectiveness of the NMEG-NMZ technique was assessed in a rat neck muscle model. Specifically, a NMEG was harvested from sternohyoid (SH) muscle and implanted to the NMZ of the denervated sternomastoid (SM) muscle. The locations of the NMZs in the recipient SM and donor SH muscles were determined (Fig. 1A, B). A NMEG pedicle contained a block of muscle (~6×6×3 mm), an intact donor nerve branch and nerve terminals, and a MEP band with numerous neuromuscular junctions (Fig. 1C-E). Three months after surgery, functional recovery of the paralyzed muscles treated with the NMEG-NMZ technique was evaluated by muscle force measurement. The extent of nerve regeneration in the target muscle was assessed using immunohistochemical techniques.

#### ■ *NMEG-NMZ with intraoperative brief electrical stimulation*

Intraoperative brief electrical stimulation (ES) was used to determine its beneficial effect on outcomes of the muscles reinnervated with the NMEG-NMZ technique. During NMEG-NMZ surgery, the SH nerve branch supplying the NMEG pedicle was stimulated for 1 hour with a continuous train of 20 Hz square pulses of 3 V, 0.1 millisecond delivered by a stimulation and recording system. The outcomes of the muscles reinnervated with NMEG-NMZ and brief ES were evaluated 3 month after treatment.

#### ■ *NMEG-NMZ with local application of nerve growth factor (NGF) and basic fibroblast growth factor (FGF-2)*

During NMEG-NMZ surgery, focal administration of NGF/FGF-2 was used to determine the beneficial effect of both neurotrophic factors on outcomes of the NMEG-NMZ technique. Specifically, The SM muscle was experimentally denervated and reinnervated with NMEG-NMZ. The muscular defect created on the target muscle was covered with 0.2 ml of fibrin sealant containing recombinant rat NGF and rat FGF-2 at a concentration of 100 ng/ml for NGF and 100 µg/ml for FGF-2. Three months after treatment, the animals underwent postoperative outcome measurements.

#### ■ *Direct nerve implantation (DNI) into the NMZ of the target muscle*

DNI-NMZ procedure was used as a technique control. The SM muscle was experimentally denervated by transecting its innervating nerve. The proximal stump of the severed SM nerve was immediately implanted into a small muscle slit made in the NMZ of the muscle where denervated MEPs were concentrated (Fig. 2). The outcomes of DNI-NMZ reinnervation were evaluated 3 months after surgery.

#### ■ *Denervation (DEN) control surgeries*

Denervation of the SM muscle was conducted to serve as a control. Twenty-one rats were randomly allocated into 3 groups each comprising 7 animals on the basis of the observation period (3, 6, and 9 months) after SM nerve resection. This study was designed to determine

spatiotemporal alterations of the myofibers, MEPs, and axons in the NMZ of long-term denervated muscles.

***Task 1.3. Evaluate the extent of functional recovery (Months 4-36)***

At the end of the 3-month recovery period, outcomes of the NMEG-NMZ technique were evaluated functionally and histochemically.

Maximal tetanic force measurement was used to evaluate the functionality of the NMEG-NMZ reinnervated muscles. The force was measured on the experimental and the contralateral control side and expressed in percentage of the control side. The right reinnervated and the left control SM muscles in each animal were exposed and dissected free from the surrounding tissues. The rostral tendon of each muscle was severed close to the insertion, tied with a 2-0 suture, and attached to a servomotor lever arm (model 305B Dual-Mode Lever Arm System; Aurora Scientific Inc, Aurora, Ontario, Canada). Muscle force of the right reinnervated SM was measured by stimulating the SH nerve branch supplying the NMEG, whereas that of the left control muscle was measured by stimulating the intact SM nerve. Isometric contraction of the SM muscle was produced with 200-millisecond trains of biphasic rectangular pulses. The duration of each phase of stimulation pulse was set at 0.2 milliseconds and the train frequency was set at 200 pulses per second. The stimulation current was gradually increased until the tetanic force reached a plateau. A break of at least 1 min was taken between two stimulations. The maximum value of muscle force during the 200-millisecond contraction was identified, as well as initial passive tension before stimulation. The difference between the maximal active force and the preloaded passive force was used as the muscle force measurement. At the moment of force measurement, the lever arm was stationary, and the muscle was adjusted to the optimal length for the development of maximum force. The core body temperature was monitored with a rectal thermistor and maintained at 36°C. The muscle and nerve examined were bathed regularly with warmed mineral oil throughout the testing to maintain muscle temperature between 35°C and 36°C. The force data were obtained and processed by an acquisition system built from a multifunction I/O National Instruments Acquisition Board (NI USB 6251; 16 bit, 1.25 Ms/s; National Instruments) connected to a Dell laptop with a custom-written program using LabVIEW 8.2 software.

- *The muscles reinnervated with NMEG-NMZ technique produced 82% of the muscle force of the contralateral control.*

The passive tension was set at a moderate level (0.08 N). Nerve stimulation was made with a 0.2-second train of 0.2-millisecond-wide biphasic pulses at frequency of 200 Hz. Operated SM muscle with implanted NMEG pedicle when compared to control muscle at the opposite side has larger stimulation threshold, reach the level of maximal force with larger stimulation current and has smaller maximal force. The NMEG-NMZ reinnervated SM showed an average maximum tetanic force of  $0.87 \pm 0.23$  N (control,  $1.06 \pm 0.10$  N;  $p < 0.005$ ). Clearly, NMEG-NMZ technique resulted in more optimal functional recovery (82% of the control) (Figs. 3 and 4A) as compared with the implantation of the NMEG pedicle into a MEP-free area (Fig. 4B) in the target muscle (67%) [Mu et al., *Neurosurgery* 69(ONS Suppl 2):ons208-ons224, 2011].

- *The muscles treated with NMEG-NMZ and intraoperative brief electrical stimulation (ES) produced 90% of the maximal tetanic force of the contralateral control.*

Maximal muscle force was successfully measured from both sides treated with NMEG-NMZ and intraoperative 1-hour ES. There was a higher average threshold of nerve stimulation current to generate muscle contraction for operated muscles (mean, 0.027 mA) than control muscles (mean, 0.019 mA), but this difference did not reach statistical significance ( $p = 0.17$ ,  $t = 1.47$ , two-tailed, paired  $t$ -test). Maximal muscle force was calculated as average muscle contraction to 5 stimulation currents ranging from 0.6 to 1.0 mA. For each rat, the percentage of functional recovery of the treated SM muscles was determined as compared with the force value of the contralateral control muscle. The treated SM muscles produced 90% of the maximal tetanic tension of the contralateral control muscles (Fig. 5). Averaged maximal muscle force at the treated side was 1.08 N, whereas 1.21 N at the contralateral control side. The difference between these averages (0.13 N) was statistically significant ( $p = 0.035$ ,  $t = 2.35$ , two-tailed, paired  $t$ -test).

- *The muscles treated with NMEG-NMZ and focal application of NGF/FGF-2 produced 91% of the maximal tetanic force of the contralateral control.*

Three months after surgery, electric stimulation of the SH nerve innervating the implanted NMEG resulted in vigorous contractions of all treated muscles. The average threshold of nerve stimulation current that produced visible muscle contraction was 0.031 mA (standard deviation 0.010 mA, median 0.030 mA) on the treated side, but was only about one third of this value on the control side (mean 0.013 mA, standard deviation 0.009 mA, median 0.008 mA). Increasing stimulation current was accompanied by a greater muscle force until it reached horizontal asymptote. This saturation level was reached with higher current (0.2 mA) on the treated side than the control side (0.05 mA). The group average values of tetanic force of SM muscles from the treated muscles (mean 1.193 N, standard deviation 0.195 N, median 1.239 N) were close to those of the controls (mean 1.316 N, standard deviation 0.101 N, median 1.335 N). The treated SM produced 91% of the maximal tetanic tension of the contralateral control (Fig. 6). Clearly, focal administration of NGF/FGF-2 promotes efficacy of NMEG technique.

- *The muscles reinnervated with DNI-NMZ produced 64% of the maximal tetanic force of the contralateral control.*

The degree of functional recovery of the reinnervated SM muscle was determined as compared with the force value of the contralateral control muscle in each rat. The DNI-NMZ reinnervated SM muscles produced 63.6% of the maximal tetanic tension of the contralateral control muscles (Fig. 7). Averaged maximal muscle force at the operated side was 0.763 N, whereas 1.200 N at the contralateral control side. The difference between these averages (0.437 N) was statistically significant ( $p = 0.0013$ ,  $t = 4.08$ ,  $df = 13$ , two-sided  $t$ -test). The average rate (calculated between operated and control muscles) was 0.640. This rate was statistically different from 1 ( $p = 0.0022$ ,  $t = 3.80$ , two-sided single sample  $t$ -test).

## **Objective 2 – Determine the extent of neural regeneration and axon-endplate connections in the treated muscles.**

### ***Task 2.1. Assess the extent of nerve regeneration (Months 12-40)***

Regenerated axons in the target muscle were examined histochemically. Some muscle sections were immunostained with a monoclonal antibody SMI-31 against phosphorylated

neurofilament (NF) as a marker for all axons. The muscle sections immunostained for NF permit to show how the regenerating axons from the implanted NMEG reinnervate the denervated SM and quantify the density and spatial distribution of the regenerating axons in the target muscle. The extent of axonal regeneration and muscle reinnervation was evaluated by quantifying the NF-immunoreactive (NF-ir) axons within the treated muscles. The intramuscular axonal density was assessed by estimating the number of the NF-ir axons and the area fraction of the axons within a section area (1.0-mm<sup>2</sup>). For a give muscle, three sections stained for NF were selected at different spatial levels to count NF-ir axons. For each section, five microscopic fields with NF-ir axons were identified and photographed. Areas with NF-positive staining were outlined, measured with public domain ImageJ software (v. 1.45s; NIH, Bethesda, Maryland). For each rat, the number and the area fraction of the NF-ir axons in the operated muscle were compared with those in the contralateral control.

- *The mean number of the regenerated axons in the NMEG-NMZ reinnervated muscles was computed to be 76.8% of the control.*

The muscle sections from NMEG-NMZ reinnervated SM processed with NF staining exhibited abundance of NF-ir axons. In the reinnervated SM, the regenerating axons from the implanted NMEG supplied the denervated NMZ and reached the most distal portion of the muscle, achieving almost full muscle reinnervation (Fig. 8). On average, the regenerated axons in the NMEG-NMZ reinnervated muscles were calculated to be 76.8% of the controls.

- *The mean number of the regenerated axons in the muscles cotreated with NMEG-NMZ and intraoperative brief ES was 81% of the control.*

The muscle sections stained with NF staining showed that NF-ir axons were confined in the NMZ of the treated and contralateral control SM muscles. The mean number and area fraction of the NF-ir axons in SM muscles treated by NMEG-NMZ plus intraoperative brief ES were measured to be 81 and 84% of the contralateral control muscles (Table 1), respectively.

- *The mean number of the regenerated axons in the muscles cotreated with NMEG-NMZ and focal application of NGF/FGF-2 was 84% of the control.*

NF staining showed that the SM muscles treated with NMEG-NMZ and focal administration of NGF/FGF-2 exhibited extensive axonal regeneration. By counting NF-ir axons per field, we observed that, in the treated SM, the regenerating axons from the implanted NMEG supplied the denervated NMZ and reached the most distal portion of the muscle. Table 2 shows the mean number and area fraction of the NF-ir axons for each muscle in each animal. The mean number of the NF-ir axons in the treated muscles was 84% of the control. Regenerated axons in the treated muscles were more abundant than those in the muscles reinnervated by NMEG-NMZ surgery alone (77% of the control;  $P = 0.049$ ,  $t = 2.05$ , unpaired  $t$ -test).

- *The mean number of the regenerated axons in the muscles reinnervated with DNI-NMZ procedure was 62% of the control.*

The regenerating axons were derived from the implanted SM nerve and supplied the denervated NMZ of the treated muscle. The density of the regenerated axons in the reinnervated muscles as indicated by the number and the area fraction of labeled axons is summarized in Table 3. The mean number and area of the NF-ir axons in the reinnervated SM muscles was computed to be 62% and 51% of the contralateral control muscles, respectively.

***Task 2.2. Examine innervated and noninnervated MEPs in the target muscle (Months 12-40)***

Some sections were stained with double fluorescence staining to label axons and MEPs. The sections were incubated with primary antibodies (SMI-31 to detect neurofilaments and SMI-81 to label thinner axons). The sections were then incubated with a secondary antibody (goat anti-mouse antibody conjugated to Alexa 488) and with  $\alpha$ -bungarotoxin conjugated with Alexa 596. The stained sections were viewed under a Zeiss fluorescence microscope and photographed. SMI-31 and SMI-81 detected axons (green), while  $\alpha$ -bungarotoxin labeled postsynaptic acetylcholine receptor (AChR) site in the MEPs (red). For each muscle sample, at least 100 labeled MEPs were randomly selected from three stained sections at different spatial levels through the muscle to determine the percentages of the innervated (visible axon attachment) and noninnervated (no visible axon attachment) MEPs.

- *Approximately 80% of the denervated MEPs in the NMEG-NMZ reinnervated muscles were reinnervated by regenerated axons.*

The sections of the treated SM muscles immunostained with double fluorescence staining showed the innervated and noninnervated MEPs. In the SM muscles reinnervated with NMEG-NMZ, the regenerating axons grew across the NMZ to innervate the denervated MEPs (Fig. 9A). The majority of the denervated MEPs (80%) in the treated muscles were reinnervated by regenerating axons, while the remaining MEPs were unoccupied by axons (Fig. 9B, C). In addition, axonal sprouts and newly formed small MEPs were identified in the NME-NMZ reinnervated muscles.

- *In the muscles cotreated with NMEG-NMZ and intraoperative brief ES, 83% of the denervated MEPs were reinnervated by regenerated axons.*

Double fluorescence labeling showed the innervated and noninnervated MEPs in the target muscle. In the SM muscles cotreated with NMEG-NMZ and brief ES, the regenerated axons were identified in the NMZ of the target muscle to innervate the denervated MEPs. On average, 83% of the denervated MEPs in the treated muscles were reinnervated by regenerating axons and only 17% of the MEPs were unoccupied by axons. In the treated muscles, innervated and noninnervated MEPs (Fig. 10A,B), small newly formed MEPs (Fig. 10C), and axonal sprouts (Fig. 10D,E) were identified. Terminal axons within the innervated MEPs were visualized (Fig. 10F).

- *In the muscles cotreated with NMEG-NMZ and focal application of NGF/FGF-2, 86% of the denervated MEPs were reinnervated by regenerated axons.*

The muscle sections immunostained with double-fluorescence staining showed that the regenerating axons grew across the NMZ to innervate the denervated MEPs. The majority of the denervated MEPs (86%) in the treated muscles were reinnervated by regenerating axons. In the treated muscles, innervated and non-innervated MEPs, small, newly-formed MEPs, axonal sprouts, and terminal axons within the innervated MEPs were identified (Fig. 11).

- *In the DNI-NMZ reinnervated muscles, 66% of the denervated MEPs were reinnervated by regenerated axons.*

In the DNI-NMZ reinnervated SM, the regenerated axons were identified in the NMZ of the target muscle to innervate the denervated MEPs. On average, 66% of the denervated MEPs in

the treated muscles were reinnervated by regenerated axons and 34% of the endplates were unoccupied by axons.

### **Objective 3 – Document histological and immunohistochemical alterations in the treated muscles.**

#### ***Task 3.1. Assess muscle weight and myofiber morphology (Months 16-48)***

Wet muscle weight and myofiber morphology are indicators for the effectiveness of muscle reinnervation. At the end of the experiments, SM muscles on both sides in each animal were removed, weighed, and photographed. The wet muscle weights were reported as a ratio of the treated side to the contralateral control side. A muscle mass ratio was calculated (muscle mass ratio = weight of reinnervated muscle/weight of contralateral muscle).

■ *The average ratio of the NMEG-NMZ reinnervated muscles to control muscles was 0.89.*

In each rat, gross appearance and size of the operated SM was similar to those of the contralateral control muscle. The reinnervated SM muscles were greater in size than the SM muscles with complete denervation for 3 months. The mean value and standard deviation of the wet weight was  $0.332 \pm 0.047$  g for the reinnervated SM muscles, whereas  $0.374 \pm 0.044$  g for the contralateral control muscles (Table 4). The differences in muscle weights of the reinnervated and control muscles were relatively small but consistent across all animals and therefore statistically significant ( $p < 0.0001$ ). The reinnervated SM muscles weighed 89% of the weight of contralateral control muscles. The mean percent of wet weight (89% of the control) of NMEG-NMZ reinnervated SM muscles was much higher than that of the denervated SM muscles (44% of the control;  $p < 0.0001$ ) (Fig. 12A-C).

Three months after surgery, NMEG-NMZ reinnervated SM exhibited very good preservation of muscle structure and myofiber morphology with less fiber atrophy as compared with the normal and denervated muscles (Fig. 12A'-C').

■ *The average ratio of the muscles cotreated with NMEG-NMZ and intraoperative brief ES to control muscles was 0.90.*

The mean wet weight of the treated SM muscles (0.309 g) was 90% of the control muscles (0.344 g) 3 months after NMEG-NMZ procedure and intraoperative brief ES, whereas that of 3-month denervated SM muscles was 0.138 g (Fig. 13A-C). The mean wet weight of the treated SM muscles was significantly higher than that of the denervated SM muscles ( $p < 0.0001$ ).

H&E-stained cross muscle sections showed the histological profiles of the treated, control, and denervated SM muscles. The treated SM (Fig. 13A') exhibited better muscle structure and myofiber morphology with less fiber atrophy as compared with the contralateral control (Fig. 13B') and denervated muscle which exhibited prominent fiber atrophy (Fig. 13C').

■ *The average ratio of the muscles cotreated with NMEG-NMZ and focal application of NGF/FGF-2 to control muscles was 0.92.*

Three months after cotreatment with NMEG-NMZ and focal administration of NGF/FGF-2, the size of the treated SM was similar to that of the contralateral control, but larger

than that of 3-month-denervated SM (Fig. 14A-C). The mean weight of the denervated SM muscles was  $0.138 \pm 0.062$  g. The difference in average muscle weight was relatively small between treated and control muscles, but consistent across rats and, therefore, statistically significant ( $P < 0.00001$ ,  $t = 6.839$ , paired  $t$ -test). The average ratio of treated to control muscles (0.92) was substantially larger than the average ratio (0.38) of denervated to control muscles in rats that had SM muscle denervation without treatment ( $p < 0.00001$ ,  $t = 14.226$ , unpaired  $t$ -test).

Muscle sections stained with H&E staining showed that myofiber morphology of the treated SM (Fig. 14A') was similar to that of the contralateral control (Fig. 14B') and better than that of the denervated muscle (Fig. 14C'). Remarkable fiber atrophy was found in the denervated muscles.

■ *The average ratio of the DNI-NMZ reinnervated muscles to control muscles was 0.71.*

The mean value of the wet weight of the reinnervated SM muscles (0.251 g) was smaller compared with that of the control muscles (0.352 g), but larger than that of the denervated SM muscles (0.199 g). The DNI-NMZ reinnervated SM muscles weighed 71% of the weight of the control muscles. (Fig. 15A-B). The mean percent rate of DNI-NMZ reinnervated SM muscles in relation to normal contralateral side (71%, with standard deviation = 0.11) was much higher than the rate of the denervated SM muscles in relation to normal contralateral side (44%, with standard deviation = 0.20,  $n = 17$ ;  $t = 4.72$ ,  $df = 30$ ,  $p < 0.00001$ ). Man-Whitney U test confirmed strong significant difference in percentage rates between the two groups ( $U_A = 223.5$ ,  $U_B = 31.5$ ,  $P = 0.00012$ ).

Stained histological sections showed that the DNI-NMZ reinnervated muscles exhibited slight-to-moderate fiber atrophy as compared with the controls (Fig. 15C-D).

**Task 3.2. Evaluate neuromuscular alterations in the long-term denervated muscles (Months 37-48)**

Denervation-induced changes in muscle weight, myofiber size, MEPs, and intramuscular nerve axons were evaluated histomorphometrically and immunohistochemically at the end of 3, 6, and 9 months after denervation.

■ *Progressive reduction in muscle weight*

We found that the denervated SM muscles exhibited a progressive reduction in muscle weight (38%, 31%, and 19% of the control), respectively (Table 5, Fig. 16A). The average muscle weight was significantly smaller in denervated than in control muscles ( $t = 19.7$ ,  $df = 20$ ,  $P < 0.00001$ ). Statistical analysis (one-way ANOVA) of the averaged rates of SM muscle weight (denervated to control) in these three groups indicated a strong trend toward decreasing rate with denervation time, but did not show statistical significant differences between these three groups ( $F = 3.25$ ,  $df = 2/18$ ,  $P = 0.0627$ ). Note that the analysis was performed on assumption of normality holds; however, when sample sizes are less than 10 (such as 7), the Shapiro-Wilk test of normality has little power to detect deviations from normality. In fact, the Kruskal-Wallis test reported a statistically significant difference between these groups ( $P = 0.0422$ ). The box plots illustrating the distribution of data in 3-month, 6-month, and 9-month groups are shown in Figure 17. Clearly, the reduction in the muscle mass is associated with denervation time.

■ *Progressive reduction in muscle fiber size*

H&E stained muscle cross sections from the control and denervated SM muscles showed a progressive reduction in fiber size of the denervated muscle (Fig. 16B). Fiber diameter measurement showed that fiber diameter was reduced to 52%, 40%, and 28% of the control for 3-, 6-, and 9-month denervation, respectively (Fig. 18).

■ *Fragmented axons and progressive decrease in the number of MEPs*

Degenerated axons in the denervated muscles became fragmented. In the stained muscle sections, fragments and/or accumulations of axonal debris were identified. The denervated MEPs were still detectable even 9 months after denervation. The mean number of the denervated MEPs was 79%, 65%, and 43% of the control in the 3-, 6-, and 9-month denervated SM muscles, respectively (Table 6; Fig. 19). Statistical analysis (one-way ANOVA) of the rates (denervated to control) of MEP counts showed strong statistical significant difference between these three groups ( $F= 30.2$ ,  $df= 2/18$ ,  $p < 0.0001$ ). Posthoc testing (Tukey HSD test) shows statistical difference between means of each pair of three groups. Average of 3-month denervation group is significantly larger than average of 6-month ( $p < 0.05$ ) and 9-month ( $p < 0.01$ ) denervation groups. Also average of 6-month group is significantly larger than that of 9-month group ( $p < 0.05$ ).

The long-term denervated muscles, especially 9-month denervated muscles (Fig. 19D-D'), showed the presence of small, shrunken and distorted MEPs. Some of the denervated MEPs displayed broken and fragmented forms, and thin lengthened shapes. Persistence of MEPs in the long-term denervated SM suggests that some surgeries targeting the MEPs such as NMEG-NMZ techniques should be effective for delayed reinnervation. However, more work is needed to develop strategies for preservation of muscle mass and MEPs after denervation.

■ *Alterations in muscle fiber types*

Skeletal muscle fibers contain three major fiber types (types I, IIA and IIB) and corresponding myosin heavy chain (MyHC) isoforms. In general, decreased neuromuscular activation, which is usually caused by neurologic diseases, denervation or disuse, results in muscle fiber atrophy and fiber type and MyHC transformation. MyHC conversion could lead to fast-to-slow shift in the fast-twitch muscle or slow-to-fast shift in the slow-twitch muscle.

Some cross sections from the denervated and control muscles were stained with type-specific anti-MyHC monoclonal antibodies (mAbs) against type I (NOQ7-5-4D), type IIA (SC-71), and all fast type II (MY-32). Immunohistochemically stained cross sections from the denervated SM showed fiber type grouping in the slow type I muscle fiber population (Fig. 20). These findings indicate that motor innervation is one of the most important factors influencing the fiber type and MyHC composition as well as morphologic profile of muscle fibers.

## **Key Research Accomplishments**

- Demonstrated that NMEG-NMZ technique results in optimal (82% of the control) functional recovery of the reinnervated muscle.
- Documented that the regenerated axons in the NMEG-NMZ reinnervated muscle reach up to 77% of the control.

- Documented that approximately 80% of the denervated MEPs in the target muscle regain motor reinnervation following NMEG-NMZ procedure.
- Documented that the wet weight of the NMEG-NMZ reinnervated muscle is 89% of the contralateral control.
- Demonstrated that intraoperative brief ES improves outcomes of the NMEG-NMZ technique. Cotreatment of NMEG-NMZ and brief ES results in better functional recovery (90% of the control) as compared with NMEG-NMZ alone (82%).
- Documented that the regenerated axons in the muscles treated with NMEG-NMZ and brief ES are 81% of the control.
- Documented that 83% of the denervated MEPs in the muscles treated with NMEG-NMZ and brief ES are reinnervated by regenerating axons.
- Documented that the wet weight of the muscles treated with NMEG-NMZ and brief ES reaches 90% of the control.
- Demonstrated that focal administration of NGF/FGF-2 improves outcomes of the NMEG-NMZ technique. The muscles cotreated with NMEG-NMZ and NGF/FGF-2 produce more optimal functional recovery (91% of the control) compared to those reinnervated with NMEG-NMZ alone.
- Documented that the regenerated axons in the muscles treated with NMEG-NMZ and NGF/FGF-2 are 84% of the control.
- Documented that 86% of the denervated MEPs in the muscles treated with NMEG-NMZ and NGF/FGF-2 are reinnervated by regenerating axons.
- Documented that the wet weight of the muscles treated with NMEG-NMZ and NGF/FGF-2 reaches 92% of the control.
- Demonstrated that the DNI-NMZ reinnervated muscles result in suboptimal functional recovery (63.6% of the control).
- Documented that the regenerated axons in the muscles reinnervated with DNI-NMZ are 62% of the control.
- Documented that in the muscles reinnervated with DNI-NMZ procedure 66% of the denervated MEPs regain innervation by regenerated axons.
- Documented that the wet weight of the muscles reinnervated with DNI-NMZ procedure is 71% of the weight of the control.
- Demonstrated that the muscles denervated for 3, 6, and 9 months exhibit a progressive reduction in muscle weight to 38%, 31%, and 19% of the control, respectively.
- Documented that fiber diameters are reduced to 52%, 40%, and 28% of the control for 3-, 6-, and 9-month denervation, respectively

- Documented that the denervated MEPs are 79%, 65%, and 43% of the control in the 3-, 6-, and 9-month denervated muscles, respectively.

## **Conclusions**

Our results allow us to make the following conclusions.

First, the NMZ of the target muscle is an ideal site for implantation of NMEG as the denervated MEPs in the NMZ can be rapidly reinnervated by the regenerating axons from the implanted NMEG. In the muscles reinnervated with NMEG-NMZ technique 80% of denervated MEPs could regain motor innervation.

Second, NMEG-NMZ technique results in better functional recovery (82%) as compared with nerve end-to-end anastomosis (57%) and DNI-NMZ (64%). This is most likely due to such a fact that the NMEG-NMZ procedure physically shortens regeneration distances and facilitates rapid MEP reinnervation, thereby avoiding irreversible loss of the denervated MEPs in the target muscle.

Third, functional recovery of the muscles reinnervated with NMEG-NMZ can be further improved by a combination of NMEG-NMZ technique with focal administration of NGF/FGF-2 or intraoperative 1-hour ES. Cotreatment of NMEG-NMZ and NGF/FGF-2 or 1-hour ES results in more optimal functional recovery (90%) as compared with NMEG-NMZ surgery alone (82%). This should be attributed to the beneficial effects of NGF/FGF-2 or ES on axonal regeneration and MEP reinnervation.

Fourth, prolonged denervation results in a progressive reduction of muscle mass, myofiber size, and MEPs. Therefore, further studies are needed for the development of therapeutic strategies to rescue muscle from atrophy and protect MEPs from degradation after muscle denervation. Maintenance of original MEPs in the long-term denervated muscle could facilitate rapid axon-MEP connections, thereby improving functional outcomes of NMEG-NMZ, DNI-NMZ, and/or other nerve repair procedures.

Finally, NMEG-NMZ has the potential for head and neck muscle reinnervation. However, more work is needed to investigate the effectiveness of the NMEG-NMZ for reinnervation of large limb muscles following PNIs.

## **4. Impact**

Traumatic PNIs commonly seen in both the military and civilian populations are the major source of chronic disabilities that have a potentially devastating impact on a patient's quality of life. There are 200,000 patients with PNIs which result in approximately \$150 billion spent in annual healthcare dollars in the USA and an estimated \$300 billion spent annually on care for disabled Americans. As currently available nerve repair methods result in poor outcomes, there is a pressing need in military medicine to improve functional recovery following PNIs.

The proposed studies were conducted to evaluate the efficacy of our recently developed NMEG technique for muscle reinnervation. This research project has yielded some notable discoveries that may impact military health care in the near future. We have demonstrated that the NMEG-NMZ results in better functional recovery of the reinnervated muscle compared to

primary nerve repair. Our NMEG-NMZ technique favors rapid MEP reinnervation because the regenerating axons from the NMEG can easily reach and reinnervate the MEPs in the target muscle, thereby contributing to optimal outcomes. We do believe that NMEG-NMZ can be an alternative option to treat PNI-induced muscle paralysis.

We have also shown that outcomes of NMEG-NMZ can be further improved by strategies that enhance axonal regeneration. Specifically, the combination of NMEG-NMZ surgery with focal application of NGF/FGF-2 or intraoperative brief ES resulted in better nerve regeneration and functional recovery as compared with NMEG-NMZ surgery alone.

Our ultimate goal is to translate the NMEG-NMZ technique to clinical practice in the near future for treating our military Service members, Veterans and civilians with PNI-induced paralyzed muscles. Our studies indicate that the NMEG-NMZ technique holds great promise for optimal functional recovery and would have broad utility for muscle reinnervation.

The NMEG-NMZ procedure will not require extensive specialized training, enabling near term transferability to surgeons to improve clinical outcomes in both the military and civilian communities. If functionality can be restored or improved, Service members can remain on active duty. Optimal functional recovery could improve return-to-work rates and quality of life.

## **5. Changes/Problems**

Nothing to report.

## **6. Products**

### **■ *Peer-Reviewed Publications (see Appendix)***

1. Mu L, Sobotka S, Chen J, Nyirenda T. Reinnervation of denervated muscle by implantation of nerve-muscle-endplate band graft to the native motor zone of the target muscle. *Brain Behav* 7(6):e00668. doi:10.1002/brb3.668, 2017. PMID: 28638701
2. Sobotka S, Chen J, Nyirenda T, Mu L. Intraoperative one-hour electrical nerve stimulation enhances outcomes of nerve-muscle-endplate band grafting technique for muscle reinnervation. *J Reconstr Microsurg* 33:533-543, 2017. PMID: 28575920
3. Sobotka S, Chen J, Nyirenda T, Mu L. Outcomes of muscle reinnervation with direct nerve implantation into the native motor zone of the target muscle. *J Reconstr Microsurg* 33:77-86, 2017. PMID: 27737470
4. Mu L, Sobotka S, Chen J, Nyirenda T. Nerve growth factor and basic fibroblast growth factor promote reinnervation by nerve-muscle-endplate grafting. *Muscle Nerve* 57:449-459, 2018. PMID: 28632904
5. Mu L, Chen J, Li J, Nyirenda T, Fowkes M, Sobotka S. Immunohistochemical detection of motor endplates in the long-term denervated muscle. *J Reconstr Microsurg* 34:348-358, 2018.

### **■ *Conference Presentations***

1. Sobotka S, Chen J, Nyirenda T, Mu L. Modified nerve-muscle-endplate band grafting technique for muscle reinnervation. Presented at the Gorge Perez Research Colloquium at the Seton Hall University, South Orange, NJ, April 24, 2015.
2. Sobotka S, Chen J, Nyirenda T, and Mu L. Outcomes of muscle reinnervation with direct implantation into the native motor zone of the target muscle. *46th Annual Meeting of Neuroscience Society*, San Diego, CA, November 12-16, 2016.
3. Mu L, Sobotka S, Chen J, Nyirenda T. Muscle reinnervation: Modified nerve-muscle-endplate band grafting technique. *46th Annual Meeting of Neuroscience Society*, San Diego, CA, November 12-16, 2016.

## Supporting Data

**Table 1.** Comparison of count and %area of NF-ir axons between right SM treated with NMEG-NMZ plus intraoperative electrical stimulation and left control in rats

Animal (no.)	Right SM		Left SM		Ratio (R/L)	
	Count	Percentage of area	Count	Percentage of area	Count	Percentage of area
1	559	0.721	798	0.945	0.701	0.763
2	670	0.640	729	0.724	0.919	0.884
3	725	0.728	913	0.946	0.794	0.770
4	630	0.621	824	0.789	0.765	0.787
5	610	0.658	816	0.827	0.748	0.796
6	655	0.710	904	0.900	0.725	0.789
7	978	0.697	1,014	0.811	0.964	0.859
8	601	0.803	988	0.970	0.608	0.828
9	894	1.060	1,043	1.200	0.857	0.883
10	792	0.736	967	0.856	0.819	0.860
11	993	1.102	1,103	1.205	0.900	0.915
12	839	0.735	993	0.840	0.845	0.875
13	1,008	0.833	1,186	0.997	0.850	0.836
14	781	0.638	883	0.704	0.884	0.906
15	683	0.596	837	0.698	0.816	0.854
Average	761	0.752	933	0.894	0.813	0.840
SD	151	0.149	125	0.156	0.093	0.051

L, left; R, right; SD, standard deviation.

**Table 2.** The count and %area of NF-ir axons in the right SM treated with NMEG-NMZ plus focal administration of NGF/FGF-2 and the left control in rats

Animal (no.)	Right SM		Left SM		Ratio (R/L)	
	Count	Percentage of area	Count	Percentage of area	Count	Percentage of area
1	683	0.738	896	1.056	0.762	0.699
2	866	0.605	995	0.803	0.870	0.753
3	926	0.801	1,033	0.982	0.896	0.816
4	901	0.674	1,128	0.874	0.799	0.771
5	587	0.509	898	0.786	0.654	0.648
6	955	1.200	1,074	0.996	0.889	1.205
7	493	0.605	723	0.862	0.682	0.702
8	889	0.826	834	0.974	1.066	0.848
9	510	0.721	670	0.865	0.761	0.834
10	809	1.002	876	1.033	0.924	0.970
11	917	0.801	1,056	0.796	0.868	1.006
12	558	0.725	801	0.854	0.697	0.849
13	779	0.824	902	0.899	0.864	0.917
14	882	0.879	997	1.120	0.885	0.785
15	970	0.934	993	0.982	0.977	0.951
Average	782	0.790	925	0.925	0.840	0.850
SD	170	0.170	131	0.100	0.110	0.140

L, left; R, right; SD, standard deviation.

**Table 3.** The number and %area of NF-ir axons in the right SM reinnervated with DNI-NMZ and the left control in rats

Animal (no.)	Right SM		Left SM		Ratio (R/L)	
	Count	Percentage of area	Count	Percentage of area	Count	Percentage of area
1	511	0.412	1,640	1.336	0.312	0.308
2	668	0.430	678	0.626	0.985	0.687
3	420	0.552	1,160	1.145	0.362	0.482
4	300	0.456	720	0.566	0.417	0.806
5	473	0.762	510	0.908	0.927	0.839
6	441	0.560	1,074	1.358	0.411	0.412
7	312	0.370	600	1.100	0.520	0.336
8	340	0.247	649	0.931	0.524	0.265
9	624	0.623	861	1.295	0.725	0.481
10	671	0.660	752	1.303	0.892	0.507
11	499	0.640	623	1.557	0.801	0.411
12	435	0.511	814	1.496	0.534	0.342
13	319	0.509	893	1.280	0.357	0.398
14	748	0.630	751	0.716	0.996	0.880
15	533	0.636	947	1.479	0.563	0.430
Average	486	0.533	845	1.140	0.622	0.506
SD	142	0.134	283	0.321	0.244	0.201

L, left; R, right; SD, standard deviation.

**Table 4.** Wet muscle weight measurement for the right NMEG-NMZ reinnervated and left control SM muscles in rats

Animal (no.)	Body weight (g)	Right treated SM (g)	Left control SM (g)	Ratio R/L
1	333	0.309	0.333	0.928
2	328	0.332	0.397	0.836
3	319	0.318	0.357	0.891
4	285	0.287	0.328	0.875
5	386	0.245	0.316	0.775
6	373	0.373	0.407	0.916
7	281	0.320	0.343	0.933
8	330	0.396	0.437	0.906
9	329	0.305	0.327	0.933
10	355	0.335	0.358	0.936
11	380	0.341	0.392	0.870
12	304	0.326	0.338	0.964
13	358	0.433	0.462	0.937
14	315	0.373	0.410	0.910
15	328	0.290	0.398	0.729
Average	334	0.332	0.374	0.889
SD	31.8	0.047	0.044	0.065

L, left; R, right; SD, standard deviation.

**Table 5.** Wet muscle weights of 3-month-, 6-month-, and 9-month-denervated and control SM muscles in rats

Animal (no.)	Body weight (g)	Denervated SM (g)	Control SM (g)	Ratio D/C
<b>3-month DEN</b>				
1	259	0.15	0.342	0.439
2	370	0.151	0.335	0.451
3	353	0.075	0.311	0.241
4	324	0.101	0.357	0.283
5	319	0.075	0.309	0.243
6	379	0.164	0.413	0.397
7	386	0.25	0.425	0.588
Average	341.4	0.138	0.356	0.377
SD	44.6	0.062	0.046	0.129
<b>6-month DEN</b>				
1	296	0.258	0.386	0.668
2	390	0.117	0.372	0.315
3	378	0.039	0.38	0.103
4	282	0.075	0.298	0.252
5	304	0.047	0.39	0.121
6	296	0.166	0.374	0.444
7	324	0.101	0.391	0.258
Average	324.3	0.115	0.37	0.309
SD	42.8	0.077	0.033	0.196
<b>9-month DEN</b>				
1	323	0.082	0.376	0.218
2	330	0.138	0.415	0.333
3	300	0.066	0.353	0.187
4	394	0.049	0.371	0.132
5	398	0.037	0.369	0.1
6	412	0.052	0.382	0.136
7	408	0.073	0.378	0.193
Average	366.4	0.071	0.378	0.186
SD	46.9	0.033	0.019	0.077

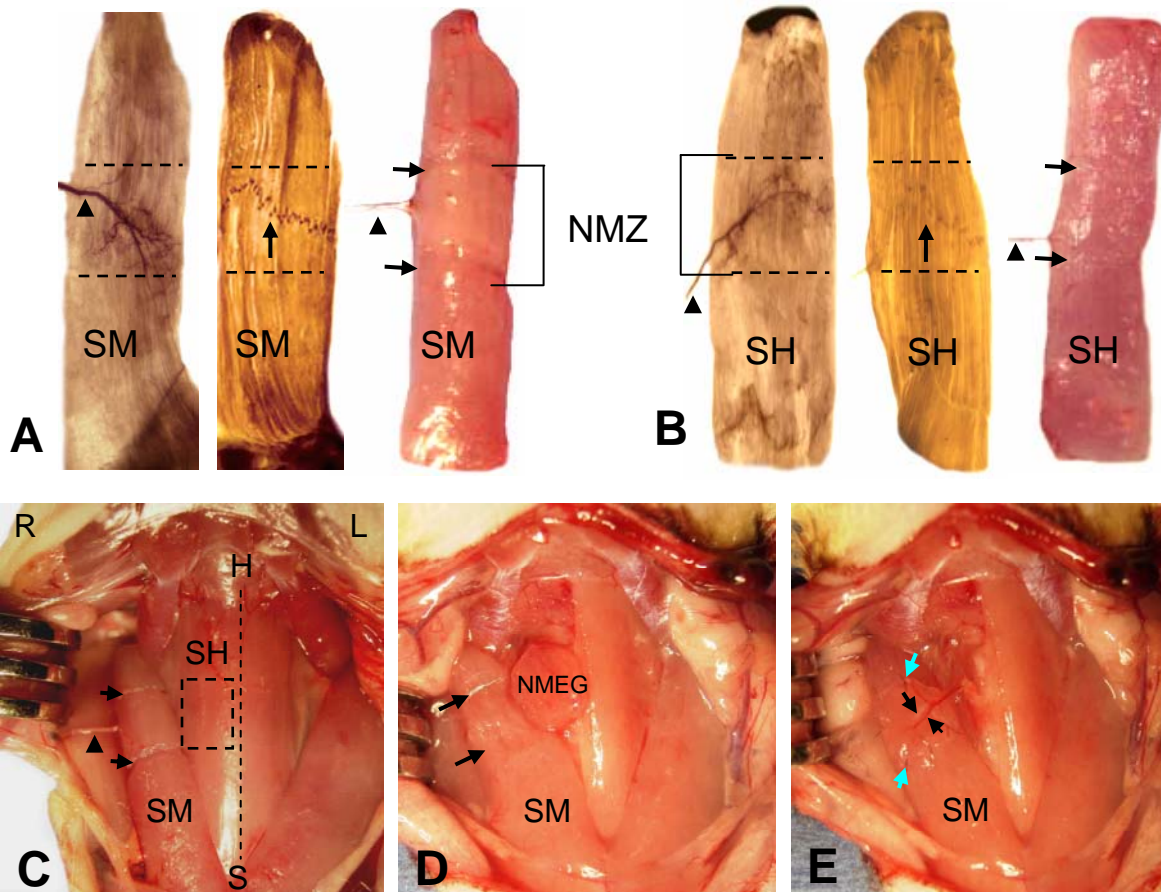
DEN, denervation; D/C, denervated/control; SD, standard deviation.

**Table 6.** MEP counts for the 3-month-, 6-month-, and 9-month-denervated and control SM muscles in rats

Animal (no.)	Denervated SM (g)	Control SM (g)	Ratio D/C
<b>3-month DEN</b>			
1	81	115	0.704
2	76	104	0.730
3	72	93	0.774
4	87	110	0.790
5	69	87	0.793
6	109	121	0.900
7	98	118	0.830
Average	84.6	106.9	0.789
SD	14.5	12.9	0.064
<b>6-month DEN</b>			
1	68	101	0.673
2	71	115	0.617
3	39	88	0.443
4	94	128	0.734
5	63	98	0.643
6	78	104	0.750
7	52	79	0.658
Average	66.4	101.9	0.645
SD	17.7	16.3	0.101
<b>9-month DEN</b>			
1	58	123	0.471
2	65	108	0.601
3	47	99	0.474
4	40	112	0.357
5	38	104	0.365
6	43	111	0.387
7	46	128	0.359
Average	48.1	112.1	0.431
SD	9.9	10.2	0.091

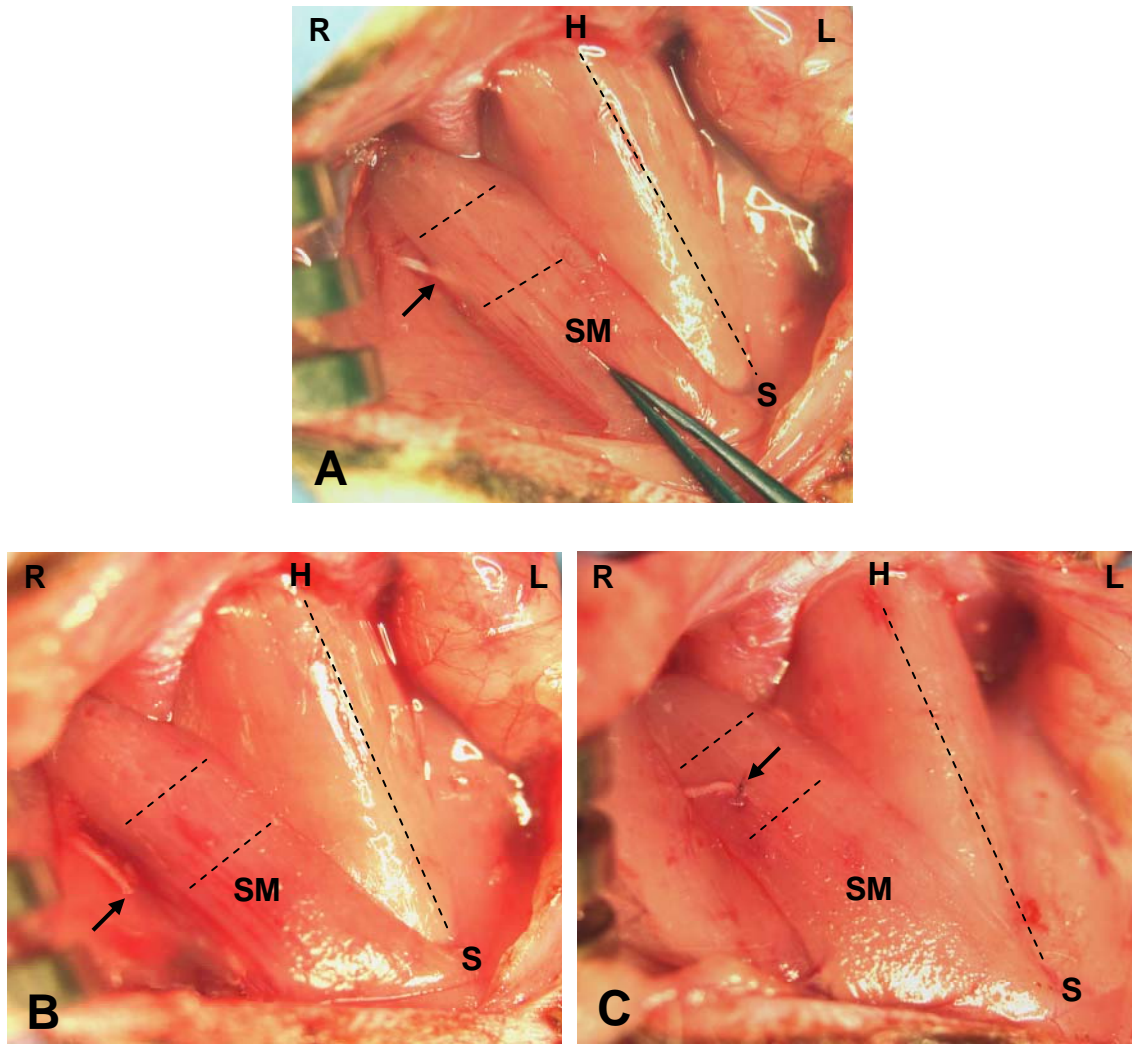
DEN, denervation; D/C, denervated/control; SD, standard deviation.

**Figure 1.** Images showing the locations of native motor zones (NMZ) of the recipient SM and donor SH muscles of the rat and surgical procedures for NMEG-NMZ transplantation.



(A) Stained and fresh right SM showing the NMZ of the muscle (outlined region). SM nerve (arrowhead) and its intramuscular nerve terminals were mapped out with Shiner's stain (left image), whereas the MEP band (arrow in the middle image) was visualized with whole mount acetyl cholinesterase staining. A fresh SM (right image) illustrated the NMZ outlined during surgery (between fiber cuts on the surface of the muscle as indicated by arrows and bracket). (B) Stained and fresh right SH showing that the NMZ of the SH is also located in the middle of the muscle. (C) A photograph from a rat during surgery, showing surgically outlined NMZ in the recipient SM (between fiber cuts as indicated by arrows) and in the donor SH (boxed region). The arrowhead indicates the SM nerve. The dashed line indicates the midline between both SH muscles. H = hyoid bone; L = left; R = right; S = sternum. (D) A NMEG pedicle was harvested from the NMZ of the right SH and a muscular defect (between arrows) was made on the SM muscle. (E) The NMEG was implanted into the recipient bed and sutured (green arrows). The SH nerve branch (large black arrow) and its accompanying blood vessels (small black arrow) can be seen on the implanted NMEG.

**Figure 2.** Surgical procedures for reinnervation of the experimentally denervated SM with direct nerve implantation (DNI)



(A) Entrance point (arrow) of the SM nerve into the muscle was visualized after lateral retraction of muscle tissue. (B) The SM nerve was transected at the motor point (arrow) and isolated from surrounding tissues. (C) The proximal stump of the severed SM nerve was buried into a small muscle slit made in the NMZ (between dashed lines) of the denervated SM muscle, and secured in position with an epineurial suture of 10-0 nylon (arrow). The oblique dashed line in A-C indicates the midline. H, hyoid bone; L, left; R, right; S, sternum.

**Figure 3.** Muscle force as a function of stimulation current in the NMEG-NMZ reinnervated and contralateral control SM muscles

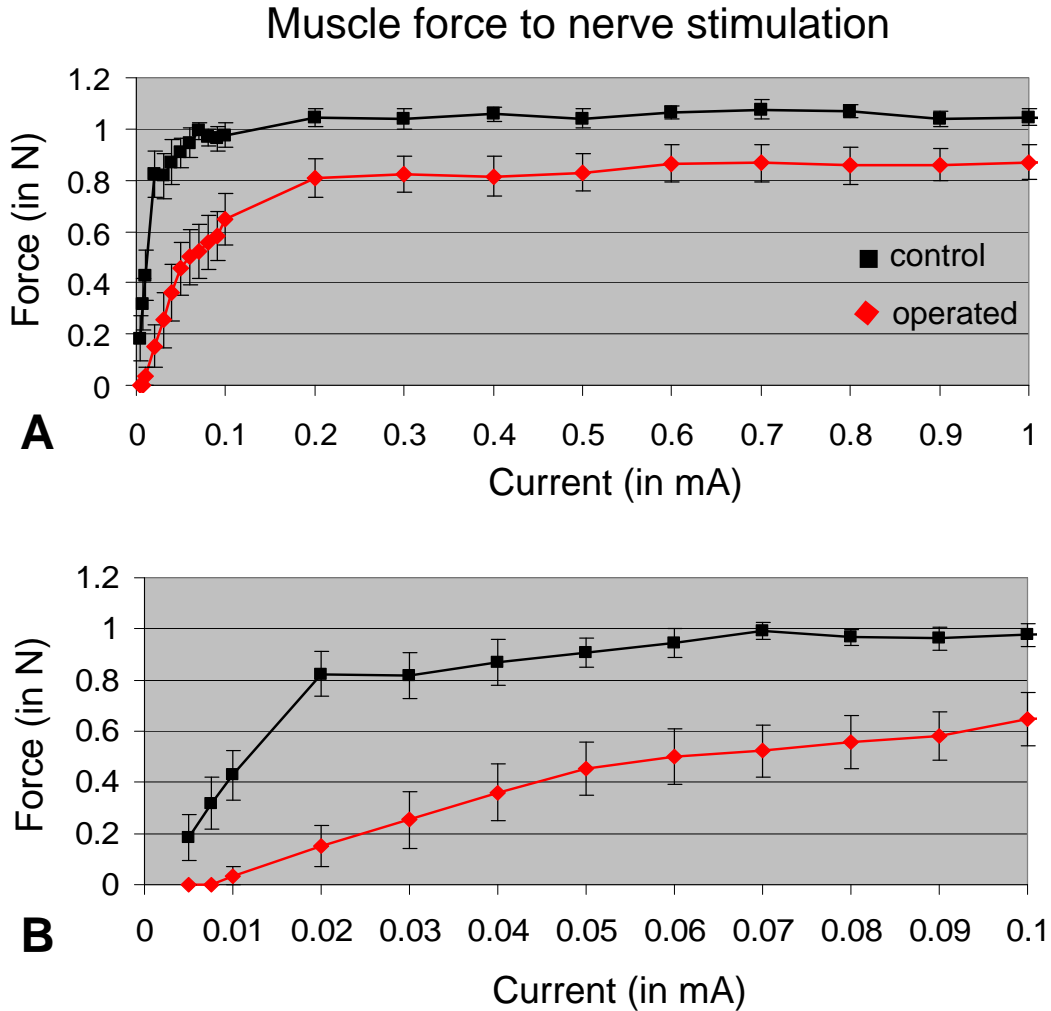
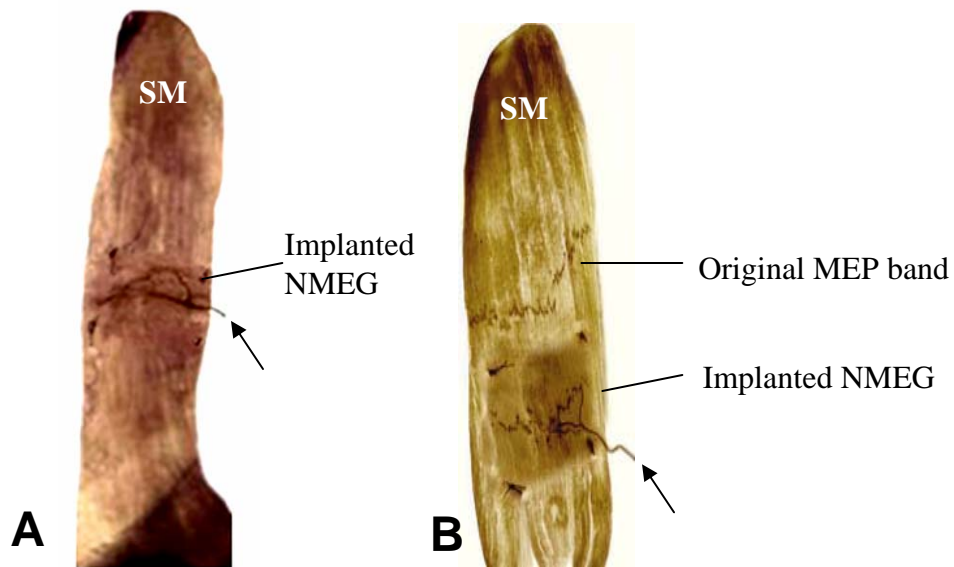


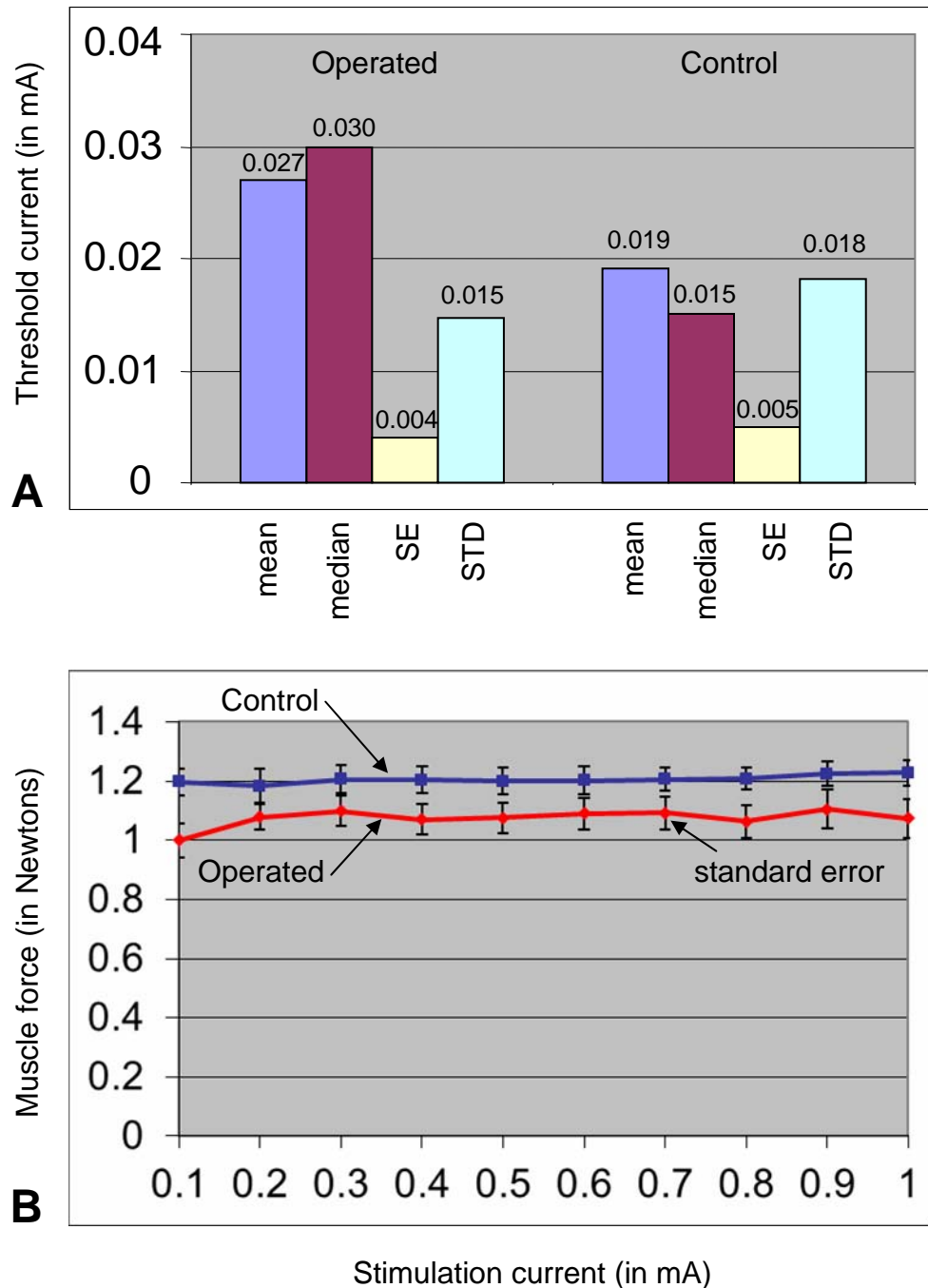
Figure 3B shows in expanded scale the early portion of Figure 3A. Maximal muscle force level was calculated as the average muscle force to stimulation currents from 0.6-1 mA. The reinnervated SM showed an average maximum tetanic force of  $0.87 \pm 0.23$  N (control,  $1.06 \pm 0.10$  N;  $p < 0.005$ ). Vertical bars represent the standard deviation of the mean. NMEG-NMZ technique resulted in optimal functional recovery (82% of the control).

**Figure 4.** Images showing the implantation sites of the NMEG in the SM muscles



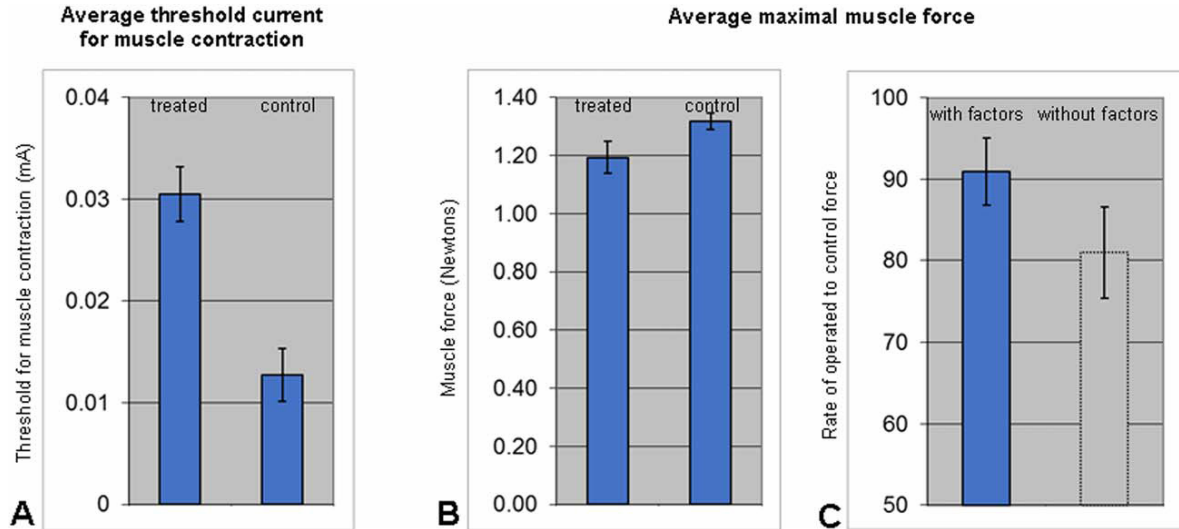
(A) Implantation of the NMEG into the NMZ of the target muscle as shown by Sihler's stain, a wholemount nerve staining technique, after NMEG-NMZ surgery. (B) Implantation of the NMEG to a MEP-free area in the target muscle as shown by wholemount acetylcholinesterase and silver staining. Arrow indicates the SH nerve supplying the NMEG.

**Figure 5.** Muscle force recovery of the SM muscles treated with NMEG-NMZ and intraoperative brief electrical stimulation



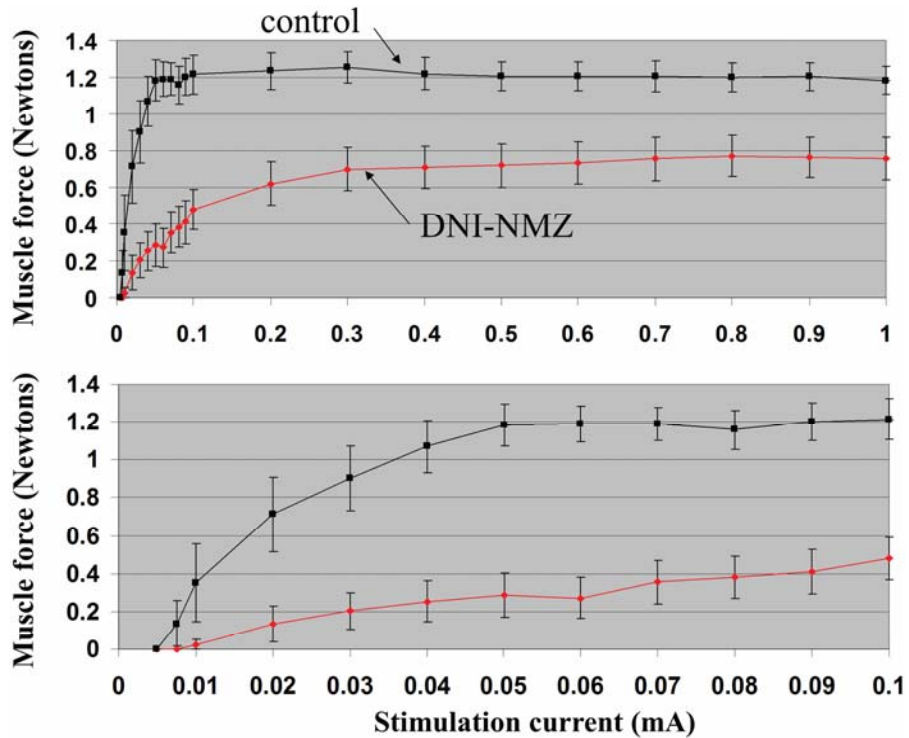
(A) Comparison of current thresholds eliciting muscle contraction between operated and control muscles. (B) Comparison of average muscle force between operated and control muscles. The treated SM muscles produced 90% of the maximal tetanic tension of the contralateral control muscles.

**Figure 6.** Muscle force from rats treated with NMEG-NMZ and focal application of NGF/FGF-2



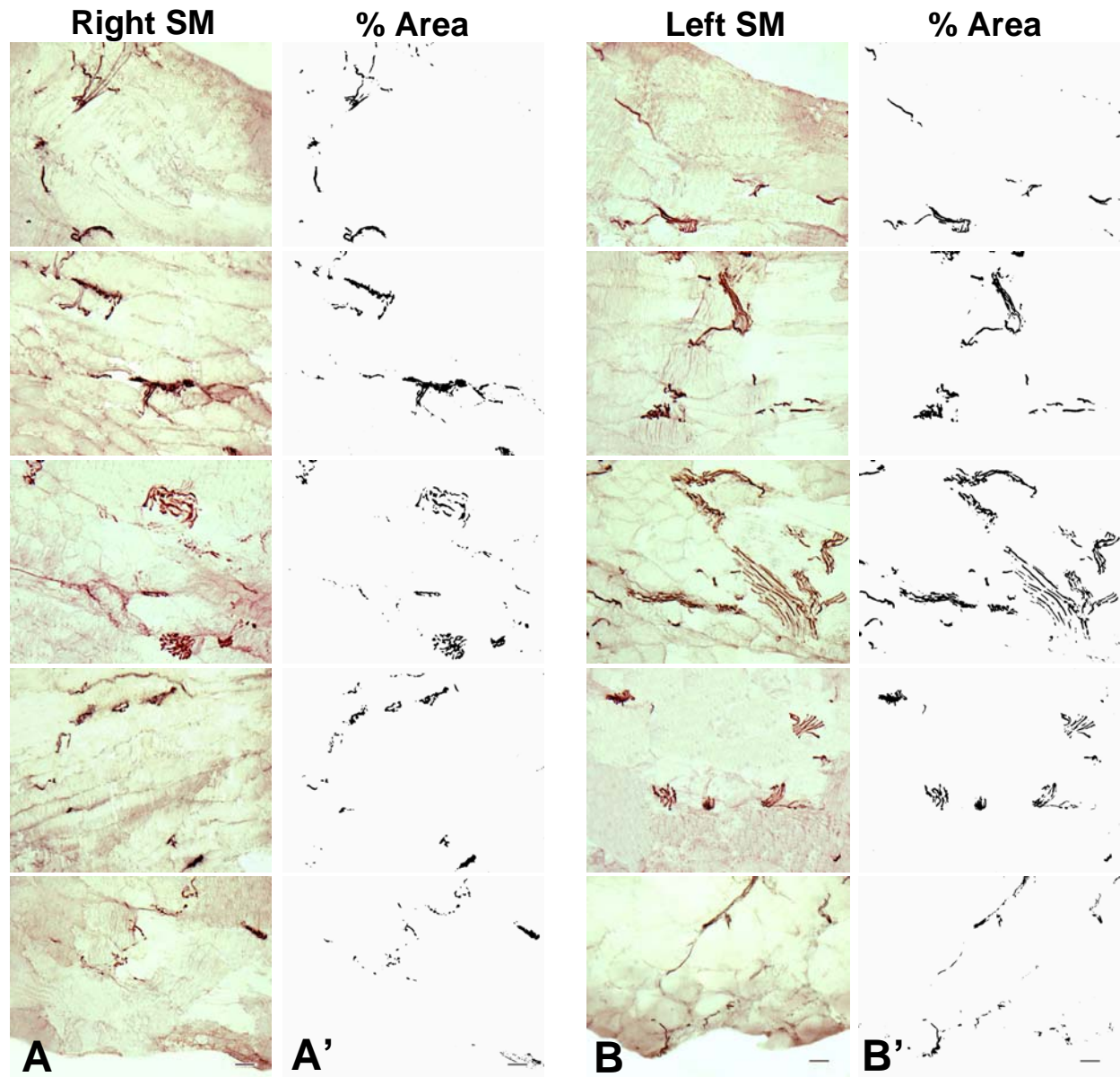
(A) Comparison of current thresholds for muscle contraction between treated and control muscles. (B) Comparison of maximal muscle force between treated and control muscles. Maximal muscle force was calculated as the average force to stimulation currents from 0.6 to 1.0 mA. (C) Average maximal force of the SM muscles treated with NMEG-NMZ and NGF/FGF-2 (factors) was 91% of the controls (left bar). The right dotted bar illustrates average percent rate of maximal force of the SM muscles treated with NMEG-NMZ alone (82% of the control).

**Figure 7.** Muscle force from rats treated with DNI-NMZ technique



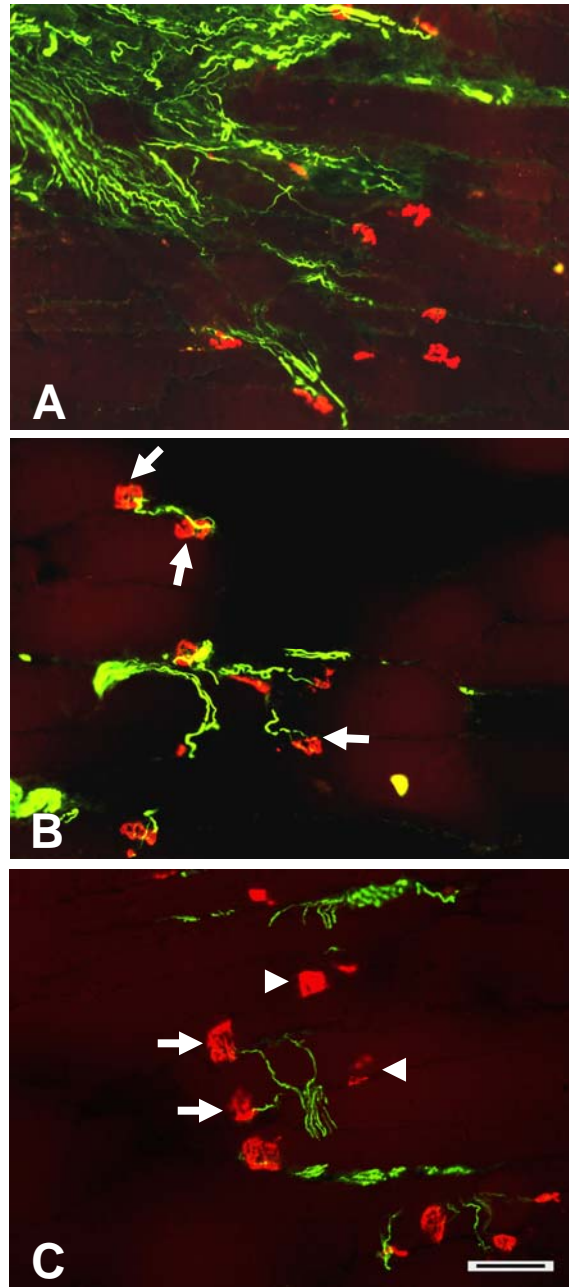
Muscle force as a function of stimulation current in operated and control sternomastoid (SM) muscles. The passive tension was set at a moderate level (0.08 N). Stimulation was made with a 0.2-second train of 0.2-millisecond-wide biphasic pulses at frequency of 200 Hz. The lower graph shows, in expanded scale, the early portion of the upper graph. Note that operated SM muscle (with DNI-NMZ label) when compared with control muscle at the opposite side (with control label) has larger stimulation threshold (0.02 vs 0.0075 mA), reach the level of maximal force with larger stimulation current (0.3 vs 0.05 mA), and has smaller maximal force. Maximal muscle force level was calculated as the average muscle force to stimulation currents from 0.6–1 mA. Average maximal muscle force level at the operated side (0.76 N) was 63.6% of muscle force at the control side (1.20 N). Vertical bars represent the standard deviation of the mean.

**Figure 8.** Axonal regeneration of the right SM muscle reinnervated with the NMEG-NMZ technique



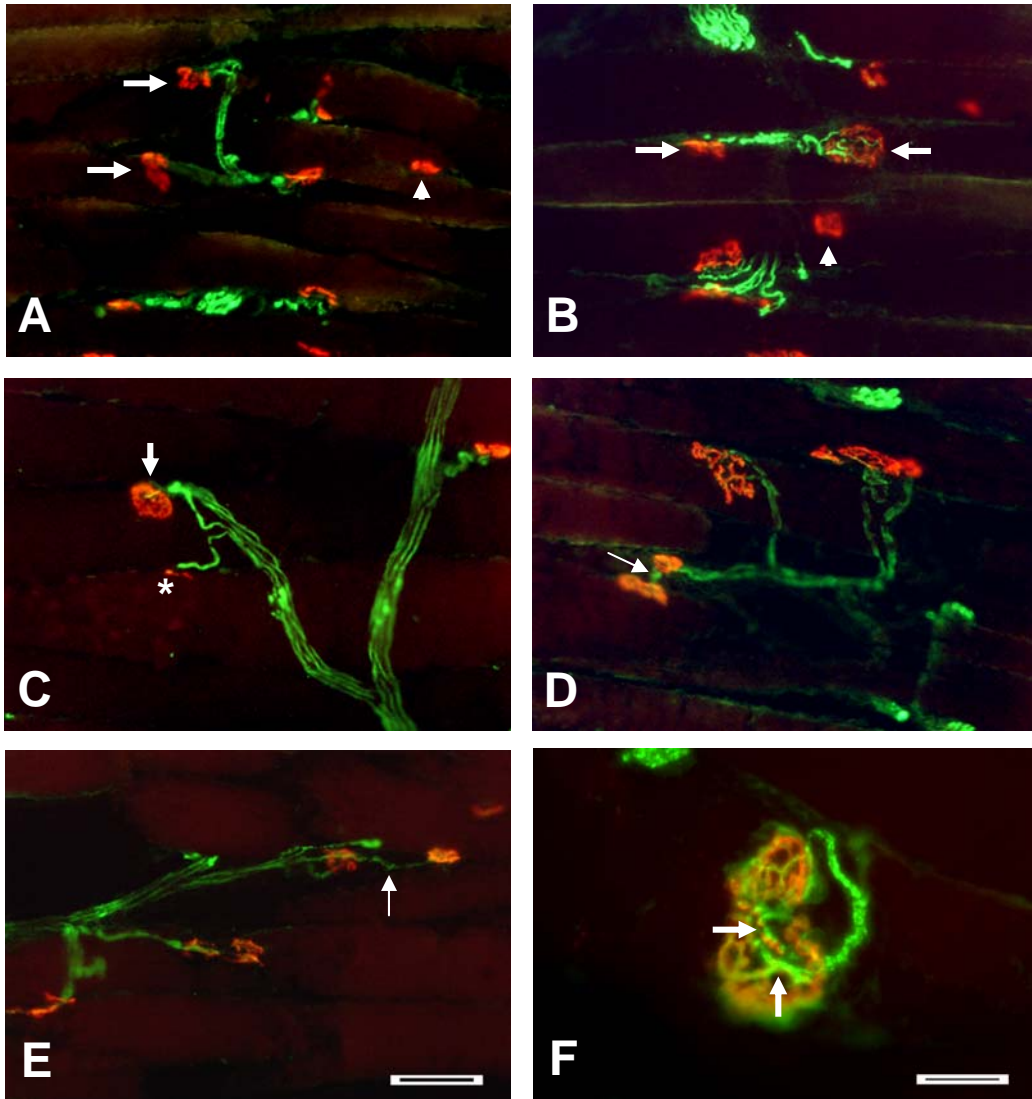
(A) Immunostained muscle sections from the right reinnervated SM. (B) Muscle sections from the left control SM. The nerve fascicles and axons were darkly stained. (A'-B') The number and area fraction of the NF-positive axons were calculated by using ImageJ software. For this case, the right SM exhibited very muscle reinnervation as indicated by the mean axon count (283, 71% of the control) and the mean area (2.32; 80% of the control).

**Figure 9.** Reinnervation of the MEPs in the muscles reinnervated with NMEG-NMZ technique



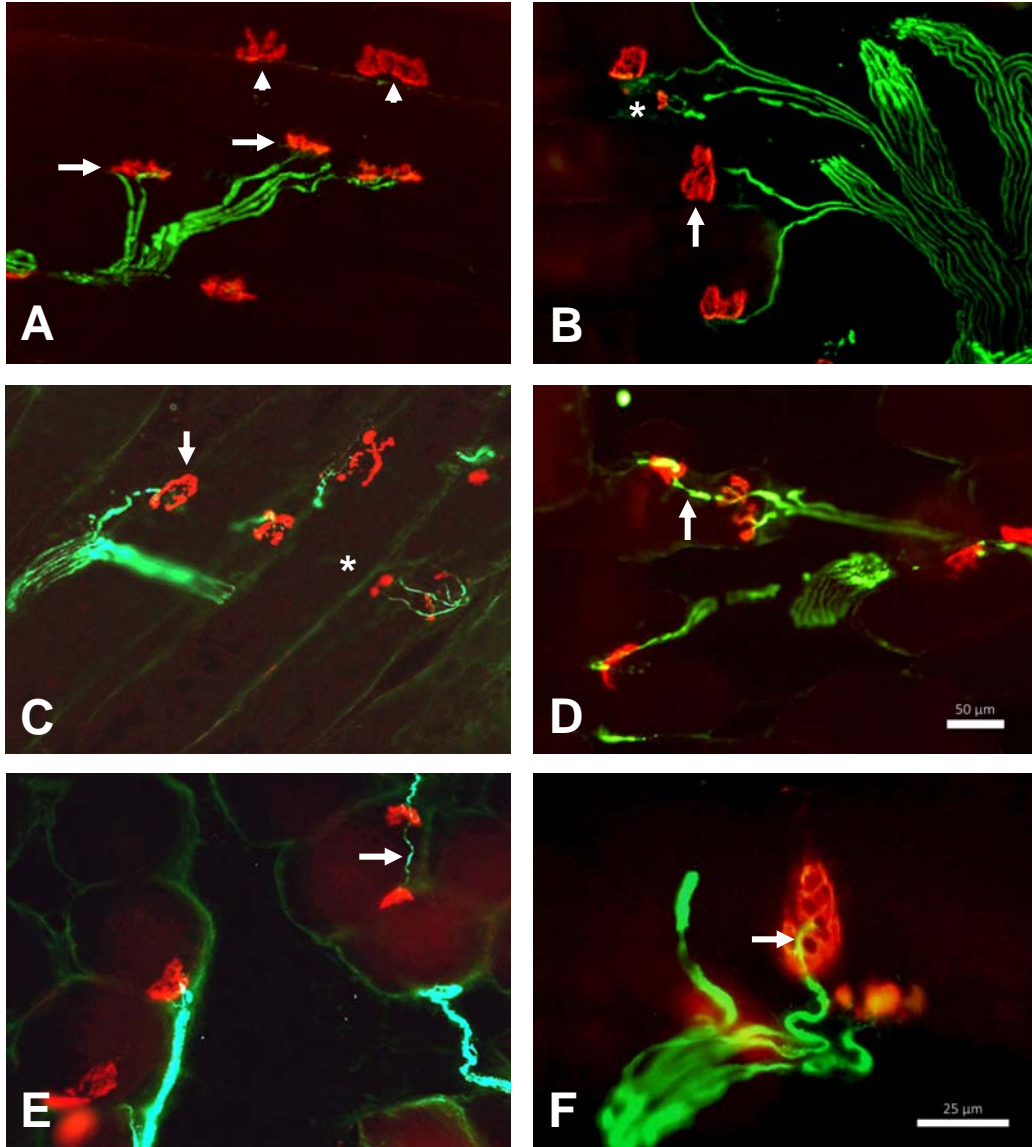
(A) Regenerated axons (green) branched extensively into fields of MEPs in the NMZ of the target muscle. (B-C) The majority of the MEPs in the treated muscle were reinnervated by regenerated axons (arrows), while some MEPs in the same muscle were unoccupied by regenerated axons (arrowheads).

**Figure 10.** Reinnervation of the MEPs in the right SM muscle of a rat cotreated with NMEG-NMZ and intraoperative brief ES



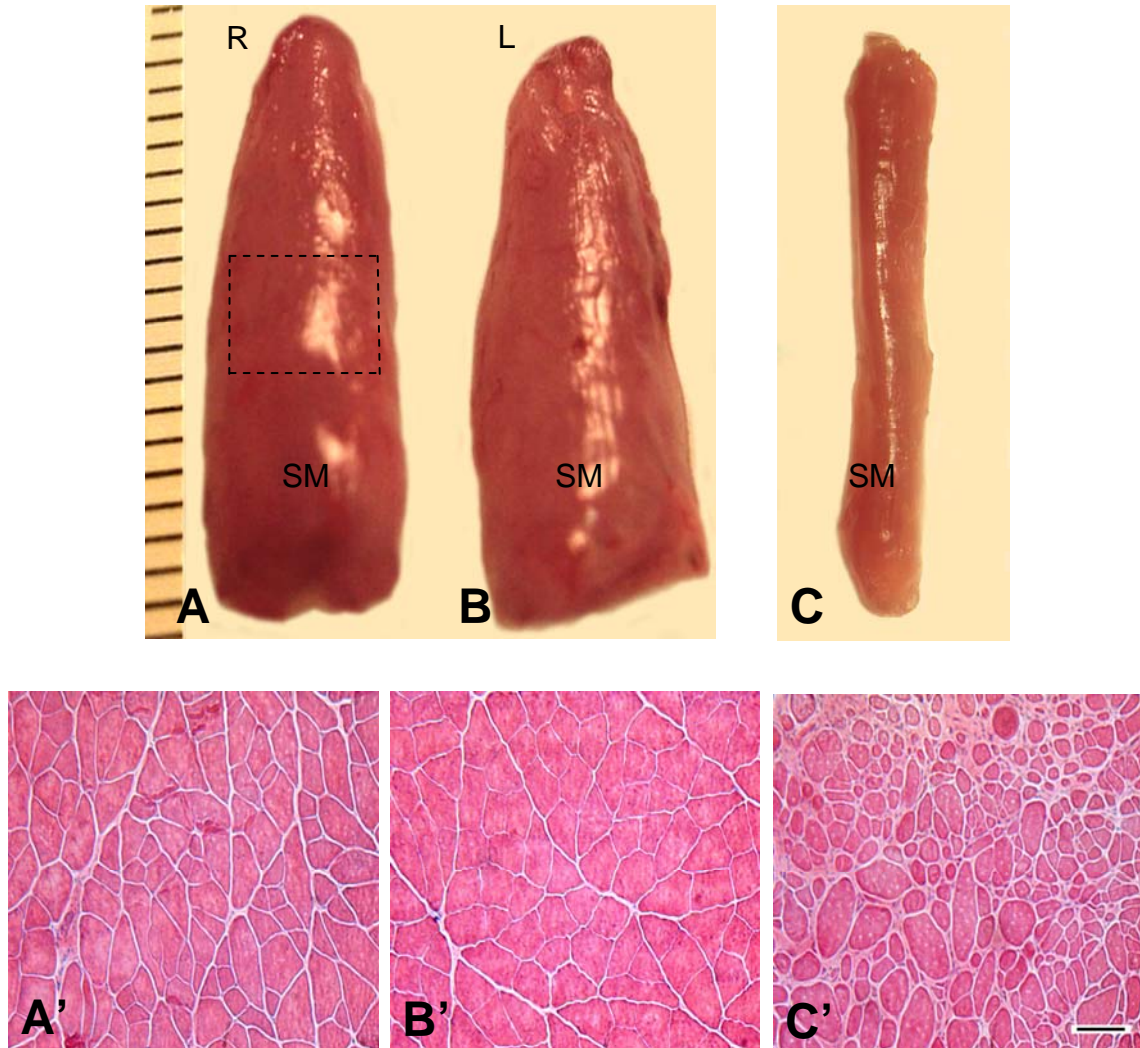
(A-B) Images showing innervated (arrows) and non-innervated (arrowheads) MEPs . (C) An image showing small newly-formed MEPs (asterisks). (D-E) Images showing ultraterminal sprouts (arrows). Bar = 100  $\mu$ m for A through E. (F) Close-up photograph of an innervated MEP, showing terminal axons (arrows, green) and acetylcholine receptors (red) at the MEP. Bar = 50  $\mu$ m.

**Figure 11.** Reinnervation of the MEPs in the right SM muscle cotreated with NMEG-NMZ and NGF/FGF-2



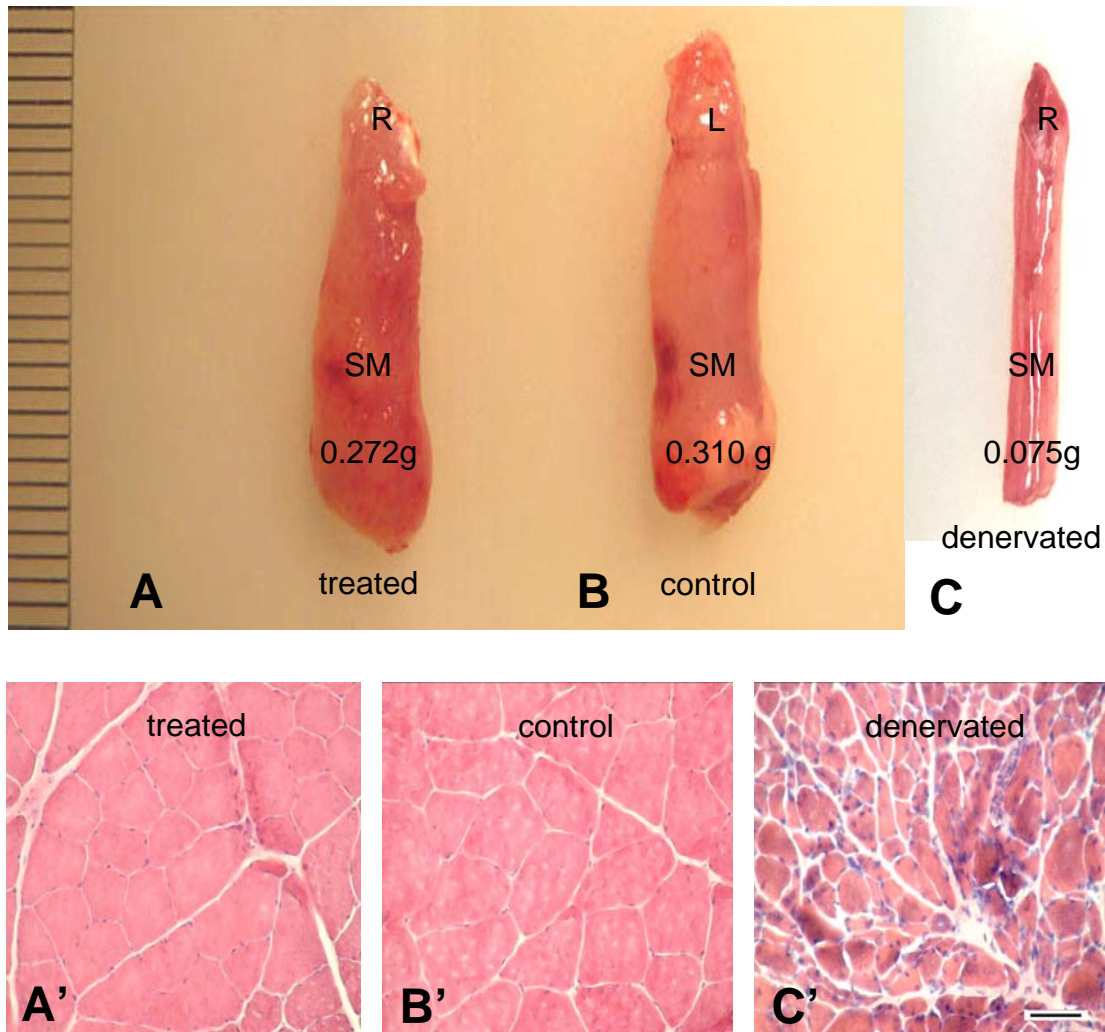
(A) Photomicrographs of the immunostained sections from right treated SM of a rat, showing innervated (arrows) and non-innervated (arrowheads) MEPs. (B-C) Images showing small, newly-formed MEPs (asterisks). (D-E) Images showing ultraterminal sprouts (arrows). (F) Close-up photograph of innervated MEPs, showing terminal axons (arrow, green) and acetylcholine receptors (red) at the MEPs.

**Figure 12.** Muscle mass and myofiber morphology of the NMEG-NMZ reinnervated SM muscle



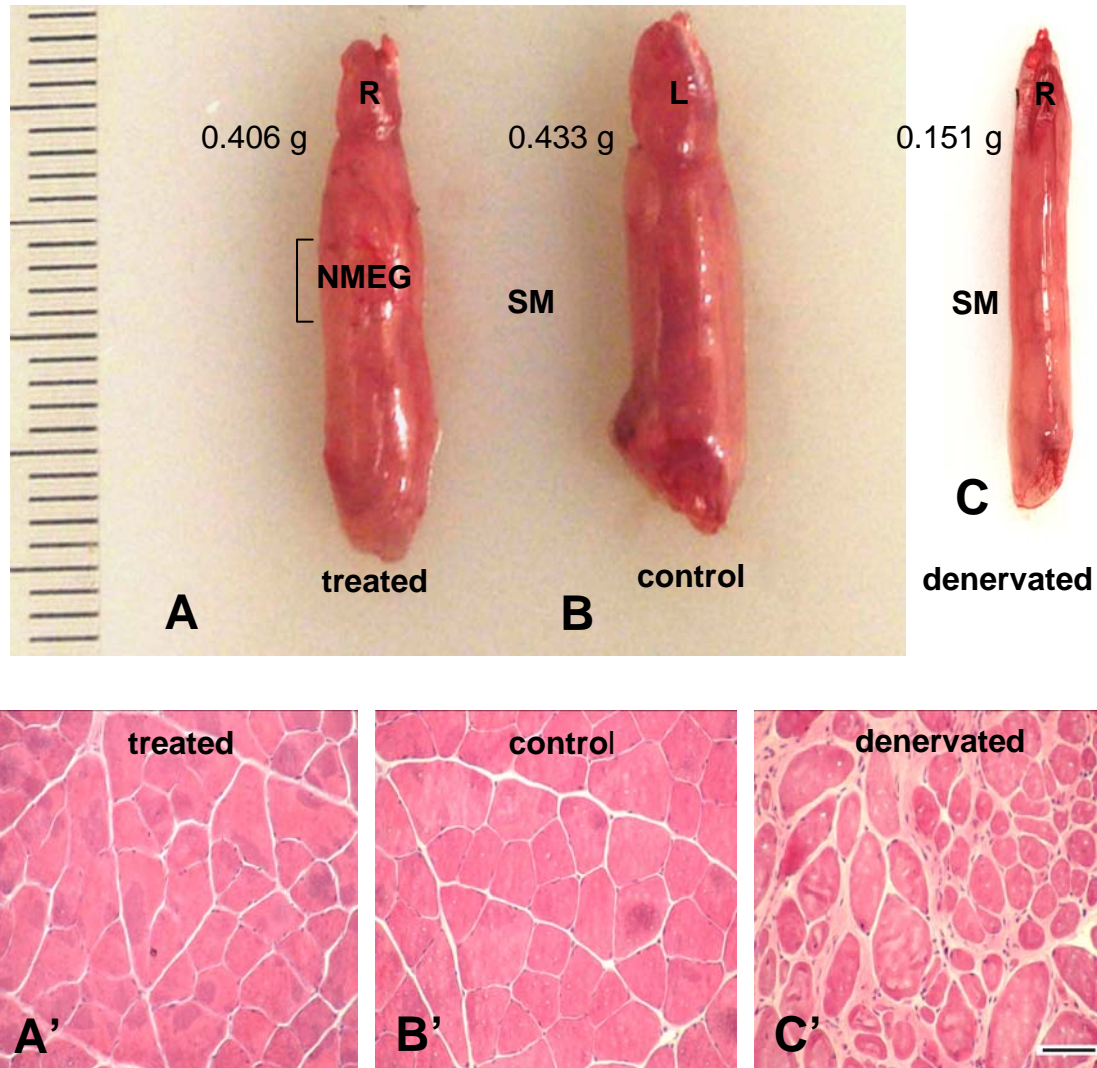
(A) A 3-month NMEG-NMZ reinnervated SM muscle. (B) A contralateral control. Note that the mass of the right (R) reinnervated SM muscle was close to that of the left (L) control muscle. The boxed region in the right SM is the location of the implanted NMEG. (C) A 3-month denervated SM muscle. (A'-C') H&E stained transverse sections from the reinnervated, control, and denervated SM muscles, respectively. Note that NMEG-NMZ reinnervated SM (A') exhibited very good preservation of muscle structure and myofiber morphology with less fiber atrophy as compared with the control (B') and denervated (C') muscles. Bar = 100 $\mu$ m for A' through C'.

**Figure 13.** Muscle mass and myofiber morphology of the SM cotreated with NMEG-NMZ and intraoperative brief ES



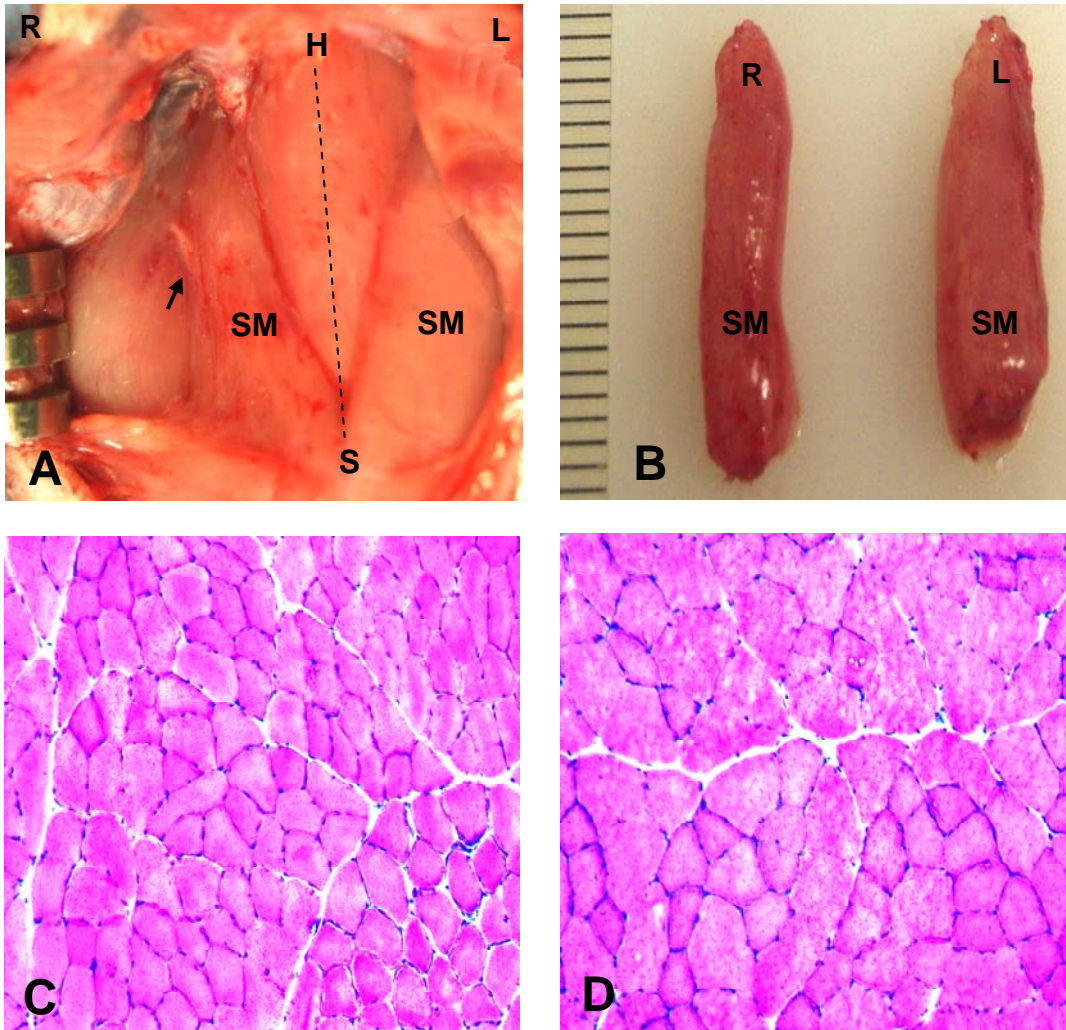
(**A**) A SM muscle 3 months after NMEG-NMZ/ES treatment. (**B**) A contralateral control. Note that the mass of the right (R) treated SM muscle was close to that of the left (L) control muscle. (**C**) A SM muscle denervated for 3 months. (**A'**-**C'**) H&E-stained transverse sections from the treated, control, and denervated SM muscles, respectively. Note that the SM muscle cotreated with NMEG-NMZ and brief ES (**A'**) exhibited very good preservation of muscle structure and myofiber morphology with less fiber atrophy as compared with the control (**B'**) and denervated (**C'**) muscles. Bar = 100  $\mu$ m for A' through C'.

**Figure 14.** Muscle mass and myofiber morphology of the SM cotreated with NMEG-NMZ and focal application of NGF/FGF-2



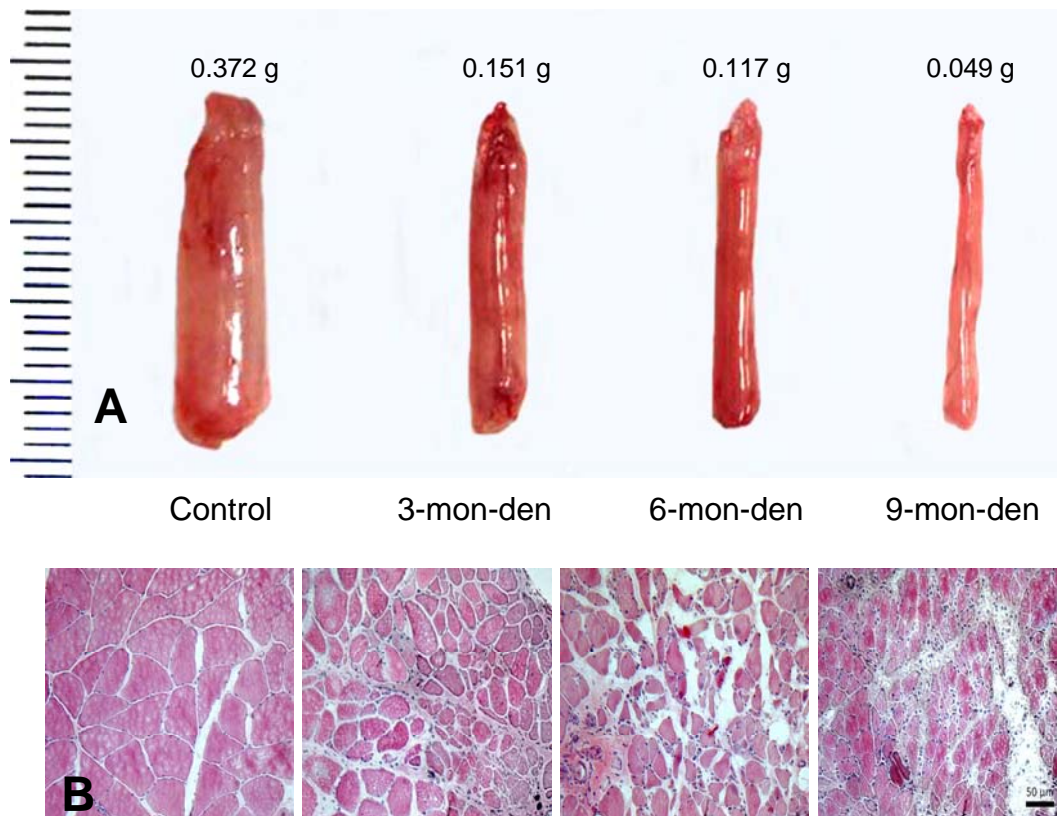
Images from a SM muscle cotreated with NMEG-NMZ and focal application of NGF/FGF-2 for 3 months (**A**), a contralateral control SM (**B**), and a 3-month denervated SM (**C**). Note that the mass of the right (R) treated SM muscle was close to that of the left (L) control muscle. (**A'**-**C'**) Muscle sections stained with H&E staining showed that the treated SM (**A'**) exhibited very good preservation of muscle structure and myofiber morphology with less fiber atrophy as compared with the control (**B'**) and denervated (**C'**) SM muscles. Bar = 100  $\mu$ m for **A'** through **C'**.

**Figure 15.** Muscle mass and myofiber morphology of the SM reinnervated with DNI-NMZ



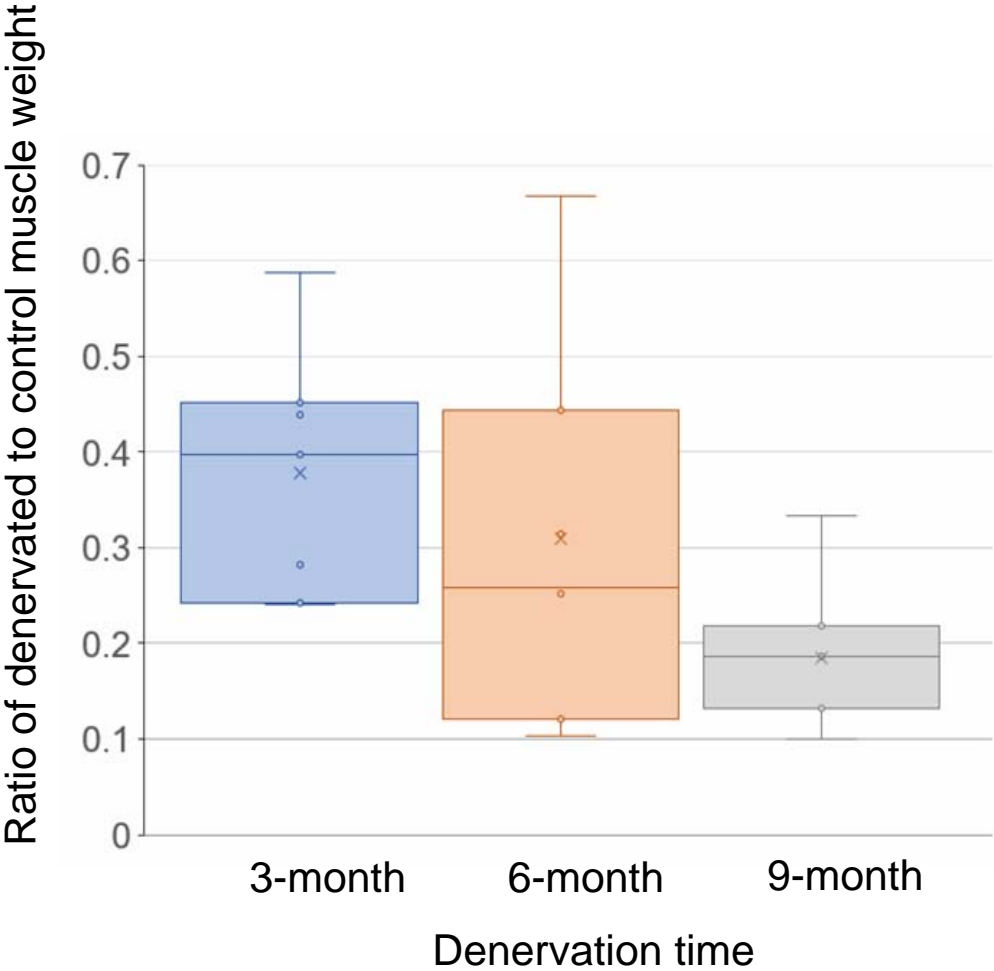
Images of a pair of SM muscles removed from a rat 3 months after DNI-NMZ surgery. (A) An image taken before removal of the SM muscles, showing the implanted SM nerve (arrow). (B) Removed SM muscles from the same animal in A. Note that the mass of the right (R) operated SM muscle (0.312 g) was smaller as compared with that of the left (L) control muscle (0.390 g). (C-D) H&E-stained cross sections from the SM muscles in B. Note that the right reinnervated SM muscle (C) exhibited mild to moderate myofiber atrophy as compared with the control (D). Initial magnification 200x for C and D.

**Figure 16.** Muscle mass and fiber morphology of the long-term denervated and control SM muscles



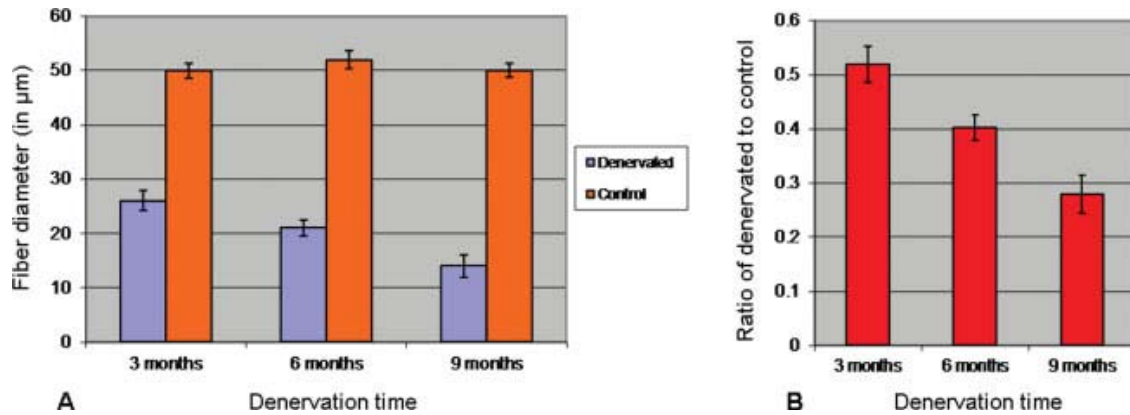
**(A)** Photographs of the removed control SM and denervated SM muscles, showing a progressive decline in muscle mass with denervation time. **(B)** Sections stained with H&E staining from the control and denervated SM muscles, showing a progressive reduction in fiber size of the denervated SM. 3-mon-den, 3-month-denervation; 6-mon-den, 6-month-denervation; 9-mon-den, 9-month-denervation.

**Figure 17.** Box plots showing the distribution of SM muscle weight ratios (denervated to control) in 3-month, 6-month, and 9-month denervation groups



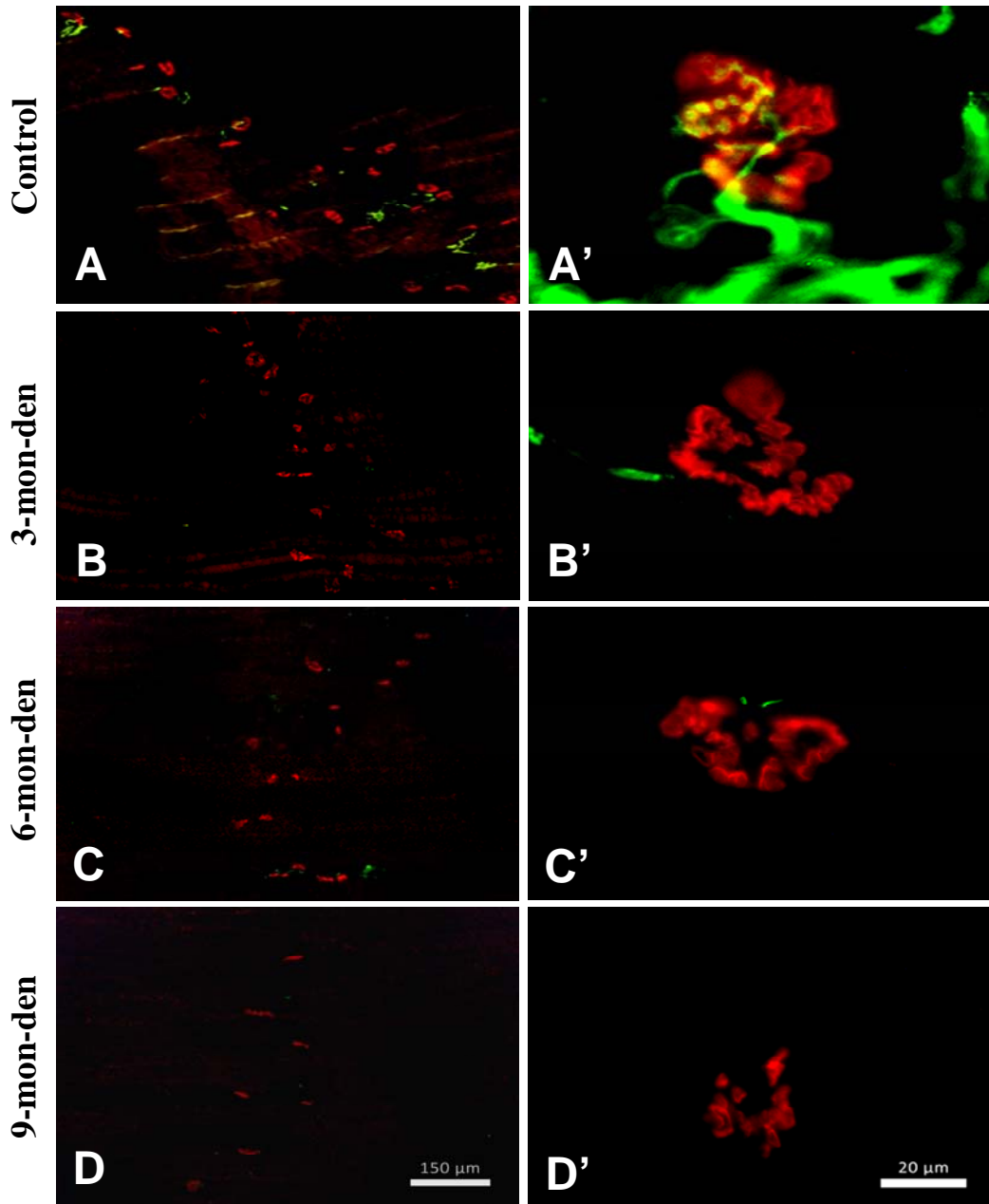
Note that median ratio is the largest in 3-month group (0.40) and decreases with length of denervation time to 0.26 in 6-month group and finally to 0.19 in the 9-month group.

**Figure 18.** Comparison of fiber diameters of the long-term denervated and control SM muscles



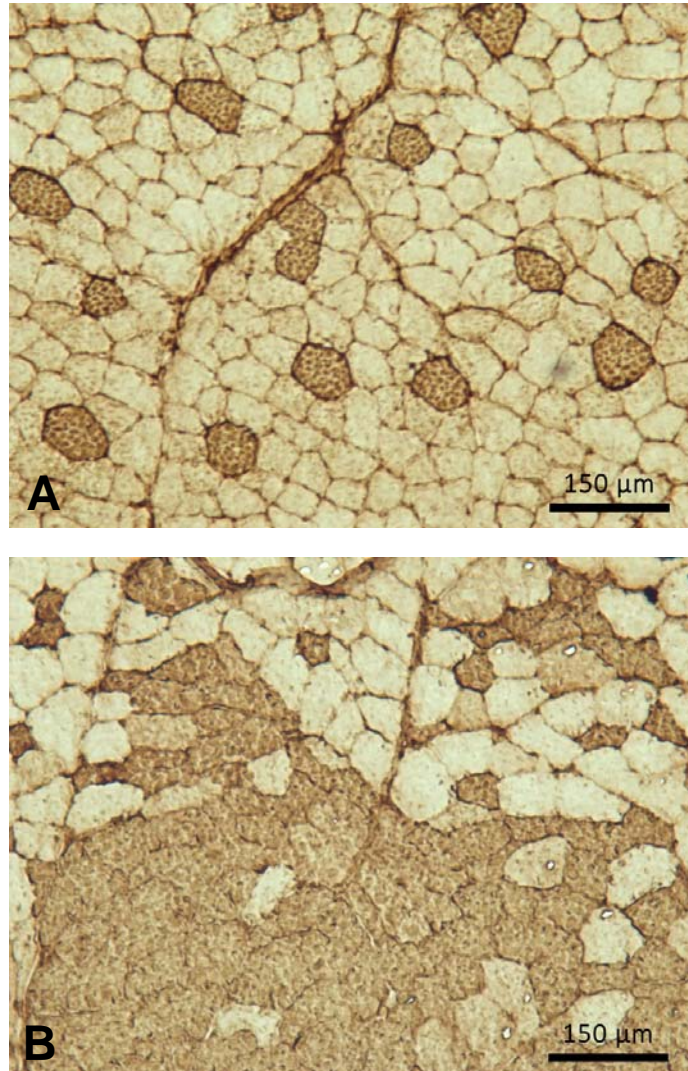
(A) Distribution of mean fiber diameters of the denervated and control SM muscles. (B) Ratio of the mean fiber size of the denervated to control muscles. Note that the fiber diameters of the denervated muscles are reduced progressively with denervation time. Vertical bars represent standard error.

**Figure 19.** Images showing alterations of the axons and MEPs in the long-term denervated SM muscles



Immunofluorescence labeling of axons (green) and MEPs (red) in the normal (A–A') and denervated (B–D') SM muscles. The low-magnification images (left column) show progressive reduction in the number of the MEPs, whereas the high-magnification images (right column) show alterations in acetylcholine receptor clusters in the denervated SM muscles. 3-mon-den, 3-month denervation; 6-mon-den, 6-month denervation; 9-mon-den, 9-month denervation.

**Figure 20.** Fiber type grouping identified in the denervated SM muscles



Immunostained cross sections from a control SM (**A**) and a 3-month denervated SM (**B**). The sections were stained with monoclonal antibody NOQ7-5-4D against type I MyHC. Type I fibers were stained dark. Type I grouping is identified in the denervated muscle.

## List of Our Publications

**The following 5 attached articles are derived from our currently completed research funded by DOD**

W81XWH-14-1-0442

Mu, Liancai (PI)

09/15/2014-09/14/2018

DOD

Reinnervation of Paralyzed Muscle by Nerve-Muscle-Endplate Band Grafting (NMEG)

The goal of this research is to assess the efficacy of our modified NMEG technique for muscle reinnervation in a rat neck muscle model. The NMEG pedicle was harvested from a noncritical muscle and implanted to the native motor zone (NMZ) of a denervated muscle.

1. Mu L, Sobotka S, Chen J, Nyirenda T. Reinnervation of denervated muscle by implantation of nerve-muscle-endplate band graft to the native motor zone of the target muscle. *Brain Behav* 7(6):e00668. doi:10.1002/brb3.668, 2017.
2. Sobotka S, Chen J, Nyirenda T, Mu L. Intraoperative one-hour electrical nerve stimulation enhances outcomes of nerve-muscle-endplate band grafting technique for muscle reinnervation. *J Reconstr Microsurg* 33:533-543, 2017.
3. Sobotka S, Chen J, Nyirenda T, Mu L. Outcomes of muscle reinnervation with direct nerve implantation into the native motor zone of the target muscle. *J Reconstr Microsurg* 33:77-86, 2017.
4. Mu L, Sobotka S, Chen J, Nyirenda T. Nerve growth factor and basic fibroblast growth factor promote reinnervation by nerve-muscle-endplate grafting. *Muscle Nerve* 57:449-459, 2018.
5. Mu L, Chen J, Li J, Nyirenda T, Fowkes M, Sobotka S. Immunohistochemical detection of motor endplates in the long-term denervated muscle. *J Reconstr Microsurg* 34:348-358, 2018.

**ORIGINAL RESEARCH**

# Reinnervation of denervated muscle by implantation of nerve-muscle-endplate band graft to the native motor zone of the target muscle

Liancai Mu<sup>1</sup>  | Stanislaw Sobotka<sup>1,2</sup> | Jingming Chen<sup>1</sup> | Themba Nyirenda<sup>1</sup>

<sup>1</sup>Department of Research, Hackensack University Medical Center, Hackensack, NJ, USA

<sup>2</sup>Department of Neurosurgery, Icahn School of Medicine at Mount Sinai, New York, NY, USA

**Correspondence**

Liancai Mu, Department of Research, Hackensack University Medical Center, Hackensack, NJ, USA.  
Email: lmu@hackensackumc.org

**Funding information**

Office of the Assistant Secretary of Defense for Health Affairs, Grant/Award Number: W81XWH-14-1-0442

**Abstract**

**Introduction:** Motor endplate reinnervation is critical for restoring motor function of the denervated muscle. We developed a novel surgical technique called nerve-muscle-endplate band grafting (NMEG) for muscle reinnervation.

**Methods:** Experimentally denervated sternomastoid muscle in the rat was reinnervated by transferring a NMEG from the ipsilateral sternohyoid muscle to the native motor zone (NMZ) of the target muscle. A NMEG pedicle contained a block of muscle (~ 6 × 6 × 3 mm), a nerve branch with axon terminals, and a motor endplate band with numerous neuromuscular junctions. At 3 months after surgery, maximal tetanic muscle force measurement, muscle mass and myofiber morphology, motoneurons, regenerated axons, and axon-endplate connections of the muscles were analyzed.

**Results:** The mean force of the reinnervated muscles was 82% of the contralateral controls. The average weight of the treated muscles was 89% of the controls. The reinnervated muscles exhibited extensive axonal regeneration. Specifically, the mean count of the regenerated axons in the reinnervated muscles reached up to 76.8% of the controls. The majority (80%) of the denervated endplates in the target muscle regained motor innervation.

**Conclusions:** The NMZ of the denervated muscle is an ideal site for NMEG implantation and for the development of new microsurgical and therapeutic strategies to achieve sufficient axonal regeneration, rapid endplate reinnervation, and optimal functional recovery. NMEG-NMZ technique may become a useful tool in the treatment of muscle paralysis caused by peripheral nerve injuries in certain clinical situations.

**KEYWORDS**

motor endplate, muscle force measurement, muscle reinnervation, native motor zone, nerve regeneration, nerve-muscle-endplate band grafting, peripheral nerve injury

## 1 | INTRODUCTION

Traumatic peripheral nerve injuries (PNIs) to the head/neck and extremity are a significant cause of morbidity and disability in both

military and civil circumstances today (Brininger, Antczak, & Breland, 2008; Eser, Aktekin, Bodur, & Atan, 2009; Kretschmer, Antoniadis, Braun, Rath, & Richter, 2001; Noble, Munro, Prasad, & Midha, 1998). There are 200,000 and 300,000 cases with PNIs in the United States

This is an open access article under the terms of the Creative Commons Attribution License, which permits use, distribution and reproduction in any medium, provided the original work is properly cited.

© 2017 The Authors. *Brain and Behavior* published by Wiley Periodicals, Inc.

and Europe, respectively, each year (Ichihara, Inada, & Nakamura, 2008; Wiberg & Terenghi, 2003). Approximately, 100,000 patients undergo peripheral nerve surgery in the United States and Europe annually (Kelsey, Praemer, Nelson, Felberg, & Rice, 1997). In the past decades, multiple techniques such as nerve end-to-end anastomosis (EEA), end-to-side neurorrhaphy, nerve grafting, nerve transfer, muscular neurotization, tubulization techniques, and many others have been developed for the reinnervation of denervated muscles (McAllister, Gilbert, Calder, & Smith, 1996; de Medinaceli, Prayon, & Merle, 1993; Siemionow & Brzezicki, 2009). However, the currently available methods result in poor muscle reinnervation and functional recovery. For example, EEA is commonly used when the two stumps of an injured nerve can be approximated without tension. Unfortunately, only about 50% of patients regain useful function (Lee & Wolfe, 2000; Wong & Crumley, 1995). Factors behind poor functional recovery include tension of the anastomosis, neuroma formation, scarring, and loss of the nerve fiber population (Green, Berke, & Graves, 1991). Studies have shown that in EEA, fewer nerve fibers could pass through the coaptation site and reach the target muscle (Mykатыn & Mackinnon, 2004). When a tension-free EEA is not technically possible, end-to-side neurorrhaphy is an alternative to repair an injured nerve when the proximal nerve stump is unavailable (Al-Qattan, 2001). The distal stump of an injured nerve is sutured to the side of an intact donor nerve. However, this procedure induces less axon regeneration and functional recovery compared to EEA (De Sa, Mazzer, Barbieri, & Barriera, 2004; Sanapanich, Morrison, & Messina, 2002).

A significant nerve defect is a common clinical situation. At present, autologous nerve grafts, nerve transfers, and tubulization techniques with natural or artificial conduits are used for nerve-gap repair. Unfortunately, nerve grafting has been associated with poor functional outcomes when there is a long distance from the level of the injury to the target muscle. The recovery rate of motor function after autogenous nerve grafting is <40% (Moneim & Omer, 1998). *Tubulization* techniques are feasible only in short nerve gaps. If the gap exceeds 1.0–1.5 cm, regeneration is poor. Longer defects (4.0–6.0 cm) result in useful reinnervation in only 13% of cases with reconstruction of upper extremity PNIs with conduits (Merle, Dellon, Campbell, & Chang, 1989; Stanec & Stanec, 1998). For the PNIs in which the proximal nerve stump is unavailable, nerve transfer is an option. Nerve transfer is the surgical coaptation of a healthy nerve donor to a denervated nerve. A nerve branch that innervates expendable muscles can be used to repair a functionally more important distal stump of an injured nerve. Many nerve-to-nerve transfers have been employed to repair the injured nerves in the hand and upper extremity with mixed results (Lee & Wolfe, 2012). In some cases, nerve repair or nerve-grafting procedures are inapplicable because of the lack of a nerve stump. In this situation, direct nerve implantation or muscular neurotization may be used (Brunelli & Brunelli, 1980, 1993). In neurotization, the proximal stump of the original nerve or a healthy but less valuable foreign motor nerve is implanted into the target muscle to reinnervate a more important motor territory that has lost its innervation through irreparable damage to its nerve.

More recently, we have developed a new reinnervation technique called “nerve-muscle-endplate band grafting (NMEG)” (Mu, Sobotka,

& Su, 2011). The development of the NMEG procedure for muscle reinnervation is based on the idea that a paralyzed muscle could be reinnervated by transferring a NMEG from a neighboring donor muscle. A healthy endplate band with a nerve branch and terminals that innervates an expendable muscle can be transplanted to a more functionally important denervated muscle for restoring its motor function. Over the past years, we have studied the NMEG technique by determining innervation patterns (Mu et al., 2011; Zhang, Mu, Su, & Sobotka, 2011) and contractile properties of the rat recipient and donor muscles (Sobotka & Mu, 2010), and conducted surgical feasibility studies and a series of reinnervation experiments using the NMEG technique and conventional EEA in a rat model (Mu et al., 2011; Sobotka & Mu, 2011, 2013a,b, 2015). Several lines of evidence from a number of quantitative analyses demonstrated that the NMEG procedure results in encouraging functional recovery (67% of the control) (Mu et al., 2011). However, entire muscle reinnervation and complete functional recovery was not achieved. We found that approximately one-third of the distal myofibers in the target muscle were not reinnervated 3 months after surgery (Mu et al., 2011; Sobotka & Mu, 2015). These findings suggest that partial muscle reinnervation accounts for incomplete functional recovery. We assumed that implantation site of the NMEG would be a critical factor influencing outcomes. In our previous studies, a NMEG was implanted into an aneural region in the recipient muscle. In this case, regenerating axons from the NMEG pedicle may need more time to reach the most distal muscle fibers and form new motor endplates (MEPs).

The purpose of this study was to test our hypothesis that optimal outcomes may be achieved by implanting the NMEG into the NMZ in the target muscle, as such a procedure (NMEG-NMZ) could reduce nerve regeneration distances and facilitate rapid MEP reinnervation. At 3 months after surgery, maximal tetanic force measurement, muscle mass and myofiber morphology, motoneurons, regenerated axons, and axon-endplate connections of the reinnervated muscles were analyzed and compared with those of the contralateral controls.

## 2 | MATERIALS AND METHODS

### 2.1 | Animals

Thirty-two adult female Sprague-Dawley rats (Taconic Laboratories, Cranbury, NJ, USA), weighing 200–250 g, were used. The animal experiments were reviewed and approved by the Institutional Animal Care and Use Committee. All animals were handled in accordance with the Guide for Care and Use of Laboratory Animals published by the US National Institutes of Health (NIH publication no. 85–23, revised 1996). The animals were kept in a 22°C environment in a 12:12-hour light–dark cycle, with food and water ad libitum. The rats were individually housed in standard cages in the state-of-the-art animal housing facilities of Hackensack University Medical Center.

### 2.2 | Surgical procedures

Thirty-two rats were randomly distributed into reinnervation ( $n = 15$ ) and denervation ( $n = 17$ ) groups. In this study, SH and SM muscles

were chosen to serve as a donor and recipient, respectively, because they were used in our previous studies (Mu et al., 2011; Sobotka & Mu, 2010, 2013b, 2015). On the day of the experiment, the rats were anesthetized via an intraperitoneal injection of a ketamine (80 mg/kg) and xylazine (5 mg/kg) mixture. With the rat supine, a midline cervical incision was made extending from the hyoid bone to the sternum to expose the right SM and SH muscles and their innervating nerves.

All the rats in both groups underwent denervation of the right SM muscle. With the aid of an Olympus SZX12 Stereo zoom surgical microscope (Olympus America Inc, Center Valley, PA, USA), the right SM

muscle was denervated by resecting a 5-mm segment of its innervating nerve and the cut ends of the nerve were then coagulated with a bipolar cautery to prevent nerve regeneration.

Immediately after muscle denervation, the rats in reinnervation group were subjected to NMEG-NMZ transplantation. First, the NMZs in the right SM and SH muscles were outlined according to the motor point (the entry point of the motor branch into the muscle) (Figure 1a and b). The NMZ of either SM or SH in the rat is located in the middle segment of the muscle that contains intramuscular nerve terminals and a MEP band as demonstrated by our previous studies (Mu

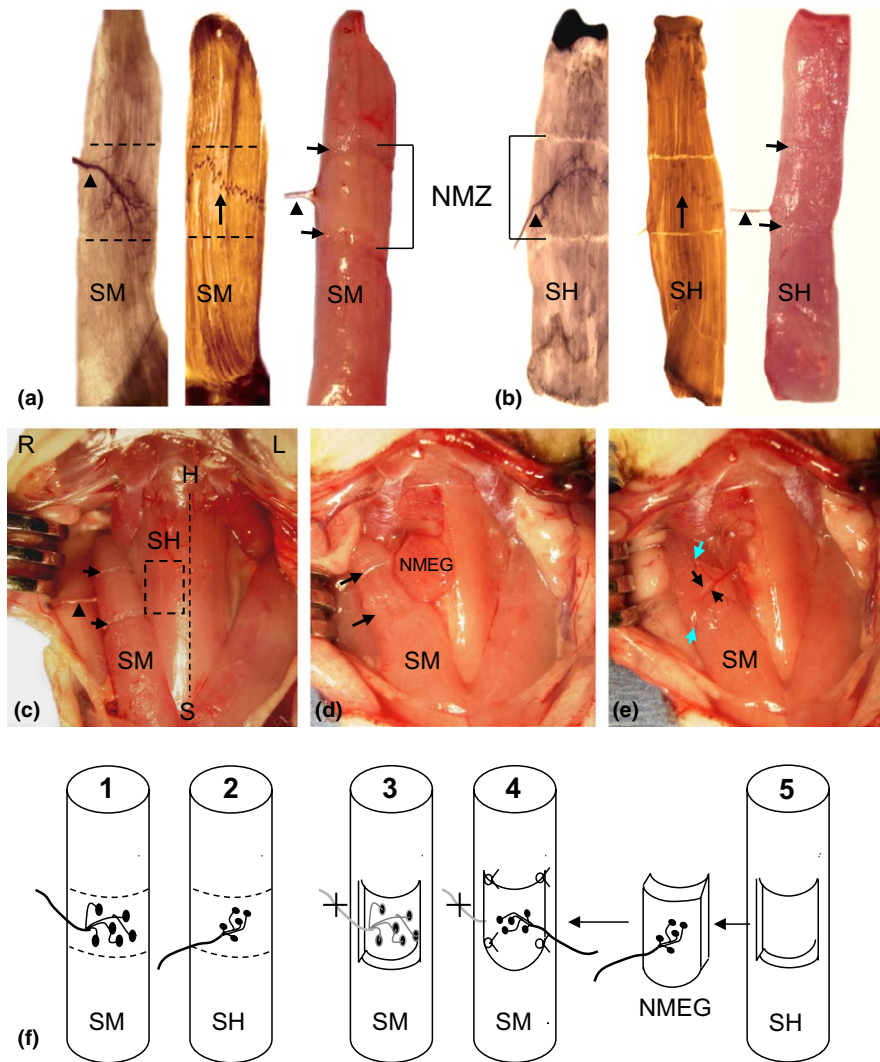


**FIGURE 1** Images showing the locations of native motor zones (NMZ) of the recipient sternomastoid (SM) and donor sternohyoid (SH) muscles of the rat and surgical procedures for NMEG-NMZ transplantation. (a) Stained and fresh right SM showing the NMZ of the muscle (outlined region). SM nerve (arrowhead) and its intramuscular nerve terminals were mapped out with Shiner's stain (left image), whereas the motor endplate (MEP) band (arrow in the middle image) was visualized with whole mount acetylcholinesterase (AChE) staining. A fresh SM (right image) illustrated the NMZ outlined during surgery (between fiber cuts on the surface of the muscle as indicated by arrows and bracket). (b) Stained and fresh right SH showing that the NMZ of the SH is also located in the middle of the muscle. (c) A photograph from a rat during surgery, showing surgically outlined NMZ in the recipient SM (between fiber cuts as indicated by arrows) and in the donor SH (boxed region). The arrowhead indicates the SM nerve. The dashed line indicates the midline between both SH muscles. H = hyoid bone; L = left; R = right; S = sternum. (d) A NMEG pedicle was harvested from the NMZ of the right SH and a muscular defect (between arrows) was made on the SM muscle. (e) The NMEG was implanted into the recipient bed and sutured (green arrows). The SH nerve branch (large black arrow) and its accompanying blood vessels (small black arrow) can be seen on the implanted NMEG. (f) Schematic illustrations summarize the surgical procedures by localizing the NMZs of the SM (F1) and SH (F2), denervating the SM and creating a muscular defect in the NMZ of the muscle (F3), and suturing the NMEG pedicle (F4) harvested from the SH (F5)

et al., 2011; Zhang et al., 2011). Second, a muscular defect (recipient bed) with the same dimensions as the NMEG pedicle was made in the NMZ of the right denervated SM muscle (Figure 1c and d). Third, a NMEG pedicle was harvested from the NMZ of the right SH donor muscle as described in our previous publication (Mu et al., 2011). Briefly, the SH nerve branch was identified on the lateral margin of the NMZ of the muscle. A NMEG pedicle containing a block of muscle (~6 × 6 × 3 mm), axon terminals, and a MEP band with numerous neuromuscular junctions was outlined and harvested from the SH muscle in continuity with its pedicle of motor nerve branch and feeding vessels (Figure 1e). A functioning NMEG was confirmed by observing its twitch contractions on nerve stimulation. Fourth, the superficial muscle fibers on the ventral aspect of the NMEG pedicle were removed to create a denuded surface for better neural regeneration. Finally, the well-prepared NMEG was embedded in the SM muscle defect and sutured with four to six 10-0 nylon microsutures (Figure 1e). Thus, the denervated SM muscle was reinnervated with NMEG-NMZ technique. Figure 1f summarizes the surgical procedures for NMEG-NMZ implantation. After surgery, the wound was closed in layers with interrupted simple sutures of 4-0 prolene.

## 2.3 | Postoperative evaluations

At the end of the 3-month recovery period, outcomes of the NMEG-NMZ technique was evaluated functionally and histochemically. The removed SM muscles from the rats in the reinnervation and denervation groups were analyzed using histological and immunohistochemical methods.

### 2.3.1 | Determining the degree of functional recovery

Maximal tetanic force measurement was used to evaluate the functionality of the NMEG-NMZ reinnervated muscles. The force was measured on the experimental and the contralateral control side and expressed in percentage of the control side. Muscle force measurement is a useful approach to assess the mechanical function and contractile properties of a muscle (van der Meulen, Urbanek, Cederna, Eguchi, & Kuzon, 2003; Yoshimura et al., 2002). Our studies (Mu et al., 2011; Sobotka & Mu, 2011, 2013a,b, 2015) and others' (Goding, Cummings, & Bright, 1989; Marie et al., 1999; Meikle, Trachy, & Cummings, 1987) used force measurement to detect the degree of functional recovery of the reinnervated cervical strap muscles. The details regarding the force measurement of the rat SM muscle have been given in our publications (Mu et al., 2011; Sobotka & Mu, 2010, 2011, 2013a,b, 2015). Briefly, the right reinnervated and the left control SM muscles in each animal were exposed and dissected free from the surrounding tissues. The rostral tendon of each muscle was severed close to the insertion, tied with a 2-0 suture, and attached to a servomotor lever arm (model 305B Dual-Mode Lever Arm System; Aurora Scientific Inc, Aurora, Ontario, Canada). Muscle force of the right reinnervated SM was measured by stimulating the SH nerve branch supplying the NMEG, whereas that of the left control

muscle was measured by stimulating the intact SM nerve. Each of the nerves was identified, isolated, and draped over a bipolar stimulating electrode for nerve stimulation. Trains of biphasic rectangular pulses of different current were delivered to the stimulated nerve using our stimulation and recording system that is built based on a multifunction National Instruments Acquisition Board (National Instruments Corp, Austin, TX, USA) and is controlled by user-written LabVIEW software (National Instruments Corp).

Isometric contraction of the SM muscle was produced with 200-millisecond trains of biphasic rectangular pulses. The duration of each phase of stimulation pulse was set at 0.2 milliseconds and the train frequency was set at 200 pulses per second. The stimulation current was gradually increased until the tetanic force reached a plateau. A break of at least 1 min was taken between two stimulations. The maximum value of muscle force during the 200-millisecond contraction was identified, as well as initial passive tension before stimulation. The difference between the maximal active force and the preloaded passive force was used as the muscle force measurement. The force generated by the contraction of the SM muscle was transduced with the servomotor of a 305B lever system and displayed on a computer screen. At the moment of force measurement, the lever arm was stationary, and the muscle was adjusted to the optimal length for the development of maximum force. During the experiment, the animal was placed supine on a heating pad (homoeothermic blanket system; Stoelting, Wood Dale, IL, USA). The core body temperature was monitored with a rectal thermistor and maintained at 36°C. The muscle and nerve examined were bathed regularly with warmed mineral oil throughout the testing to maintain muscle temperature between 35°C and 36°C.

The force data were obtained and processed by an acquisition system built from a multifunction I/O National Instruments Acquisition Board (NI USB 6251; 16 bit, 1.25 Ms/s; National Instruments) connected to a Dell laptop with a custom-written program using LabVIEW 8.2 software. The system produced stimulation pulses, which, after isolation from the ground through an optical isolation unit (Analog Stimulus Isolator model 2200; AM Systems, Inc, Carlsborg, Washington, DC, USA), were used for the current controlled nerve stimulation. The acquisition system was also used to control muscle length and to collect a muscle force signal from the 305B Dual-Mode Lever System. Collected data were analyzed offline with DIAdem 11.0 software (National Instruments).

### 2.3.2 | Tracking the origin of the axons in the SM muscles reinnervated with NMEG-NMZ technique

Immediately after tetanic tension measurements, five experimental animals were subjected to retrograde horseradish peroxidase (HRP) neuronal labeling to track the origin of the axons innervating the reinnervated SM muscles. As the NMEG was harvested from the right SH muscle and transplanted into the denervated right SM muscle, the HRP injected into the right SM should label SH motoneurons if muscle reinnervation was successful. The details regarding HRP labeling have been given in our previous publications (Mu et al., 2011;

Zhang et al., 2011). Briefly, 30% HRP (type VI A; Sigma Chemical, St. Louis, MO, USA) solution was injected at two points (5  $\mu$ l per point) into the MEP band in the right reinnervated SM and the left SH (control) with Hamilton microsyringe. After a survival time of 48 h, the animals were deeply anesthetized with sodium pentobarbital (60 mg/kg intraperitoneally) and perfused transcardially with 200 ml of a fixative solution containing 1% paraformaldehyde, 1.25% glutaraldehyde, and 3% dextrose in 0.1 mol/L phosphate buffer at pH 7.4 and 4°C. After perfusion, the fixed lower medulla oblongata and cervical spinal cord (C1-C4) were dissected out, postfixed 4 hr at 4°C in the same fixative, and then stored in graded concentrations (10% and 25%) of phosphate-buffered sucrose solution at pH 7.4 and 4°C for 2 hr and overnight, respectively. The fixed medulla and upper cervical spinal cord were frozen and sectioned at 40  $\mu$ m on a cryostat in the transverse plane. The sections were reacted for 20 min in the dark with 3,3',5,5'-tetramethylbenzidine as the chromogen to develop the HRP reaction product. The processed sections were mounted on gelatin-coated slides and counterstained with 1% aqueous neutral red (pH 4.8).

The stained serial sections were examined under a Zeiss photomicroscope (Axiophot-2; Carl Zeiss, Goettingen, Germany) and photographed with a digital camera (Spot-32; Diagnostic Instruments, Keene, NH, USA) attached to the photomicroscope. The distributions of the SM and SH motoneurons in the medulla oblongata and spinal cord were recorded to see if the right-treated SM was controlled by SH motoneurons.

### 2.3.3 | Examining muscle mass, implanted NMEG, and myofiber morphology

At the end of the experiments, SM muscles on both sides in each animal were removed, weighed, and photographed. A muscle mass ratio was calculated (muscle mass ratio = weight of reinnervated muscle/weight of contralateral muscle). Five NMEG-NMZ reinnervated right SM muscles were processed with Sihler's stain, a whole mount nerve mapping technique to see if the NMEG was precisely implanted into the NMZ of the target muscle. The details regarding Sihler's stain have been given in our previous publication (Mu & Sanders, 2010). Briefly, the removed muscles were fixed for 3 weeks in 10% unneutralized formalin; macerated for 2 weeks in 3% aqueous potassium hydroxide (KOH) solution; decalcified for 1 week in Sihler solution I (one volume glacial acetic acid, one volume glycerin, and six volumes 1% w/v aqueous chloral hydrate); stained for 3 weeks in Sihler solution II (one volume stock Ehrlich's hematoxylin, one volume glycerin, and six volumes 1% w/v aqueous chloral hydrate); destained for 3 hr in Sihler solution I; immersed for 1 hr in 0.05% w/v lithium carbonate solution to darken the nerves; cleared for 3 days in 50% v/v aqueous glycerin; and preserved for 4 weeks in 100% glycerin with a few thymol crystals for transparency. After transillumination by a xenon light source (model 610; Karl Storz, Endoscopy-America, Culver City, CA, USA), the stained muscles were dissected and photographed.

The removed SM muscles ( $n = 30$ ) from 10 rats with NMEG-NMZ reinnervation and five rats with denervation were sectioned

and stained using histological and immunohistochemical techniques. Each SM muscle was divided into three segments: rostral, middle, and caudal. The muscle segments were frozen in melting isopentane cooled with dry ice and cut on a cryostat (Reichert-Jung 1800; Mannheim, Germany) at  $-25^{\circ}\text{C}$ . The rostral and caudal segments were cut transversely and serial cross sections (10  $\mu$ m) were stained with routine hematoxylin and eosin (H&E) staining to examine the effects of NMEG-NMZ reinnervation or denervation on the muscle mass and myofiber morphology. In contrast, the middle muscle segment containing the NMZ and/or NMEG was cut sagittally (60  $\mu$ m) and sections were stained using immunohistochemical methods to detect axons and MEPs as described below.

### 2.3.4 | Documenting nerve regeneration and MEP reinnervation

#### Immunohistochemical staining for neurofilament (NF)

Some sagittal sections were immunostained with a monoclonal antibody against phosphorylated NF (SMI-31; Covance Research Products, Berkeley, CA, USA) as a marker for all axons as described in our previous publication (Mu et al., 2015). Briefly, the sections were: (1) treated in PBS containing 0.3% Triton and 2% BSA for 30 min; (2) incubated with primary antibody SMI-31 (dilution 1:800) in PBS containing 0.03% Triton at 4°C overnight; (3) incubated for 2 hr with the biotinylated secondary antibody (anti-mouse, 1:1000; Vector, Burlingame, CA, USA); (4) treated with avidin-biotin complex method with a Vectastain ABC kit (1:1000 ABC Elite; Vector); and (5) treated with diaminobenzidine-nickel as chromogen to visualize peroxidase labeling. Control sections were stained as described except that the incubation with the primary antibody was omitted.

The muscle sections immunostained for NF permit to show how the regenerating axons from the implanted NMEG reinnervate the denervated SM and quantify the density and spatial distribution of the regenerating axons in the target muscle. The extent of axonal regeneration and muscle reinnervation was evaluated by quantifying the NF-immunoreactive (NF-ir) axons within the treated muscles as described in our previous publications (Sobotka & Mu, 2013a, 2015). The intramuscular axonal density was assessed by estimating the number of the NF-ir axons and the area fraction of the axons within a section area (1.0-mm<sup>2</sup>). For a given muscle, three sections stained for NF were selected at different spatial levels to count NF-ir axons. For each section, five microscopic fields with NF-ir axons were identified and photographed in an order from ventral to dorsal aspect of the muscle. Areas with NF-positive staining were outlined, measured with public domain ImageJ software (v. 1.45s; NIH, Bethesda, Maryland). For each rat, the number and the area fraction of the NF-ir axons in the operated muscle were compared with those in the contralateral control.

#### Double fluorescence staining

Double fluorescence staining was used to label axons and MEPs as described (Grumbles, Sesodia, Wood, & Thomas, 2009) with some modifications. Briefly, some sagittal muscle sections were: (1) dried and then placed in Zamboni fixative with 5% sucrose for 20 min at

4°C; (2) washed several times with 1.5-T buffer with 0.05% Tween-20 and treated with 0.1 mol/L of glycine in 1.5 T buffer for 30 min, and dipped in 100% methanol at -20°C; (3) blocked in 1.5 T buffer containing 4% normal goat serum for 30 min to inhibit nonspecific protein binding; (4) incubated overnight at 4°C with primary antibodies (SMI-31 to detect neurofilaments and SMI-81 to label thinner axons; Covance Research Products Inc); (5) washed in 1.5 T buffer with 0.05% Tween-20 and incubated at room temperature for 2 hr both with a secondary antibody (goat anti-mouse antibody conjugated to Alexa 488) and with  $\alpha$ -bungarotoxin conjugated with Alexa 596 (Invitrogen Corporation, Carlsbad, CA, USA); and (6) washed in 1.5 T buffer with 0.05% Tween-20 and coverslipped.

The stained sections were viewed under a Zeiss fluorescence microscope and photographed. SMI-31 and SMI-81 detected axons (green), while  $\alpha$ -bungarotoxin labeled postsynaptic acetylcholine receptor (AChR) site in the MEPS (red). For each muscle sample, at least 100 labeled MEPS were randomly selected from three stained sections at different spatial levels through the muscle to determine the percentages of the innervated (visible axon attachment) and noninnervated (no visible axon attachment) MEPS.

## 2.4 | Data analysis

Wet muscle weights, force values, the number and area fraction of NF-ir axons, and innervated and noninnervated MEPS of the SM muscles in each rat were computed. The variables of the reinnervated SM muscles were expressed as the percentages of the values of the contralateral control muscles. All data were reported as mean  $\pm$  SD. The Student *t*-test (paired, two tailed) was used to compare differences in the mean muscle force, mean muscle weight, and mean number and area fraction of NF-ir axons between operated and unoperated SM muscles. A difference was considered statistically significant at  $p < 0.05$ .

## 3 | RESULTS

### 3.1 | Maximal tetanic muscle force

Maximum tetanic tension in the NMEG-NMZ reinnervated SM and the contralateral control muscles were evaluated at the end of the 3-month recovery period. The averaged force values for the treated and control muscles are summarized in Figure 2. For each rat, the percentage of functional recovery of the SM muscle reinnervated with NMEG-NMZ technique was determined as compared with that of the contralateral control muscle. Our previous studies have demonstrated that optimal muscle length could be achieved by stretching the muscle with moderate tension of 0.08 N (Mu et al., 2011; Sobotka & Mu, 2010). Electric stimulation of the nerve branch innervating the NMEG at low intensity (0.02–0.03 mA) produced visible muscle contraction. A lower (0.0075–0.01 mA) stimulation threshold was obtained when the nerve innervating the left intact SM muscle was stimulated. An increase in the stimulation current resulted in an increase in muscle force until it reached horizontal asymptote. During nerve stimulation

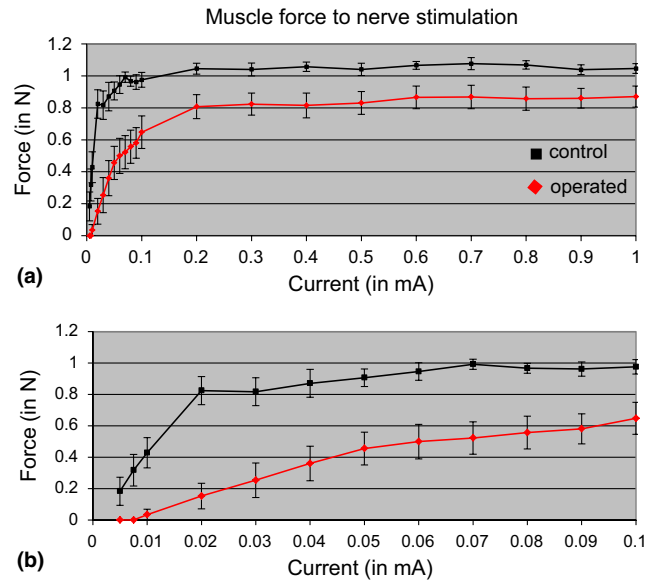


**FIGURE 2** Muscle force as a function of stimulation current in operated and control SM muscles. The passive tension was set at a moderate level (0.08 N). Nerve stimulation was made with a 0.2-second train of 0.2-millisecond-wide biphasic pulses at frequency of 200 Hz. The lower graph (b) shows in expanded scale the early portion of the upper graph (a). Operated SM muscle with implanted NMEG pedicle (shown in red) when compared to control muscle at the opposite side (shown in black) has larger stimulation threshold, reach the level of maximal force with larger stimulation current and has smaller maximal force. Maximal muscle force level was calculated as the average muscle force to stimulation currents from 0.6 to 1 mA. Average maximal muscle force level at the operated side (0.865 N) was 81.6% of muscle force at the control side (1.060 N). Vertical bars represent the standard deviation of the mean

on the operated side, this saturation level was reached with 0.2 mA. The saturation level was reached at smaller current (0.1 mA) on the control side. The reinnervated SM showed an average maximum tetanic force of  $0.87 \pm 0.23$  N (control,  $1.06 \pm 0.10$  N;  $p < 0.005$ ). Therefore, the reinnervated SM muscles produced 82% of the maximal tetanic tension of the contralateral control muscles.

### 3.2 | HRP-labeled motoneurons innervating NMEG-NMZ reinnervated SM muscle

The location of HRP-labeled motoneurons on the operated side could demonstrate the source of innervation of the NMEG-NMZ reinnervated muscle. As reported in our previous studies, the SM motoneurons were concentrated in the lower medulla oblongata and spinal ventral grey horn in the C1 to C2 (Mu et al., 2011; Zhang et al., 2011). The SM motoneurons in C1 were concentrated mainly in the dorso-medial region, whereas the SH motoneurons at this level were located in the ventromedial region of the ventral horn (Mu et al., 2011). In this study, HRP injections into the right reinnervated SM muscle labeled motoneurons in the ventromedial region of the ventral horn in the C1 to C2, which were consistent with those labeled by HRP injections into the left intact SH muscle (Figure 3). These findings indicate

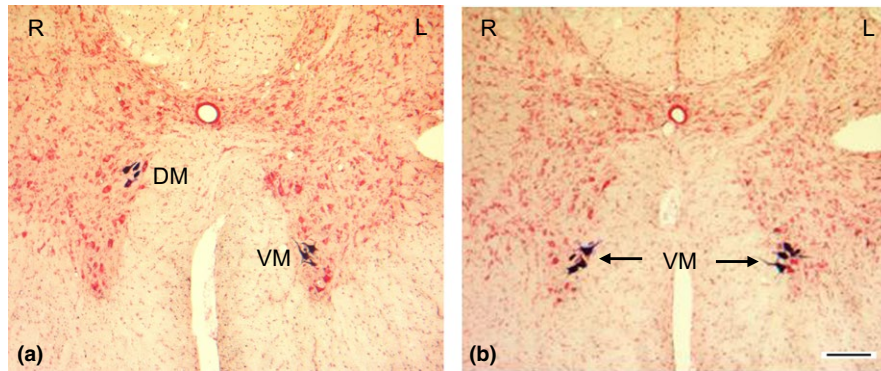


**FIGURE 3** Motoneurons labeled with retrograde horseradish peroxidase (HRP) neuronal tracing in rats. (a) A transverse section from upper cervical spinal cord segment C1 in a normal adult rat, showing different locations of the sternomastoid (SM) and sternohyoid (SH) motoneurons. The HRP solution was injected into the right (R) SM and left (L) SH muscles. Note that in C1, the SH motoneurons were confined to the ventromedial (VM) region, whereas SM motoneurons were located in the dorsomedial (DM) region of the ventral horn of the spinal cord. (b) A transverse section from C1 after HRP injections into the right reinnervated SM muscle and the left intact SH muscle in a rat. Note that the motoneurons controlling the right reinnervated SM were located in the same region as that innervating the SH (VM in C1). Bar = 100  $\mu$ m

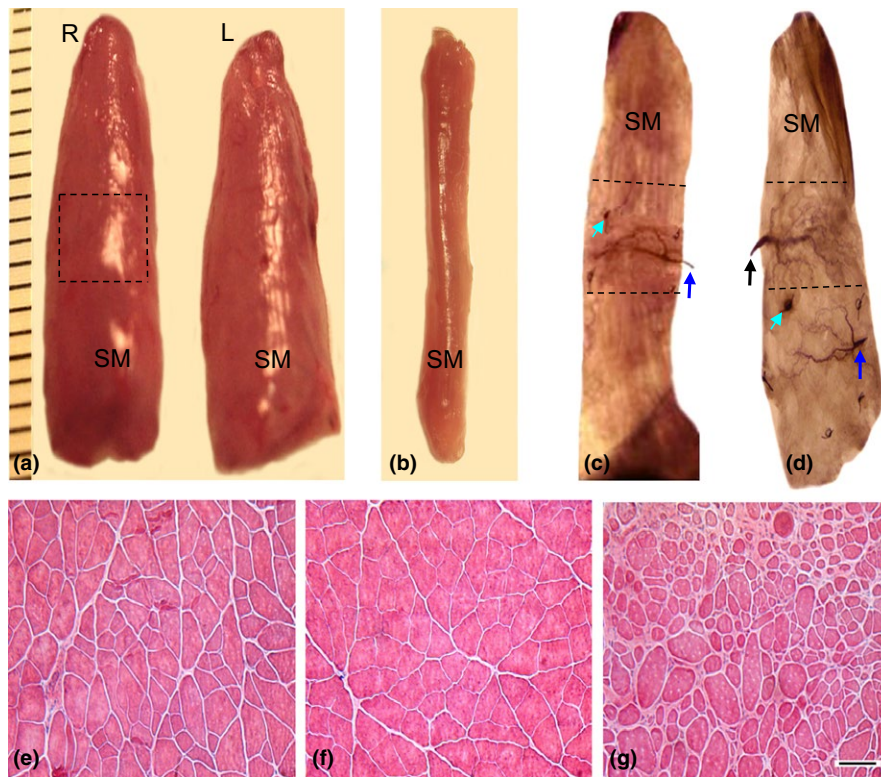


**FIGURE 4** Images from the reinnervated, normal control, and denervated SM muscles showing gross appearance, muscle mass, myofiber morphology, and NMEG implantation site. (a) A pair of SM muscles removed from a rat 3 months after NMEG-NMZ surgery. Note that the mass of the right (R) reinnervated SM muscle was close to that of the left (L) control muscle. The boxed region in the right SM is the location of the implanted NMEG. (b) A SM muscle denervated by resecting a 5-mm segment of its innervating nerve for 3 months. Note that the denervated SM showed a more significant loss of muscle mass as compared with the reinnervated and normal SM muscles. (c–d) Sihler’s stained SM muscles showing the difference in the NMEG implantation site between NMEG-NMZ technique (c) and our originally designed NMEG procedure (d). Note that the NMEG pedicle containing a SH nerve branch (blue arrow) and intramuscular nerve terminals was implanted into the NMZ (outlined region in c) of the SM in the middle portion of the muscle for NMEG-NMZ reinnervation. In contrast, the NMEG pedicle was implanted into the caudal MEP-free area of the target muscle in our originally designed NMEG procedure (d). Green arrow indicates a microsuture surrounding the implanted NMEG pedicle. The implanted NMEG contained a SH nerve branch (blue arrow) and nerve terminals. Black arrow in d indicates the SM nerve branch. (e–g) Hematoxylin and eosin-stained transverse sections of the SM muscles. Note that 3 months after surgery, NMEG-NMZ reinnervated SM (e) exhibited very good preservation of muscle structure and myofiber morphology with less fiber atrophy as compared with the normal (f) and denervated (g) muscles. Bar = 100  $\mu$ m for e through g

that the axons innervating the treated SM muscles were derived solely from the implanted SH nerve and controlled by the SH motoneurons. Retrograde HRP labeling also confirmed that the NMEG-NMZ microsurgery was successfully performed.

### 3.3 | Muscle weight, location of the implanted NMEG, and myofiber morphology

In each rat, gross appearance and size of the operated SM was similar to those of the contralateral control muscle (Figure 4a). The reinnervated SM muscles were greater in size than the SM muscles with complete denervation for 3 months (Figure 4b). The mean value and standard deviation of the wet weight was  $0.332 \pm 0.047$  g for the reinnervated SM muscles, whereas  $0.374 \pm 0.044$  g for the contralateral control muscles (Table 1). The differences in muscle weights of the reinnervated and control muscles were relatively small but consistent across all animals and therefore statistically significant ( $p < 0.0001$ ). The reinnervated SM muscles weighed 89% of the weight of contralateral control muscles (Table 1). The mean percent of wet weight (89% of the control) of NMEG-NMZ reinnervated SM muscles was much higher than that of the denervated SM muscles (44% of the control;  $p < 0.0001$ ).

The location of the implanted NMEG within the right SM muscle was determined. Sihler's stain showed that microsurgery for NMEG-NMZ reinnervation was successfully performed as indicated by precise implantation of the NMEG into the NMZ of the target muscle (Figure 4c). Each of the implanted NMEG contained a SH nerve branch and numerous nerve terminals, indicating that the treated SM was reinnervated by the SH nerve. In our original NMEG procedure, however, the NMEG pedicle obtained from the ipsilateral SH muscle was implanted into the caudal endplate-free area in the SM muscle (Figure 4d).

Hematoxylin and eosin-stained transverse muscle sections showed that the NMEG-NMZ reinnervated SM muscles exhibited very good preservation of muscle structure and myofiber morphology with less fiber atrophy (Figure 4e) as compared with the contralateral control (Figure 4f) and denervated (Figure 4g) muscles.

### 3.4 | Axonal regeneration and MEP reinnervation

The muscle sections from NMEG-NMZ reinnervated SM processed with NF staining exhibited abundance of NF-ir axons. In the reinnervated SM, the regenerating axons from the implanted NMEG supplied the denervated NMZ and reached the most distal portion of the muscle, achieving almost full muscle reinnervation (Figure 5a–b). The mean number and area fraction of the labeled axons for each muscle in each animal is summarized in Table 2. On average, the regenerated axons in the NMEG-NMZ reinnervated muscles were calculated to be 76.8% of the controls. No NF-ir axons were identified in the stained sections of the denervated SM muscles (data not shown).

The sagittal sections of the treated SM muscles immunostained with double fluorescence staining showed the innervated and non-innervated MEPs. In the SM muscles reinnervated with NMEG-NMZ, the regenerating axons grew across the NMZ to innervate the denervated MEPs (Figure 5c–e). The majority of the denervated MEPs (80%) in the treated muscles were reinnervated by regenerating axons, while the remaining MEPs were unoccupied by axons. In addition, axonal sprouts and newly formed small MEPs were identified in the NMEG-NMZ reinnervated muscles. In the stained sections from the denervated SM muscles, no axons were visualized and the denervated MEPs were characterized by reduced staining density, decreased number, and altered shape and size (data not shown).

Animal no.	Body weight, g	Right SM, g	Left SM, g	Ratio R/L
1	333	0.309	0.333	0.928
2	328	0.332	0.397	0.836
3	319	0.318	0.357	0.891
4	285	0.287	0.328	0.875
5	386	0.245	0.316	0.775
6	373	0.373	0.407	0.916
7	281	0.320	0.343	0.933
8	330	0.396	0.437	0.906
9	329	0.305	0.327	0.933
10	355	0.335	0.358	0.936
11	380	0.341	0.392	0.870
12	304	0.326	0.338	0.964
13	358	0.433	0.462	0.937
14	315	0.373	0.410	0.910
15	328	0.290	0.398	0.729
Average	333.6	0.332	0.374	0.889
STDEV	31.8	0.047	0.044	0.065

**TABLE 1** Wet muscle weight measurement for the right reinnervated and left control sternomastoid (SM) muscles in rats ( $n = 15$ )

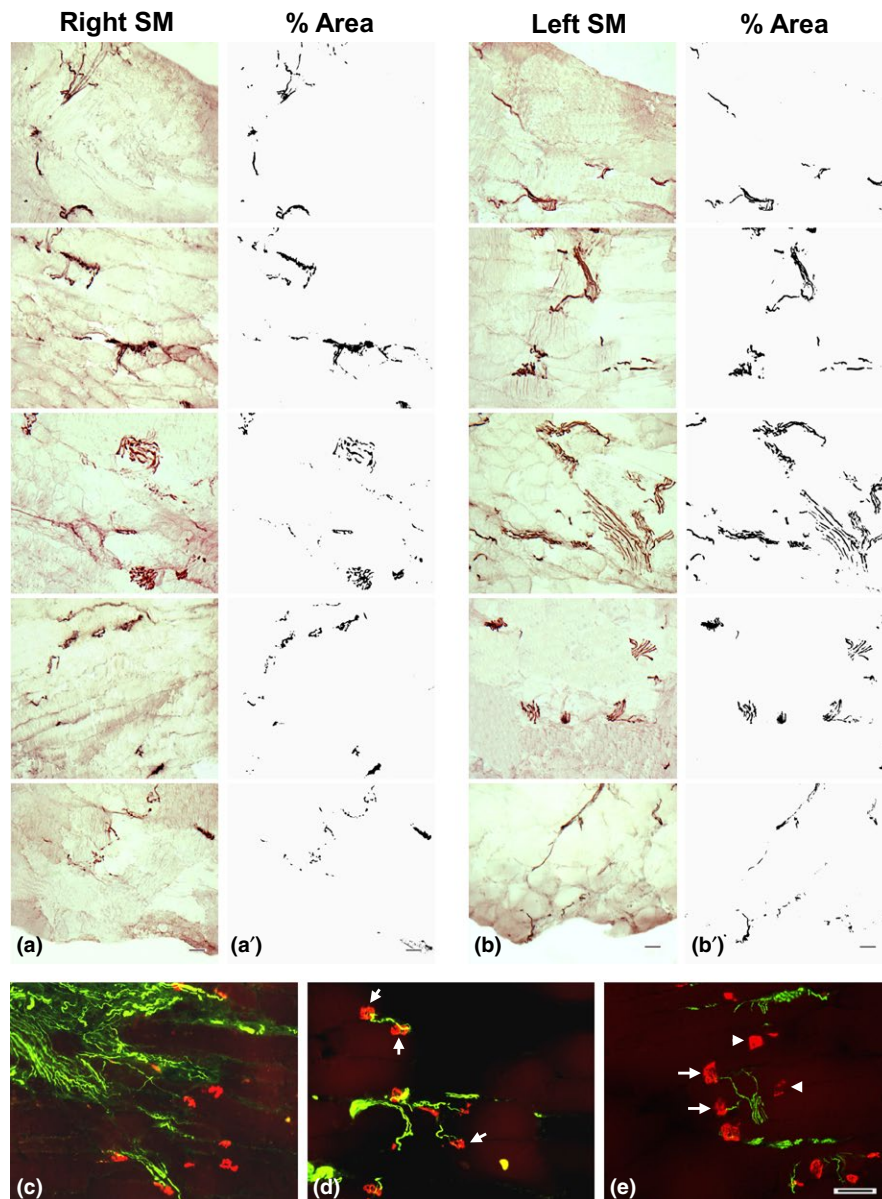


**FIGURE 5** Images of the immunostained sections of the NMEG-NMZ reinnervated and contralateral control SM muscles of a rat. (a–b) Images of sagittal sections of the right reinnervated (a) and left control (b) SM muscles. The sections were immunostained with antibody against neurofilament (NF) and photographed from ventral (top) to dorsal (bottom) surfaces of the muscle. Note that the nerve fascicles and axons (darkly stained threads and dots) in the right NMEG-NMZ reinnervated SM are distributed throughout the thickness of the muscle. (a'–b') The stained sections in a and b were opened using ImageJ software and converted to 8-bit (binary) images, color thresholded, and particle analyzed for nerve morphometry. The density of the axons was evaluated by estimating the number and area fraction of the NF-positive axons within a section area ( $1.0 \text{ mm}^2$ ). For this rat, as compared with the left control SM (mean axon count: 398; mean area: 2.92) the right SM exhibited very good muscle reinnervation as indicated by the mean axon count (283; 71% of the control) and the mean area (2.32; 80% of the control). Bar =  $100 \mu\text{m}$  for a through b. (c–e) Images of sagittal sections immunostained with double fluorescence staining of the right reinnervated SM muscle of a rat, showing axon-endplate connections. Regenerated axons (green) were detected with SMI-31 monoclonal against neurofilaments, while motor endplates (MEPs; red) were labeled with  $\alpha$ -bungarotoxin. Note that the regenerated axons branched extensively into fields of MEPs in the NMZ of the target muscle (c). The majority of the MEPs in the treated muscle were reinnervated by regenerated axons (arrows in e), while some MEPs in the same muscle were unoccupied by regenerated axons (arrowheads in d and e). Bar =  $100 \mu\text{m}$  for c through e

## 4 | DISCUSSION

In this study, we have demonstrated that NMEG-NMZ technique resulted in optimal recovery of muscle force (82% of the control). The reinnervated muscles exhibited good preservation of muscle mass

(89% of the control) and myofiber morphology. In the treated muscles, the mean count and area of the axons reached up to 76.8% and 75.6% of the controls, respectively, and the majority (80%) of the denervated MEPs regained motor innervation. The optimal outcomes are attributed to the unique advantages of the NMEG-NMZ technique.

Animal no.	Right SM		Left SM		Ratio (R/L)	
	Count	%Area	Count	%Area	Count	%Area
1	765	0.366	980	0.681	0.781	0.537
2	652	0.494	854	0.544	0.763	0.908
3	726	0.925	996	1.081	0.729	0.856
4	769	0.475	1004	0.782	0.766	0.607
5	494	0.305	708	0.478	0.698	0.638
6	822	0.303	1065	0.463	0.772	0.654
7	857	0.544	1091	1.133	0.786	0.480
8	583	0.264	696	0.484	0.838	0.545
9	576	0.601	854	0.701	0.674	0.857
10	904	0.773	1096	0.844	0.825	0.916
11	766	0.457	871	0.493	0.879	0.927
12	289	1.073	381	0.968	0.759	1.108
13	283	2.320	398	2.915	0.711	0.796
Average	653	0.685	846	0.890	0.768	0.756

L, left; R, right.

Specifically, the regenerating axons from the NMEG could rapidly reinnervate the denervated MEPs in the target muscle and form functional synapses.

A transferred NMEG could provide an abundant source of nerve terminals and MEPs for nerve regeneration and muscle reinnervation. NMEG has sufficient pedicle-recipient muscle interfaces, which provide enough space for axonal regeneration. The axons could start to regenerate at multiple points in the implanted NMEG and grow across the pedicle-recipient muscle interfaces to reach the recipient muscle fibers. The NMEG-NMZ technique described here is based on the concept that denervated MEPs in the NMZ of the target muscle are preferential sites for reinnervation. One reason for the impaired target reinnervation could be degradation of MEPs during prolonged denervation. The NMEG-NMZ procedure physically shortens regeneration distances and facilitates rapid MEP reinnervation to avoid irreversible loss of the denervated MEPs in the target muscle. The importance of nerve regeneration onto the sites of the original MEPs is highlighted by various animal experiments. Recent studies (Ma et al., 2011) have shown that poor motor recovery after peripheral nerve injury resulted from a failure of synapse reformation because of the delay in motor axons reaching their target. Barbour, Yee, Kahn, and Mackinnon (2012) emphasized that "*Functional motor recovery after peripheral nerve injury is predominantly determined by the time to motor endplate reinnervation and the absolute number of regenerated motor axons that reach target.*" The MEP is a highly specialized structure, optimized for the rapid transmission of information from the presynaptic nerve terminal to the postsynaptic muscle fiber. It serves to efficiently communicate the electrical impulse from the motor neuron to the skeletal muscle to signal contraction. MEP regions of mammalian muscle fibers are preferentially reinnervated as a consequence of some special property of the muscle fiber at this site. Studies have demonstrated that after nerve injury regenerating axons preferentially form synapses at

**TABLE 2** Quantitative comparison of count and %area of neurofilament-immunoreactive axons between right operated and left control sternomastoid (SM) muscles in rats ( $n = 13$ )

original synaptic sites (Bennett, McLachlan, & Taylor, 1973; Covault, Cunningham, & Sanes, 1987; Gorio, Carmignoto, Finesso, Polato, & Nunzi, 1983; Sanes, Marshall, & McMahan, 1978). As reported, 30 days after nerve transection, all the regenerating nerve fibers grew into and innervated the regions of the original MEPs (Iwayama, 1969). The MEPs may exert an attraction on the regenerating axons. Synaptic basal lamina at the MEP contains molecules that direct the formation of synaptic specializations on regenerating axon terminals and myofibers (McMahan & Wallace, 1989). Some other chemotropic substance released from the MEPs may attract the regenerating axons in the vicinity. Using direct nerve implantation model, some investigators observed preferential reinnervation of the native MEPs in the target muscle by abundant regenerating axons and sprouts (Guth & Zalewski, 1963; Sakellarides, Sorbie, & James, 1972).

NMEG-NMZ technique would have the potential for clinical application. It could be considered in selected clinical cases with extremity nerve injuries when no other repair options are possible. This method would be useful especially for treating laryngeal and facial paralysis. One of the most important problems involved in rehabilitation surgery of the recurrent laryngeal nerve (RLN) arises from the fact that this nerve carries fibers innervating antagonistic muscle groups (abductor and adductor muscles) which perform different functions during phonation, respiration, and swallowing. After RLN damage or nerve repair, some axons grow in a misdirected fashion. This leads to adductor axons innervating abductor muscles and vice versa, resulting in "synkinesis", in which both opening (abductor) and closing (adductor) muscles activate in a dysfunctional way (Crumley, 2000). Synkinetic reinnervation is responsible for poor functional outcome as a result of simultaneous contraction of antagonistic muscles. To avoid synkinesis and functional failures, selective reinnervation of the glottis opener and of the glottis-closing musculature is commonly performed. Up to date, ansa cervicalis is a commonly used candidate as a potential donor

for selective reinnervation of the laryngeal adductor and abductor muscles (Crumley, 1991). The donor nerve can be directly implanted into a target muscle or prepared as a nerve-muscle pedicle (NMP) to reinnervate the paralyzed muscle (Tucker, 1989). The NMP method involves transferring a donor nerve branch with a small piece of muscle tissue (a 2- to 3-mm cube) from a cervical strap muscle to a paralyzed laryngeal muscle. Surgical methods for reanimation of the paralyzed face include cross-facial nerve graft, nerve transfers, and free muscle transplantation (Hoffman, 1992; Terzis & Konofaos, 2008). The NMP transfer or direct nerve implantation has been also used for the selective reinnervation of paralyzed facial muscles to avoid synkinesis (Goding et al., 1989; Hall, Trachy, & Cummings, 1988). Although some authors (Tucker, 1989) reported good results, others reported poor muscle reinnervation and functional recovery (Fata, Malmgren, Gacek, Dum, & Woo, 1987; Rice & Burstein, 1983) after NMP transfer. There are several factors leading to poor outcome. First, a NMP is designed at the point where a nerve branch enters the muscle without consideration of the MEPs and nerve terminals. Second, the pedicle is too small to contain donor nerve terminals and MEPs. Finally, the pedicle may contain only a nerve stump, serving as direct nerve implantation as both methods resulted in similar outcomes (Goding et al., 1989; Hall et al., 1988). The results from this study suggest that NMEG-NMZ technique could be an option for the treatment of laryngeal and facial paralysis.

Although our experiments showed the potential of NNMEG-NMZ in immediate muscle reinnervation, this study also has some limitations. For example, postoperative evaluations were performed at the end of 3 months after surgery. Three-month recovery period may be not enough to provide a complete picture of what occurs after NMEG-NMZ. Further studies are needed to determine morphological and functional alterations at different time points after NMEG-NMZ reinnervation. This information would be helpful for better understanding the time-related changes of muscle reinnervation and functional recovery. In addition, it remains unknown if the NMEG-NMZ has the potential for delayed reinnervation that is not uncommon in clinical practice. One of our ongoing studies is to determine the efficacy of NMEG-NMZ for chronic muscle denervation. For this purpose, it is important to know the decreasing rate of the endplates in the completely denervated muscle and to determine the time point when all the endplates cannot be detected.

In conclusion, this study showed that the NMZ of the target muscle is the best site in the target muscle for NMEG implantation. NMEG-NMZ procedure could shorten axon regeneration distances and facilitate rapid endplate reinnervation, thereby avoiding muscle atrophy and contributing to optimal functional recovery. Our results have demonstrated that NMEG-NMZ technique resulted in extensive axonal regeneration, MEP reinnervation, and optimal functional recovery. This method can be used for treatment of laryngeal and facial paralysis. Further technical improvements and studies to identify the NMZ in laryngeal musculature will be required before this technique can be applied in a clinically meaningful fashion. In addition, it could be one alternative to reinnervate other denervated muscles when no other repair options are possible. Although NMEG-NMZ technique

has treatment potential in immediate muscle reinnervation, further work is warranted to determine its effectiveness for delayed muscle reinnervation.

## ACKNOWLEDGMENTS

This work was supported by the Office of the Assistant Secretary of Defense for Health Affairs under Award No. W81XWH-14-1-0442 (to Liancai Mu). The U.S. Army Medical Research Acquisition Activity, 820 Chandler Street, Fort Detrick MD 21702-5014 is the awarding and administering acquisition office. Opinions, interpretations, conclusions, and recommendations are those of the authors and are not necessarily endorsed by the Department of Defense. In conducting research using animals, the investigators adhere to the laws of the United States and regulations of the Department of Agriculture. This protocol was approved by the USAMRMC Animal Care and Use Review Office (ACURO) for the use of rats. The authors thank the anonymous reviewers for their constructive comments on the manuscript.

## CONFLICT OF INTEREST

None declared.

## REFERENCES

- Al-Qattan, M. M. (2001). Terminolateral neurotomy: Review of experimental and clinical studies. *Journal of Reconstructive Microsurgery*, *17*, 99–108.
- Barbour, J., Yee, A., Kahn, L. C., & Mackinnon, S. E. (2012). Supercharged end-to-side anterior interosseous to ulnar motor nerve transfer for intrinsic musculature reinnervation. *The Journal of Hand Surgery*, *37*, 2150–2159.
- Bennett, M. R., McLachlan, E. M., & Taylor, R. S. (1973). The formation of synapses in reinnervated mammalian striated muscle. *Journal of Physiology*, *233*, 481–500.
- Brininger, T. L., Antczak, A., & Breland, H. L. (2008). Upper extremity injuries in the U.S. military during peacetime years and wartime years. *Journal of Hand Therapy*, *21*, 115–122.
- Brunelli, G. A., & Brunelli, L. M. (1980). Direct neurotization of severely damaged denervated muscles. *International Surgery*, *65*, 529–531.
- Brunelli, G. A., & Brunelli, G. R. (1993). Direct muscle neurotization. *Reconstructive Microsurgery*, *9*, 81–90.
- Covault, J., Cunningham, J. M., & Sanes, J. R. (1987). Neurite outgrowth on cryostat sections of innervated and denervated skeletal muscle. *Journal of Cell Biology*, *105*, 2479–2488.
- Crumley, R. L. (1991). Update: Ansa cervicalis to recurrent laryngeal nerve anastomosis for unilateral laryngeal paralysis. *Laryngoscope*, *101*, 384–388.
- Crumley, R. L. (2000). Laryngeal synkinesis revisited. *The Annals of Otolaryngology, Rhinology, and Laryngology*, *109*, 365–371.
- De Sa, J. M., Mazzer, N., Barbieri, C. H., & Barriera, A. A. (2004). The end-to-side peripheral nerve repair. Functional and morphometric study using the peroneal nerve of rats. *Journal of Neuroscience Methods*, *136*, 45–53.
- Eser, F., Aktekin, L. A., Bodur, H., & Atan, C. (2009). Etiological factors of traumatic peripheral nerve injuries. *Neuro India*, *57*, 434–437.
- Fata, J. J., Malmgren, L. T., Gacek, R. R., Dum, R., & Woo, P. (1987). Histochemical study of posterior cricoarytenoid muscle reinnervation

- by a nerve-muscle pedicle in the cat. *The Annals of Otolaryngology, Rhinology, and Laryngology*, 96, 479–487.
- Goding, G. S. Jr, Cummings, C. W., & Bright, D. A. (1989). Extension of neuromuscular pedicles and direct nerve implants in the rabbit. *Archives of Otolaryngology - Head and Neck Surgery*, 115, 217–223.
- Gorio, A., Carmignoto, G., Finesso, M., Polato, P., & Nunzi, M. G. (1983). Muscle reinnervation. II. Sprouting, synapse formation, and repression. *Neuroscience*, 8, 403–416.
- Green, D. C., Berke, G. S., & Graves, M. C. (1991). A functional evaluation of ansa cervicalis nerve transfer for unilateral vocal cord paralysis: Future directions for laryngeal reinnervation. *Otolaryngology - Head and Neck Surgery*, 104, 453–466.
- Grumbles, R. M., Sesodia, S., Wood, P. M., & Thomas, C. K. (2009). Neurotrophic factors improve motoneuron survival and function of muscle reinnervated by embryonic neurons. *Journal of Neuropathology and Experimental Neurology*, 68, 736–746.
- Guth, L., & Zalewski, A. A. (1963). Disposition of cholinesterase following implantation of nerve into innervated and denervated muscle. *Experimental Neurology*, 7, 316–326.
- Hall, S. J., Trachy, R. E., & Cummings, C. W. (1988). Facial muscle reinnervation: A comparison of neuromuscular pedicle with direct nerve implant. *The Annals of Otolaryngology, Rhinology, and Laryngology*, 97, 229–233.
- Hoffman, W. Y. (1992). Reanimation of the paralyzed face. *Otolaryngologic Clinics of North America*, 25, 649–667.
- Ichihara, S., Inada, Y., & Nakamura, T. (2008). Artificial nerve tubes and their application for repair of peripheral nerve injury: An update of current concepts. *Injury*, 39(Suppl 4), 29–39.
- Iwayama, T. (1969). Relation of regenerating nerve terminals to original endplates. *Nature*, 224, 81–82.
- Kelsey, J., Praemer, A., Nelson, L., Felberg, A., & Rice, D. (1997). *Upper extremity disorders: Frequency, impact, and cost*. London: Churchill-Livingstone.
- Kretschmer, T., Antoniadis, G., Braun, V., Rath, S. A., & Richter, H. P. (2001). Evaluation of iatrogenic lesions in 722 surgically treated cases of peripheral nerve trauma. *Journal of Neurosurgery*, 94, 905–912.
- Lee, S. K., & Wolfe, S. W. (2000). Peripheral nerve injury and repair. *Journal of American Academy of Orthopaedic Surgeons*, 8, 243–252.
- Lee, S. K., & Wolfe, S. W. (2012). Nerve transfers for the upper extremity: New horizons in nerve reconstruction. *Journal of American Academy of Orthopaedic Surgeons*, 20, 506–517.
- Ma, C. H., Omura, T., Cobos, E. J., Latremoliere, A., Ghasemlou, N., Brenner, G. J., ... Woolf, C. J. (2011). Accelerating axonal growth promotes motor recovery after peripheral nerve injury in mice. *Journal of Clinical Investigation*, 121, 4332–4347.
- Marie, J. P., Lerosey, Y., Dehesdin, D., Jin, O., Tadie, M., & Andrieu-Guitrancourt, J. (1999). Experimental reinnervation of a strap muscle with a few roots of the phrenic nerve in rabbits. *The Annals of Otolaryngology, Rhinology, and Laryngology*, 108, 1004–1011.
- McAllister, R. M., Gilbert, S. E., Calder, J. S., & Smith, P. J. (1996). The epidemiology and management of upper limb peripheral nerve injuries in modern practice. *The Journal of Hand Surgery*, 21, 4–13.
- McMahan, U. J., & Wallace, B. G. (1989). Molecules in basal lamina that direct the formation of synaptic specializations at neuromuscular junctions. *Developmental Neuroscience*, 11, 227–247.
- de Medinaceli, L., Prayon, M., & Merle, M. (1993). Percentage of nerve injuries in which primary repair can be achieved by end-to-end approximation: Review of 2,181 nerve lesions. *Microsurgery*, 14, 244–246.
- Meikle, D., Trachy, R. E., & Cummings, C. W. (1987). Reinnervation of skeletal muscle: A comparison of nerve implantation with neuromuscular pedicle transfer in an animal model. *The Annals of Otolaryngology, Rhinology, and Laryngology*, 96, 152–157.
- Merle, M., Dellon, A. L., Campbell, J. N., & Chang, P. S. (1989). Complications from silicon-polymer intubulation of nerves. *Microsurgery*, 10, 130–133.
- van der Meulen, J. H., Urbanchek, M. G., Cederna, P. S., Eguchi, T., & Kuzon, W. M. Jr (2003). Denervated muscle fibers explain the deficit in specific force following reinnervation of the rat extensor digitorum longus muscle. *Plastic and Reconstructive Surgery*, 112, 1336–1346.
- Moneim, M., & Omer, G. (1998). Clinical outcome following acute nerve repair. In G. Omeg, M. Spinner, & A. Van Beek (Eds.), *Management of peripheral nerve problems* (pp. 414–419). Philadelphia, PA: Saunders.
- Mu, L., Chen, J., Sobotka, S., Nyirenda, T., Benson, B., Gupta, F., ... Beach, T. (2015). Alpha-synuclein pathology in sensory nerve terminals of the upper aerodigestive tract of Parkinson's disease patients. *Dysphagia*, 30, 404–417.
- Mu, L., & Sanders, I. (2010). Sihler's whole mount nerve staining technique: A review. *Biotechnic and Histochemistry*, 85, 19–42.
- Mu, L., Sobotka, S., & Su, H. (2011). Nerve-muscle-endplate band grafting: A new technique for muscle reinnervation. *Neurosurgery*, 69(Suppl. 2), 208–224.
- Myckatyn, T. M., & Mackinnon, S. E. (2004). A review of research endeavors to optimize peripheral nerve reconstruction. *Neurological Research*, 26, 124–138.
- Noble, J., Munro, C. A., Prasad, V. S., & Midha, R. (1998). Analysis of upper and lower extremity peripheral nerve injuries in a population of patients with multiple injuries. *Journal of Trauma*, 45, 116–122.
- Rice, D. H., & Burstein, F. D. (1983). Restoration of physiologic vocal fold abduction with the ansa cervicalis nerve. *Archives of Otolaryngology*, 109, 480–481.
- Sakellarides, H. T., Sorbie, C., & James, L. (1972). Reinnervation of denervated muscles by nerve transplantation. *Clinical Orthopaedics and Related Research*, 83, 195–201.
- Sanapanich, K., Morrison, W. A., & Messina, A. (2002). Physiologic and morphologic aspects of nerve regeneration after end-to-end or end-to-side coaptation in a rat model of brachial plexus injury. *The Journal of Hand Surgery*, 27, 133–142.
- Sanes, J. R., Marshall, L. M., & McMahan, U. J. (1978). Reinnervation of muscle fiber basal lamina after removal of myofibers. Differentiation of regenerating axons at original synaptic sites. *Journal of Cell Biology*, 78, 176–198.
- Siemionow, M., & Brzezicki, G. (2009). Chapter 8: Current techniques and concepts in peripheral nerve repair. *International Review of Neurobiology*, 87, 141–172.
- Sobotka, S., & Mu, L. (2010). Characteristics of tetanic force produced by the sternomastoid muscle of the rat. *Journal of Biomedicine & Biotechnology*, 2010, 194984.
- Sobotka, S., & Mu, L. (2011). Force characteristics of the rat sternomastoid muscle reinnervated with end-to-end nerve repair. *Journal of Biomedicine & Biotechnology*, 2011, 173471.
- Sobotka, S., & Mu, L. (2013a). Force recovery and axonal regeneration of the sternomastoid muscle reinnervated with the end-to-end nerve anastomosis. *Journal of Surgical Research*, 182, e51–e59.
- Sobotka, S., & Mu, L. (2013b). Comparison of muscle force after immediate and delayed reinnervation using nerve-muscle-endplate band grafting. *Journal of Surgical Research*, 179, e117–e126.
- Sobotka, S., & Mu, L. (2015). Muscle reinnervation with nerve-muscle-endplate band grafting technique: Correlation between force recovery and axonal regeneration. *Journal of Surgical Research*, 195, 144–151.
- Stanec, S., & Stanec, Z. (1998). Reconstruction of upper-extremity peripheral-nerve injuries with ePTFE conduits. *Journal of Reconstructive Microsurgery*, 14, 227–232.
- Terzis, J. K., & Konofaos, P. (2008). Nerve transfers in facial palsy. *Facial Plastic Surgery*, 24, 177–193.
- Tucker, H. M. (1989). Long-term results of nerve-muscle pedicle reinnervation for laryngeal paralysis. *The Annals of Otolaryngology, Rhinology, and Laryngology*, 98, 674–676.
- Wiberg, M., & Terenghi, G. (2003). Will it be possible to produce peripheral nerves? *Surgical Technology International*, 11, 303–310.

- Wong, B. J., & Crumley, R. L. (1995). Nerve wound healing. An overview. *Otolaryngologic Clinics of North America*, 28, 881–895.
- Yoshimura, K., Asato, H., Jejurikar, S. S., Cederna, P. S., Urbanchek, M. G., & Kuzon, W. M. Jr (2002). The effect of two episodes of denervation and reinnervation on skeletal muscle contractile function. *Plastic and Reconstructive Surgery*, 109, 212–219.
- Zhang, X., Mu, L., Su, H., & Sobotka, S. (2011). Locations of the motor endplate band and motoneurons innervating the sternomastoid muscle in the rat. *Anatomical Record (Hoboken)*, 294, 295–304.

**How to cite this article:** Mu L, Sobotka S, Chen J, Nyirenda T. Reinnervation of denervated muscle by implantation of nerve-muscle-endplate band graft to the native motor zone of the target muscle. *Brain Behav.* 2017;7:e00668.  
<https://doi.org/10.1002/brb3.668>

# Intraoperative 1-Hour Electrical Nerve Stimulation Enhances Outcomes of Nerve–Muscle-Endplate Band Grafting Technique for Muscle Reinnervation

Stanislaw Sobotka, PhD, DSc<sup>1,2</sup> Jingming Chen, MD<sup>1</sup> Themba Nyirenda, PhD<sup>1</sup> Liancai Mu, MD, PhD<sup>1</sup>

<sup>1</sup> Department of Research, Upper Airway Research Laboratory, Hackensack University Medical Center, Hackensack, New Jersey

<sup>2</sup> Department of Neurosurgery, Icahn School of Medicine at Mount Sinai, New York, New York

Address for correspondence Stanislaw Sobotka, PhD, DSc, Department of Research, Hackensack University Medical Center, Hackensack, NJ 07601 (e-mail: stanislaw.sobotka@mountsinai.org).

J Reconstr Microsurg 2017;33:533–543.

## Abstract

**Background** Increasing evidence suggests that 1-hour electrical nerve stimulation during surgery improves nerve regeneration and functional recovery. However, it remains unknown if this approach has beneficial effects on the outcomes of our recently developed nerve–muscle-endplate band grafting-native motor zone (NMEG-NMZ) technique for muscle reinnervation.

**Methods** In this study, NMEG-NMZ transplantation was performed in a rat model. The right sternomastoid muscle was experimentally denervated and immediately reinnervated by implanting a NMEG harvested from the ipsilateral sternohyoid (SH) muscle into the NMZ of the target muscle. Before implantation of the NMEG, the SH nerve branch innervating the NMEG was subjected to intraoperative 1-hour continuous electrical stimulation (20 Hz). Three months after surgery, the degree of functional recovery was evaluated with muscle force measurement and the extent of nerve regeneration and endplate reinnervation was examined using histological and immunohistochemical methods.

**Results** A combination of NMEG-NMZ with electrical nerve stimulation resulted in a greater degree of functional recovery than the NMEG-NMZ alone. The mean muscle force of the treated muscles was 90% of the contralateral control. The muscle mass was recovered up to 90% of the control. The mean number and percentage of area of the regenerated axons in the treated muscles was computed to be 81 and 84% of the control muscles, respectively. On average, 83% of the denervated endplates in the treated muscles were reinnervated by regenerated axons.

**Conclusion** Intraoperative brief nerve stimulation promotes nerve regeneration, endplate reinnervation, and functional recovery of the muscles reinnervated with NMEG-NMZ technique.

## Keywords

- ▶ electrical nerve stimulation
- ▶ nerve regeneration
- ▶ muscle force measurement

Peripheral nerve injury (PNI) is a major source of chronic disabilities and remains a challenging problem for microsurgeons. Approximately 100,000 patients undergo peripheral nerve surgery in the United States and Europe annually.<sup>1</sup> Despite advances in microsurgery and extensive studies on nerve repair, the presently available methods for muscle

reinnervation result in poor functional recovery. Therefore, there is a pressing need to seek new strategies for treating PNI-related muscle paralysis.

Increasing evidence suggests that functional motor recovery after PNI and nerve repair is predominantly determined by motor endplate (MEP) reinnervation and the

received  
January 6, 2017  
accepted after revision  
March 23, 2017  
published online  
June 2, 2017

Copyright © 2017 by Thieme Medical Publishers, Inc., 333 Seventh Avenue, New York, NY 10001, USA.  
Tel: +1(212) 584-4662.

DOI <https://doi.org/10.1055/s-0037-1602824>.  
ISSN 0743-684X.

absolute number of regenerated motor axons that reach target.<sup>2-5</sup> Recently, we developed a novel reinnervation technique called nerve-muscle-endplate band grafting (NMEG) in a rat model.<sup>6</sup> The idea is that a healthy MEP band with a nerve branch and terminals that innervates an expendable muscle can be transplanted to a more functionally important denervated muscle for restoring its motor function. Our originally designed surgical procedure that involved implantation of a NMEG into a MEP-free area in the recipient muscle yielded encouraging functional recovery (67% of the control).<sup>6</sup> As MEP reinnervation is critical for motor recovery, we modified the surgical procedures by implanting the NMEG into the native motor zone (NMZ) of the target muscle. NMEG-NMZ technique resulted in better muscle reinnervation and functional recovery (82% of the control) as compared with our original NMEG implantation.<sup>7</sup> We hypothesized that the outcomes of NMEG-NMZ might be improved by using supplementary strategies that accelerate nerve regeneration and MEP reinnervation.

Among the strategies used for enhancing axon regeneration, electrical stimulation (ES) to the injured peripheral nerve is a promising approach. Several authors<sup>8-17</sup> have developed a clinically feasible technique of 1 hour low-frequency (20 Hz) ES of the proximal nerve stump just after surgical repair of a transected peripheral nerve to enhance peripheral nerve regeneration. The authors reported that intraoperative brief ES greatly accelerates axon outgrowth across the site of nerve repair and promotes functional recovery.<sup>12-15</sup>

The purpose of this study was to explore whether 1 hour low-frequency ES of the nerve branch innervating the NMEG pedicle has beneficial effects on the outcomes of NMEG-NMZ reinnervation.

## Materials and Methods

Experiments involved the use of 23 3-month-old female Sprague-Dawley rats (Taconic Laboratories, Cranbury, NJ) weighing between 200 and 250 g at initial operation. All procedures were approved by the Animal Care and Use Committee of Hackensack University Medical Center and the USAMRMC Animal Care and Use Review Office and adhered to the Guide for the Care and Use of Laboratory Animals published by National Research Council (US) Committee, 8th edition, National Academies Press (US), Washington, DC, 2011. The animals were housed at a constant temperature (22°C) on a 12-hour light-dark cycle and were provided with food and water. All efforts were made to minimize the number of animals and their suffering in the experiments.

### Surgical Procedures and Electrical Stimulation

Twenty-two rats were randomly divided into NMEG-NMZ ( $n = 15$ ) and denervation ( $n = 7$ ) groups. For NMEG-NMZ, sternohyoid (SH) and sternomastoid (SM) muscles were chosen to serve as a donor and recipient, respectively, because this model was used in our recent studies.<sup>7</sup>

Animals were anesthetized with an intraperitoneal injection of a mixture of ketamine (80 mg/kg) and xylazine (5 mg/kg) and operated on using aseptic technique. With the rat supine, a

midline cervical incision was made extending from the hyoid bone to the sternum to expose the right SM and SH muscles and their innervating nerves. All rats in both groups underwent denervation of the right SM by the excision of a 5-mm segment of its nerve just proximal to its motor point in the middle of the muscle under an Olympus SZX12 Stereo zoom surgical microscope (Olympus America Inc, Center Valley, Pennsylvania). The cut ends of the nerve were coagulated with a bipolar cautery to prevent nerve regeneration.

Immediately after muscle denervation by the excision of a segment of the native nerve to the right SM muscle, the rats in NMEG-NMZ group underwent NMEG-NMZ transplantation as described.<sup>7</sup> Briefly, the NMZs in the right SM and SH muscles were outlined during surgery according to the entry point of the motor branch into each muscle (►Fig. 1). A muscular defect with the same dimensions as the NMEG pedicle was made in the NMZ of the right denervated SM muscle. An NMEG pedicle was harvested from the NMZ of the SH in the middle portion of the right SH muscle. The nerve to the SH muscle was not transected but dissected free along with the NMZ and muscle fibers of that zone. The NMEG pedicle was composed of a block of muscle ( $\sim 6 \times 6 \times 3$  mm), a nerve branch and vessels, intramuscular axon terminals, and a MEP band with numerous neuromuscular junctions. The superficial muscle fibers on the ventral aspect of the NMEG pedicle were removed to create a denuded surface for better reconnection of SH nerve with target SM muscle.

After harvesting of the NMEG pedicle, brief low-frequency ES was performed. The SH nerve branch supplying the NMEG pedicle was placed on bipolar stainless steel hook electrodes and stimulated using a stimulation and recording system (National Instruments Corp, Austin, Texas) controlled by user-written LabVIEW software (National Instruments Corp). The nerve was stimulated for 1 hour with a continuous train of 20 Hz square pulses of 3 V, 0.1 millisecond<sup>8</sup> delivered by a stimulation and recording system (National Instruments Corp) controlled by user-written LabVIEW software (National Instruments Corp). The nerve distance between stimulating electrode and NMEG was  $\sim 5$  mm. Throughout the stimulation procedure, the muscle pedicle and its innervating SH nerve branch stimulated were regularly bathed with warm mineral oil. Immediately after nerve stimulation, the NMEG pedicle was embedded in the SM muscle defect and sutured with four to six 10-0 nylon microsutures (►Fig. 1). After surgery, the wound was closed in layers with interrupted simple sutures of 4-0 Prolene.

Three months after NMEG-NMZ transplantation and electrical stimulation, functional recovery, nerve regeneration, and muscle reinnervation were evaluated using electrophysiological, morphohistological, and immunohistochemical techniques. For each animal, contralateral intact SM served as a control.

### Maximal Tetanic Force Measurement

The rats in the NMEG-NMZ group were subjected to maximal tetanic force measurement to examine the degree of functional recovery of the reinnervated SM muscles. The details

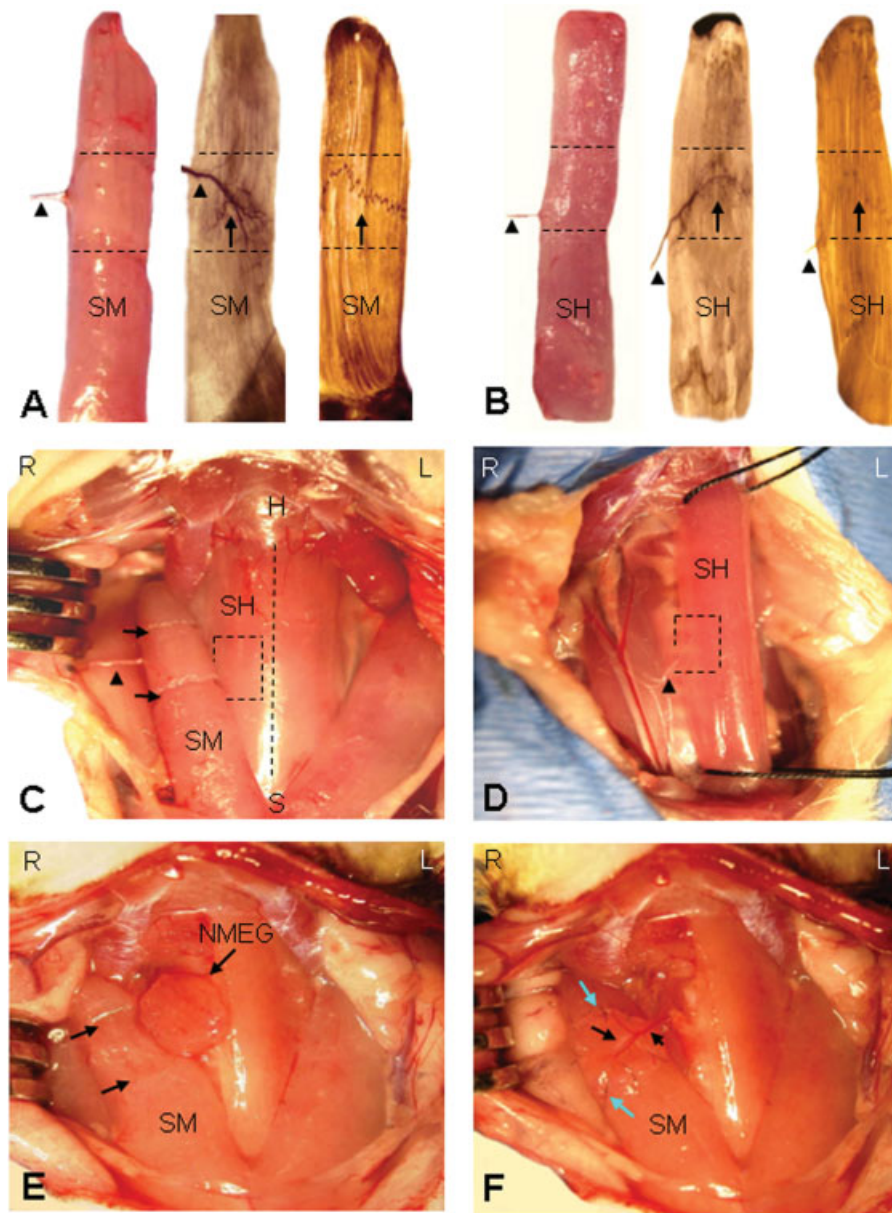


**Fig. 1** NMZs of recipient SM and donor SH muscles and operative procedures for NMEG-NMZ technique in the rat. (A) Removed right SM muscles, showing the NMZ (between dashed lines) of the muscle as indicated by motor point (arrowhead) in fresh muscle (left image), intramuscular nerve supply in Sihler's stained muscle (middle image), and MEP band in AChE-stained muscle (right image). (B) Removed right SH muscles, illustrating the NMZ of the muscle. (C) A photograph from a rat during surgery, showing surgically outlined NMZ in the right SM (between fiber cuts on the surface of the muscle as indicated by arrows) and in the SH (boxed region). The vertical dashed line indicates the midline. (D) Surgically outlined NMZ in the right SH muscle (boxed region). The right SM was removed to show the SH nerve (arrowhead). Note that either SM or SH is supplied by a single motor nerve branch (arrowheads in A–D) which enters into the middle portion of the muscle. (E) A NMEG pedicle was harvested from the NMZ of the right SH muscle and a muscular defect was made in the NMZ of the right SM muscle (between arrows). (F) The NMEG pedicle was implanted into the muscular defect made in the SM and sutured (pale arrows). Note that a nerve branch (large black arrow) and blood vessels (small black arrow) can be seen on the surface of the implanted NMEG pedicle. AChE, acetylcholinesterase; H, hyoid bone; L, left; MEP, motor endplate; NMEG, nerve–muscle–endplate band grafting; NMZs, native motor zones; R, right; S, sternum; SH, sternohyoid; SM, sternomastoid.

regarding force measurement have been given in our previous publications.<sup>6,7,18–23</sup> Briefly, the rostral tendon of the SM muscle was severed close to the insertion, tied with a 2–0 suture, and connected to a servomotor lever arm (model 305B Dual-Mode Lever Arm System; Aurora Scientific Inc, Aurora, Ontario, Canada) to record titanic force at optimal muscle length. Muscle force of the right SM was measured first by

stimulating with a bipolar electrode the SH nerve branch supplying the NMEG, whereas muscle force of the left control muscle was measured by stimulating the intact SM nerve. A stimulation and recording system (National Instruments Corp) controlled by user-written LabVIEW software (National Instruments Corp) was used to deliver biphasic rectangular pulses to the nerve stimulated.

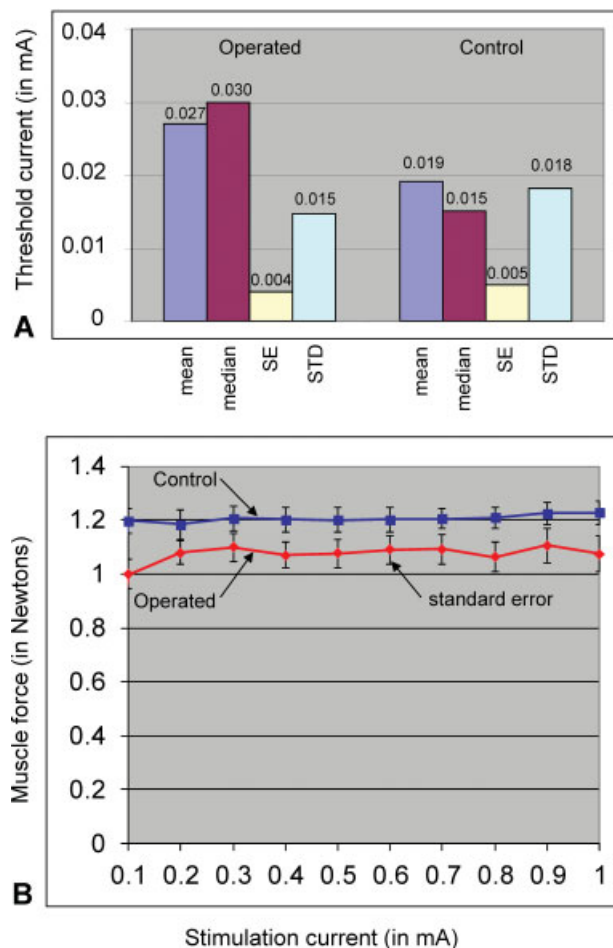


**Fig. 2** Muscle force recovery of the operated SM muscles as compared with the contralateral controls in rats. (A) Comparison of current thresholds eliciting muscle contraction between operated and control muscles. Note that operated SM muscles had a higher mean stimulation threshold to generate visible muscle contraction (mean, 0.027 mA) than contralateral control muscles (mean, 0.019 mA), but this difference did not reach statistical significance ( $p = 0.17$ ,  $t = 1.47$ , two-tailed, paired  $t$ -test). (B) Comparison of average muscle force between operated and control muscles. Maximal muscle force was computed as average muscle contraction to five stimulation currents ranging from 0.6 to 1.0 mA. Note that the mean maximal muscle force on the operated side (1.08 N) was 90% of that on the contralateral control side (1.21 N). Vertical bars represent the standard deviation of the mean. SM, sternomastoid.

Isometric contraction of the SM muscle was produced with 200-millisecond trains of biphasic rectangular pulses. The duration of each phase of stimulation pulse was set at 0.2 milliseconds and the train frequency was set at 200 pulses per second. The stimulation current was gradually increased until the tetanic force reached a plateau. A break of at least 1 minute was taken between two stimulations. The maximum value of muscle force during the 200-millisecond contraction was identified, as well as initial passive tension before stimulation. The difference between the maximal active force and the preloaded passive force was used as the muscle force measurement. The force generated by the contraction of the SM muscle was transduced with the

servomotor of a 305B lever system and displayed on a computer screen. At the moment of force measurement, the lever arm was stationary, and the muscle was adjusted to the optimal length for the development of maximum force. During the experiment, the rat was placed supine on a heating pad, and the core body temperature was monitored with a rectal thermistor and maintained at 36°C. The muscle connected at the distal end to a servomotor lever arm and nerve examined was bathed regularly with warmed mineral oil throughout the testing to maintain muscle temperature between 35 and 36°C.

The force data were obtained and processed by an acquisition system built from a multifunction I/O National Instruments Acquisition Board (NI USB-6251; 16-bit, 1.25 MS/s; National Instruments) connected to a Dell laptop with a custom-written program using LabVIEW 8.2 software. The system produced stimulation pulses, which, after isolation from the ground through an optical isolation unit (Analog Stimulus Isolator model 2200; AM Systems, Inc, Carlsborg, Washington), were used for the current controlled nerve stimulation. The acquisition system was also used to control muscle length and to collect a muscle force signal from the 305B Dual-Mode Lever System. Collected data were analyzed offline with DIAdem 11.0 software (National Instruments). Muscle force was reported as a ratio of the operated to the control side.

### Wet Muscle Weight Measurement and Tissue Preparation

After muscle force measurements, SM muscles on both sides in each rat were excised, photographed, and weighed. A muscle mass ratio was computed (muscle mass ratio = weight of operated muscle/weight of contralateral muscle).

Each of the removed SM muscles in both groups was divided into three segments: rostral, middle, and caudal. The muscle segments were then frozen in melting isopentane cooled with dry ice and cut on a cryostat (Reichert-Jung 1800; Mannheim, Germany) at  $-25^{\circ}\text{C}$ . The rostral and caudal segments were cut transversely and serial cross sections (10  $\mu\text{m}$ ) were stained with routine hematoxylin and eosin staining to examine muscle structure and myofiber morphology. The middle segment containing the NMZ and/or implanted NMEG was cut sagittally (60  $\mu\text{m}$ ) and stained using immunohistochemical methods to detect and quantify with ImageJ software regenerated axons and MEPs.

### Immunohistochemical Labeling of Regenerated Axons and Motor Endplates

Intramuscular axons and MEPs in the operated, control, and denervated SM muscles were detected with immunohistochemical methods as described later.<sup>7,23,24</sup>

### Neurofilament Staining

Some sagittal sections were immunostained with a monoclonal antibody phosphorylated neurofilament (NF) (SMI-31, Covance Research Products, Berkeley, CA) as a marker for all axons as described in our previous publications.<sup>7,23,24</sup> Briefly, the sections were treated in PBS containing 0.3%

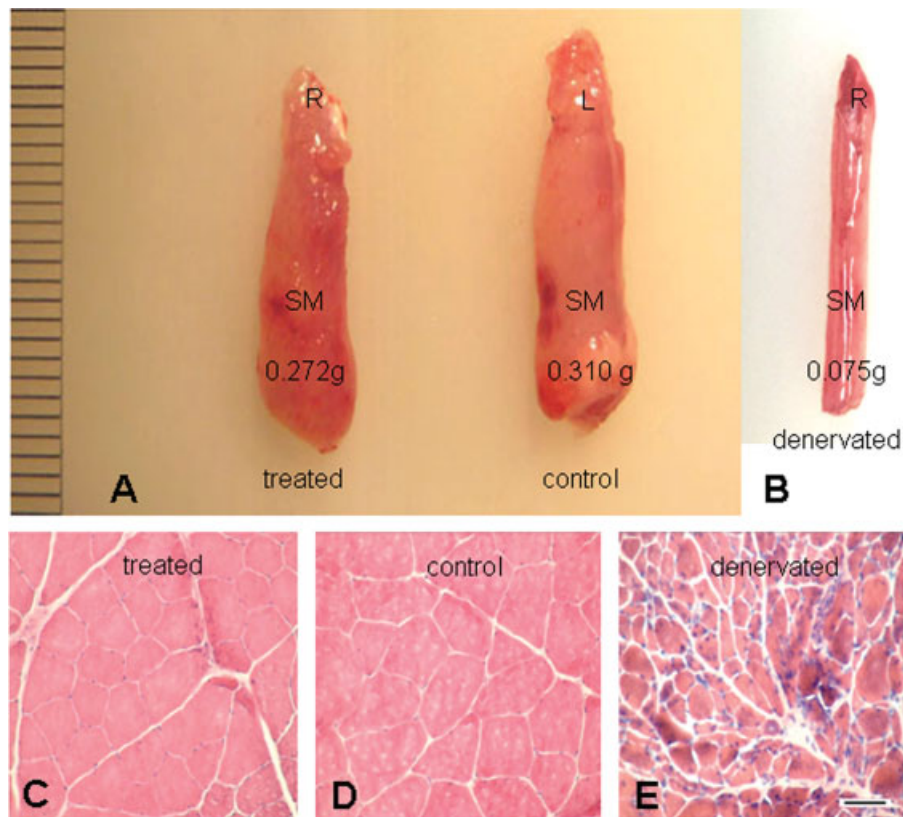


**Fig. 3** Comparison of muscle mass and histology among operated, control, and denervated SM muscles of rats. (A) The right operated and left control SM muscles from a rat 3 months after NMEG-NMZ transplantation and intraoperative 1 hour of electrical stimulation. Note that there is no significant difference in muscle mass between the R operated and L control muscles. (B) A denervated SM, noting that 3-month denervation resulted in a marked reduction of muscle mass as compared with the operated and control muscles. (C–E) Hematoxylin and eosin–stained cross sections from the (C) operated, (D) contralateral control, and (E) denervated SM muscles. Note that the operated SM had slight muscle fiber atrophy as compared with the control. The denervated SM exhibited significant muscle fiber atrophy. Bar = 100  $\mu$ m for (C) through (E). L, left; NMEG-NMZ, nerve–muscle–endplate band grafting–native motor zone; R, right; SM, sternomastoid.

triton and 2% bovine serum albumin for 30 minutes and incubated with primary antibody SMI-31 (dilution 1:800) in PBS containing 0.03% triton at 4°C overnight. The sections were then incubated for 2 hours with the biotinylated secondary antibody (antimouse, 1:1,000, Vector, Burlingame, CA). The incubated sections were processed with avidin–biotin complex method with a Vectastain ABC kit (1:1,000 ABC Elite, Vector) and reacted with diaminobenzidine–nickel as chromogen to visualize peroxidase labeling. Control sections were stained as described except that the incubation with the primary antibody was omitted.

For quantitative analysis, images were taken at  $\times 200$  with the aid of a USB digital microscope camera (INFINITY 3–3URC, Lumenera Corp., Ottawa, Canada) attached to a Zeiss fluorescence microscope (Axioplan-1; Carl Zeiss, Gottingen, Germany) and analyzed using ImageJ software (v. 1.45s; NIH, Bethesda, MD) as described in our publications.<sup>7,23</sup> The intramuscular axonal density was assessed by estimating the number of the NF-immunoreactive (NF-ir) axons and the area fraction of the axons within a section area (1.0 mm<sup>2</sup>). For a given muscle, three sections stained for NF were selected at different spatial levels to quantify NF-ir axons and areas. For each section, five microscopic fields with NF-ir axons were photographed. Areas with NF-positive staining

were outlined and measured with public domain ImageJ software. For each rat, the number and area fraction of the NF-ir axons in the treated muscle were compared with those in the contralateral control.

#### Double Fluorescence Labeling

Double fluorescence labeling was used to detect MEPs and their innervating axons in the NMZ of the SM muscles as described in our publications.<sup>7,23</sup> Briefly, some sagittal muscle sections were fixed in Zamboni fixative with 5% sucrose for 20 minutes at 4°C. The fixed sections were treated with 0.1 mol/L of glycine in 1.5 Tris buffer (pH 7.6) for 30 minutes and dipped in 100% methanol at – 20°C for 20 minutes. The sections were blocked in 1.5 Tris buffer containing 4% normal goat serum for 30 minutes and incubated overnight at 4°C with primary antibodies (SMI-31 to detect NFs and SMI-81 to label thinner axons; Covance Research Products Inc). The sections were then incubated at room temperature for 2 hours both with a secondary antibody (goat antimouse antibody conjugated to Alexa 488) and with  $\alpha$ -bungarotoxin conjugated with Alexa 596 (Invitrogen Corporation, Carlsbad, CA). The sections were washed several times with 1.5 Tris buffer with 0.05% Tween-20 between steps and the stained sectioned were coverslipped.

The stained sections were viewed under a Zeiss fluorescence microscope and photographed using USB 3.0 digital microscope camera. SMI-31 and SMI-81 detected axons (green), while  $\alpha$ -bungarotoxin-labeled postsynaptic acetylcholine receptor site in the MEPs (red). For each muscle sample, at least 100 labeled MEPs were randomly selected from stained sections to determine the percentages of the innervated (visible axon attachment) and noninnervated (no visible axon attachment) MEPs.

### Data Analysis

Force values, muscle weights, the number and the area fraction of NF-ir axons, and innervated and noninnervated MEPs of the operated and unoperated SM muscles in each rat were computed. The variables of the reinnervated SM muscles were expressed as the percentages of the values of the contralateral control muscles. Data were presented as mean  $\pm$  standard deviation. The Student's *t* test (paired, two-tailed) was used to compare differences in the mean values of the variables examined between operated and unoperated SM muscles. A difference was considered statistically significant at  $p < 0.05$ .

## Results

### Functional Recovery of the Treated Muscles

Maximal muscle force was successfully measured from both sides in 14 rats treated with NMEG-NMZ plus intraoperative 1-hour ES. As reported in our previous publications,<sup>6,7,18-23</sup> muscle force was measured when muscle was stretched at optimal tension of 0.08 N. There was a higher average threshold of nerve stimulation current to generate muscle contraction for operated muscles (mean, 0.027 mA) than control muscles (mean, 0.019 mA), but this difference did not reach statistical significance ( $p = 0.17$ ,  $t = 1.47$ , two-tailed, paired *t*-test) (**Fig. 2A**). Increasing stimulation current was accompanied by a greater muscle force until it reached horizontal asymptote. Stimulation current  $\geq 0.2$  mA produced maximal muscle force in operated muscle, whereas  $\geq 0.1$  mA in control muscle.

Maximal muscle force was calculated as average muscle contraction to five stimulation currents ranging from 0.6 to 1.0 mA. For each rat, the percentage of functional recovery of the treated SM muscles was determined as compared with the force value of the contralateral control muscle. The treated SM muscles produced 90% of the maximal tetanic tension of the contralateral control muscles (**Fig. 2B**). Averaged maximal muscle force at the treated side was 1.08 N, whereas 1.21 N at the contralateral control side. The difference between these averages (0.13 N) was statistically significant ( $p = 0.035$ ,  $t = 2.35$ , two-tailed, paired *t*-test).

### Wet Muscle Weight and Muscle Histology

Wet muscle weight and myofiber morphology are indicators for the effectiveness of muscle reinnervation. In this study, the size of the treated SM was similar to that of the contralateral control, but larger than that of 3-month-denervated SM (**Fig. 3A, B**). Specifically, the mean wet weight of the treated

**Table 1** Wet muscle weight of right treated and left control SM muscles of rats ( $n = 15$ )

Animal (No.)	Body weight (g)	Right treated SM (g)	Left control SM (g)
1	337	0.276	0.296
2	345	0.320	0.336
3	385	0.272	0.310
4	388	0.264	0.350
5	364	0.266	0.362
6	356	0.284	0.315
7	370	0.300	0.355
8	342	0.383	0.412
9	346	0.353	0.384
10	343	0.319	0.339
11	320	0.317	0.336
12	325	0.361	0.386
13	305	0.301	0.305
14	338	0.327	0.349
15	311	0.298	0.328
Average	345	0.309	0.344
SD	24.6	0.036	0.032
Ratio, %		90	100

Abbreviations: SM, sternomastoid; SD, standard deviation.

SM muscles (0.309 g) was 90% of the control muscles (0.344 g) (**Table 1**), whereas that of the denervated SM muscles was 0.138 g. The mean wet weight of treated SM muscles was much higher than that of the denervated SM muscles ( $p < 0.0001$ ).

Hematoxylin and eosin-stained cross muscle sections showed the histological profiles of the treated, control, and denervated SM muscles. The treated SM (**Fig. 3C**) exhibited better muscle structure and myofiber morphology with less fiber atrophy as compared with the contralateral control (**Fig. 3D**) and denervated muscle which exhibited prominent fiber atrophy (**Fig. 3E**).

### Regenerated Axons and Innervated Motor Endplates in the Treated Muscles

Microscopic imaging of the sagittal sections processed with NF staining showed that NF-ir axons were confined in the NMZ of the treated and contralateral control SM muscles. By counting NF-ir axons (green) per field at  $\times 200$  magnification, we observed that in the treated SM, the regenerating axons from the implanted NMEG supplied the NMZ of the treated muscle. The mean number and area fraction of the NF-ir axons in the treated SM muscles were measured to be 81 and 84% of the contralateral control muscles (**Fig. 4** and **Table 2**), respectively.

Double fluorescence labeling showed the innervated and noninnervated MEPs (**Fig. 5**). In the SM muscles cotreated

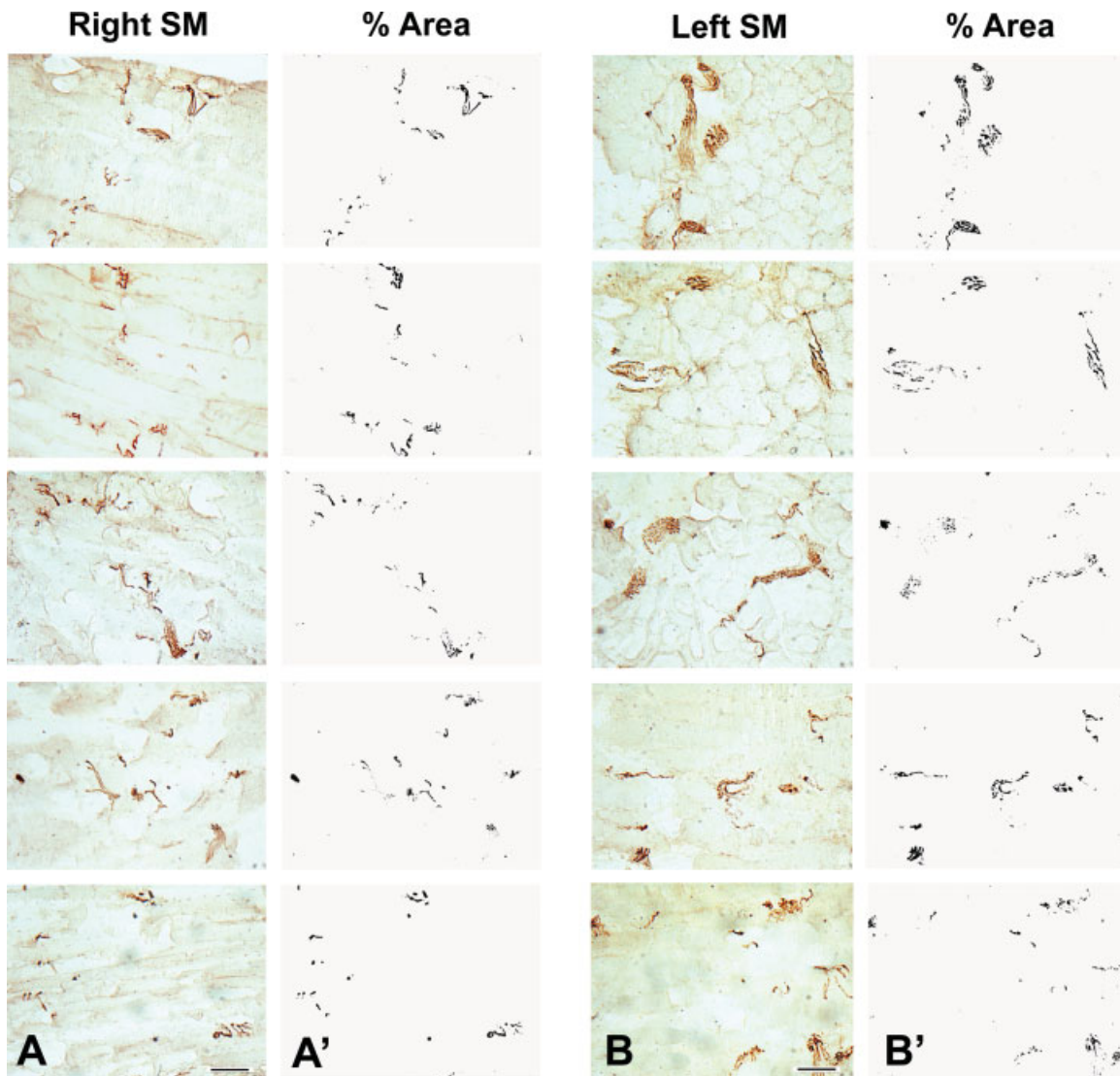


**Fig. 4** Photomicrographs of sagittal sections immunostained for NF from the right operated and left control SM muscles of the rat number 3. (A) Photographs were taken from five microscopic fields in a stained section from the right operated SM (first column), showing the NF-positive axons. (A') The photographs in the first column were converted to black and white (second column) by the use of ImageJ software to compute the number and percentage of area of the regenerated axons. (B–B') Photographs from the left control SM. Bar = 100  $\mu$ m. For this rat, as compared with the left control SM (mean axon count, 913; mean area, 0.946) the right operated SM exhibited good muscle reinnervation as indicated by the mean axon count (725, 79% of the control) and mean area (0.728, 77% of the control). NF, neurofilament; SM, sternomastoid.

with NMEG-NMZ and brief ES, the regenerated axons were identified in the NMZ of the target muscle to innervate the denervated MEPs (**Fig. 5A–J**). On average, 83% of the denervated MEPs in the treated muscles were reinnervated by regenerated axons and only 17% of the MEPs were unoccupied by axons. In the treated muscles, innervated and noninnervated MEPs (**Fig. 5A–E**), small newly formed MEPs (**Fig. 5F, G**), and axonal sprouts (**Fig. 5H, I**) were identified. Terminal axons within the innervated MEPs were visualized (**Fig. 5J**). In 3-month-denervated muscles, denervated MEPs were still present and remained noninnervated. A few fragments and/or accumulations of axon debris and noninnervated MEPs (no visible axon attachment) were observed (**Fig. 5K, L**).

## Discussion

To our knowledge, this is the first study to combine NMEG-NMZ reinnervation technique with intraoperative brief (1 hour) low-frequency (20 Hz) ES for muscle reinnervation. Our study demonstrated that NMEG-NMZ plus brief ES resulted in extensive axonal regeneration (mean number of the regenerated axons, 81% of the control), well-preserved muscle mass (mean muscle weight, 90% of the control), and optimal functional motor recovery (mean maximal tetanic force, 90% of the control). The majority of MEPs (83%) in the treated muscles regained motor innervation.

Muscle paralysis caused by PNI is frequently treated with nerve anastomosis, nerve transfer, nerve grafting, direct

**Table 2** Comparison of count and percentage of area of neurofilament-immunoreactive axons between right treated and left control SM muscles in rats ( $n = 15$ )

Animal (no.)	Right SM		Left SM		Ratio (R/L)	
	Count	Percentage of area	Count	Percentage of area	Count	Percentage of area
1	559	0.721	798	0.945	0.701	0.763
2	670	0.640	729	0.724	0.919	0.884
3	725	0.728	913	0.946	0.794	0.770
4	630	0.621	824	0.789	0.765	0.787
5	610	0.658	816	0.827	0.748	0.796
6	655	0.710	904	0.900	0.725	0.789
7	978	0.697	1,014	0.811	0.964	0.859
8	601	0.803	988	0.970	0.608	0.828
9	894	1.060	1,043	1.200	0.857	0.883
10	792	0.736	967	0.856	0.819	0.860
11	993	1.102	1,103	1.205	0.900	0.915
12	839	0.735	993	0.840	0.845	0.875
13	1,008	0.833	1,186	0.997	0.850	0.836
14	781	0.638	883	0.704	0.884	0.906
15	683	0.596	837	0.698	0.816	0.854
Average	761	0.752	933	0.894	0.813	0.840
SD	151	0.149	125	0.156	0.093	0.051

Abbreviations: L, left; R, right; SD, standard deviation.

nerve implantation, and many others.<sup>25,26</sup> Despite advances in microsurgical techniques for nerve repair, functional recovery is frequently poor. Therefore, restoration of useful function after PNI is a major challenge for reconstructive surgery and rehabilitation medicine.<sup>27</sup> Many studies have demonstrated that functional motor recovery after PNI and nerve repair is primarily determined by the absolute number of regenerated motor axons that reach target and the time to MEP reinnervation.<sup>2-5</sup> Our research efforts focus on creating strategies for MEP reinnervation to treat muscle paralysis caused by PNIs. We have demonstrated the importance of MEP reinnervation in motor recovery of the target muscle. For example, 3 months after transplantation of the NMEG into a MEP-free area, the mean maximal tetanic force of the treated muscles was 67% of the controls.<sup>6</sup> In contrast, transplantation of the NMEG into the NMZ of the target muscle yielded better functional recovery (mean maximal tetanic force, 82% of the control).<sup>7</sup> In addition, direct nerve implantation into the NMZ<sup>23</sup> also resulted in satisfactory muscle reinnervation and functional recovery. These findings suggest that NMZ in the target muscle is the best region for muscle reinnervation.

Optimal axon regeneration, MEP reinnervation, and muscle force recovery observed in this study should be attributed to several factors. First, NMEG-NMZ procedure shortens nerve regeneration distances and facilitates rapid axon-MEP connections. As the NMEG pedicle from the donor muscle was transplanted into the NMZ of the recipient

muscle, the regenerating axons derived from the transplant could easily reach and reinnervate the denervated MEPs in the target muscle. Second, the NMEG pedicle harvested from the NMZ of the donor muscle provides an abundant source of nerve terminals for axonal regeneration. Finally, there are sufficient pedicle-recipient muscle interfaces that favor axons to regenerate at multiple points and reinnervate the denervated MEPs in the target muscle. The re-established functional synapses could avoid muscle atrophy and achieve optimal functional recovery. Our findings suggest that the combination of NMEG-NMZ with 1 hour 20-Hz ES could be an option for muscle reinnervation.

Despite the regenerative capacity of injured peripheral nerves, functional recovery remains suboptimal after primary nerve repair.<sup>28-30</sup> There is an increasing interest in using brief low-frequency ES to enhance nerve regeneration for improving functional recovery after nerve transection and microsurgical repair. Recent work by Al-Majed et al (2000a)<sup>8</sup> has demonstrated that 1 hour of 20-Hz ES of the proximal stump of a transected and repaired peripheral nerve in the rat accelerates axon regeneration. The 20-Hz frequency of ES was chosen as it is the mean frequency of action potential generation in motoneurons<sup>31</sup> and 1 hour ES is considered to be a clinically feasible period in the operating room for human nerve surgical repair.<sup>8,17</sup> ES at a frequency of 20 Hz for 1 hour accelerates axon outgrowth across the site of surgical repair of transected nerve stumps, resulting in accelerated target muscle reinnervation. As

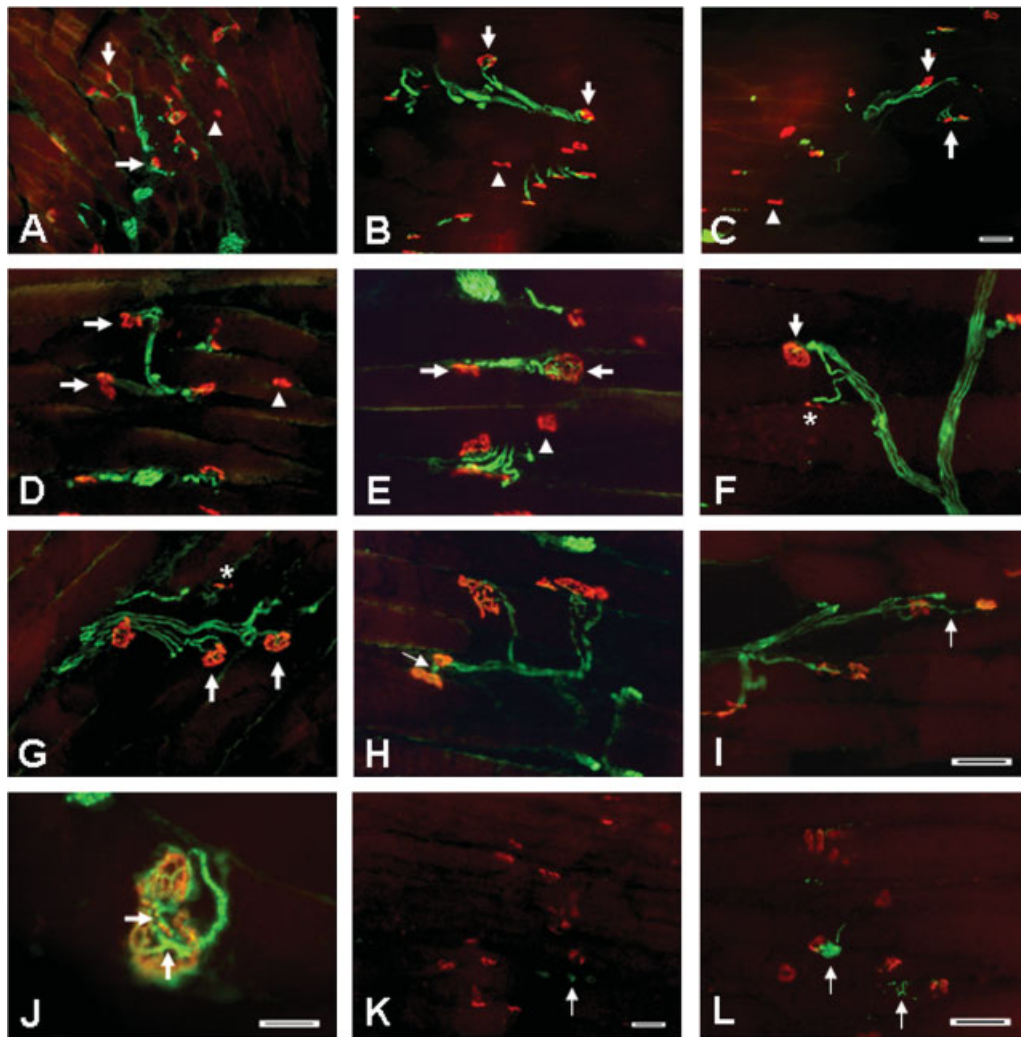


**Fig. 5** Images of double immunofluorescence staining of sagittal sections (A–J) from right operated SM muscle of a rat cotreated with NMEG-NMZ implantation and intraoperative 1-hour of electrical stimulation and (K–L) from a denervated SM muscle. (A–C) Low-power view of the stained sections, showing the distribution of MEPs and axons in the NMZ of the operated muscle. Note that the majority of the MEPs in the operated SM were reinnervated by regenerated axons (arrows). The noninnervated MEPs were indicated by arrowheads. Bar = 100  $\mu$ m for A through C. (D–I) High-power view of the stained sections, showing innervated (arrows) and noninnervated (arrowheads) (D and E) MEPs, (F and G) small newly formed MEPs (asterisks), and (H and I) ultraterminal sprouts (arrows). Bar = 100  $\mu$ m for D through I. (J) Closeup photograph of an innervated MEP, showing terminal axons (arrows) and acetylcholine receptors at the MEP. Bar = 50  $\mu$ m. (K–L) Immunostained sections from a rat SM muscle denervated for 3 months. Note that only a few fragments and/or accumulations of neurofilament-immunoreactive decomposed nerve fibers (arrows) and noninnervated MEPs (no visible axon attachment) were observed. Bar = 100  $\mu$ m. MEPs, motor endplates; NMEG-NMZ, nerve-muscle-endplate band grafting-native motor zone; SM, sternomastoid.

reported, the percentage of regenerating neurons innervating the target muscle increased from 40% without ES to 75% with ES.<sup>11</sup> These beneficial effects have been documented to be associated with a faster and enhanced upregulation of brain-derived neurotrophic factor and its tyrosine kinase B receptor in motoneurons.<sup>9,32</sup> The efficacy of the 1 hour of ES of the proximal stump of an injured nerve in promoting axon outgrowth has been confirmed not only in acute animal experiments performed in many independent studies<sup>8–16,32–39</sup> but also in delayed nerve repair model<sup>40</sup> and in human studies.<sup>41</sup> As reported by Gordon et al (2010),<sup>41</sup> the 1 hour of 20-Hz ES of the median nerve after carpal tunnel release surgery in humans also resulted in earlier recovery of muscle reinnervation and sensory com-

pound action potentials. These findings indicate that the brief low-frequency ES could become a clinically useful therapeutical approach for accelerating axon regeneration and muscle reinnervation. The combination of nerve reconstruction surgery with brief ES appears to be effective for maximizing postoperative functional recovery.

## Conclusion

First, the NMZ of the target muscle is an ideal site for implantation of NMEG and for the development of novel strategies to treat muscle paralysis caused by PNIs. Regenerating axons from a NMEG or a nerve stump implanted into the NMZ of the target muscle could easily reach and

reinnervate the denervated MEPs, re-establishing functional synapses.

Second, MEP reinnervation is critical for motor functional recovery after PNI and nerve reconstruction. This study showed that the majority (83%) of MEPs in the muscles treated with NMEG-NMZ and brief ES regained motor innervation. This is most likely due to such a fact that the NMEG-NMZ procedure physically shortens regeneration distances and facilitates rapid MEP reinnervation, thereby avoiding irreversible loss of the denervated MEPs in the target muscle.

Third, the outcomes of NMEG-NMZ technique can be further improved by a combination of NMEG-NMZ technique with intraoperative brief ES. Future directions will be to build upon this combination strategy, with other therapies targeted to various aspects of axonal regeneration.

Finally, although our experiments showed the potential of NMEG-NMZ in immediate muscle reinnervation, further work is needed to determine if the combination of NMEG-NMZ with brief ES has the potential for delayed reinnervation that is not uncommon in clinical practice.

#### Acknowledgments

This work was supported by the Office of the Assistant Secretary of Defense for Health Affairs under Award No. W81XWH-14-1-0442 (to Dr. Liancai Mu). The U.S. Army Medical Research Acquisition Activity, 820 Chandler Street, Fort Detrick, MD 21702-5014 is the awarding and administering acquisition office. Opinions, interpretations, conclusions, and recommendations are those of the authors and are not necessarily endorsed by the Department of Defense. In conducting research using animals, the investigators adhere to the laws of the United States and regulations of the Department of Agriculture. This protocol was approved by the USAMRMC Animal Care and Use Review Office for the use of rats. The authors thank the anonymous reviewers for their constructive comments on the article.

#### References

- Kelsey J, Praemer A, Nelson L, Felberg A, Rice D. Upper Extremity Disorders: Frequency, Impact, and Cost. London: Churchill-Livingstone; 1997
- Payne SH Jr, Brushart TM. Neurotization of the rat soleus muscle: a quantitative analysis of reinnervation. *J Hand Surg Am* 1997; 22(04):640-643
- Park DM, Shon SK, Kim YJ. Direct muscle neurotization in rat soleus muscle. *J Reconstr Microsurg* 2000;16(05):379-383
- Ma CHE, Omura T, Cobos EJ, et al. Accelerating axonal growth promotes motor recovery after peripheral nerve injury in mice. *J Clin Invest* 2011;121(11):4332-4347
- Barbour J, Yee A, Kahn LC, Mackinnon SE. Supercharged end-to-side anterior interosseous to ulnar motor nerve transfer for intrinsic musculature reinnervation. *J Hand Surg Am* 2012; 37(10):2150-2159
- Mu L, Sobotka S, Su H. Nerve-muscle-endplate band grafting: a new technique for muscle reinnervation. *Neurosurgery* 2011; 69(2, Suppl Operative):ons208-ons224, discussion ons224
- Mu L, Sobotka S, Chen J, Nyirenda T. Reinnervation of denervated muscle by implantation of nerve-muscle-endplate band graft to the native motor zone of the target muscle. *Brain Behav* 2016; in press
- Al-Majed AA, Neumann CM, Brushart TM, Gordon T. Brief electrical stimulation promotes the speed and accuracy of motor axonal regeneration. *J Neurosci* 2000a;20(07):2602-2608
- Al-Majed AA, Brushart TM, Gordon T. Electrical stimulation accelerates and increases expression of BDNF and trkB mRNA in regenerating rat femoral motoneurons. *Eur J Neurosci* 2000b; 12(12):4381-4390
- Brushart TM, Hoffman PN, Royall RM, Murinson BB, Witzel C, Gordon T. Electrical stimulation promotes motoneuron regeneration without increasing its speed or conditioning the neuron. *J Neurosci* 2002;22(15):6631-6638
- Brushart TM, Jari R, Verge V, Rohde C, Gordon T. Electrical stimulation restores the specificity of sensory axon regeneration. *Exp Neurol* 2005;194(01):221-229
- Gordon T, Sulaiman O, Boyd JG. Experimental strategies to promote functional recovery after peripheral nerve injuries. *J Peripher Nerv Syst* 2003;8(04):236-250
- Gordon T, Brushart TM, Amirjani N, Chan KM. The potential of electrical stimulation to promote functional recovery after peripheral nerve injury-comparisons between rats and humans. *Acta Neurochir Suppl (Wien)* 2007;100:3-11
- Gordon T, Brushart TM, Chan KM. Augmenting nerve regeneration with electrical stimulation. *Neurol Res* 2008;30(10):1012-1022
- Gordon T, Chan KM, Sulaiman OA, Udina E, Amirjani N, Brushart TM. Accelerating axon growth to overcome limitations in functional recovery after peripheral nerve injury. *Neurosurgery* 2009; 65(Suppl):A132-A144
- Gordon T, Sulaiman OA, Ladak A. Chapter 24: electrical stimulation for improving nerve regeneration: where do we stand? *Int Rev Neurobiol* 2009;87:433-444
- Gordon T, English AW. Strategies to promote peripheral nerve regeneration: electrical stimulation and/or exercise. *Eur J Neurosci* 2016;43(03):336-350
- Sobotka S, Mu L. Characteristics of tetanic force produced by the sternomastoid muscle of the rat. *J Biomed Biotechnol* 2010; 2010:194984
- Sobotka S, Mu L. Force characteristics of the rat sternomastoid muscle reinnervated with end-to-end nerve repair. *J Biomed Biotechnol* 2011;2011:173471
- Sobotka S, Mu L. Force recovery and axonal regeneration of the sternomastoid muscle reinnervated with the end-to-end nerve anastomosis. *J Surg Res* 2013;182(02):e51-e59
- Sobotka S, Mu L. Comparison of muscle force after immediate and delayed reinnervation using nerve-muscle-endplate band grafting. *J Surg Res* 2013;179(01):e117-e126
- Sobotka S, Mu L. Muscle reinnervation with nerve-muscle-endplate band grafting technique: correlation between force recovery and axonal regeneration. *J Surg Res* 2015;195(01):144-151
- Sobotka S, Chen J, Nyirenda T, Mu L. Outcomes of muscle reinnervation with direct nerve implantation into the native motor zone of the target muscle. *J Reconstr Microsurg* 2017; 33(02):77-86
- Mu L, Chen J, Sobotka S, et al; Arizona Parkinson's Disease Consortium. Alpha-synuclein pathology in sensory nerve terminals of the upper aerodigestive tract of Parkinson's disease patients. *Dysphagia* 2015;30(04):404-417
- Lee SK, Wolfe SW. Peripheral nerve injury and repair. *J Am Acad Orthop Surg* 2000;8(04):243-252
- Siemionow M, Brzezicki G. Chapter 8: current techniques and concepts in peripheral nerve repair. *Int Rev Neurobiol* 2009; 87:141-172
- Lundborg G. Richard P. Bunge memorial lecture. Nerve injury and repair—a challenge to the plastic brain. *J Peripher Nerv Syst* 2003; 8(04):209-226

- 28 Terzis JK, Smith KL. *The Peripheral Nerve: Structure, Function and Reconstruction*. New York: NY; Raven; 1990
- 29 Kim DH, Han K, Tiel RL, Murovic JA, Kline DG. Surgical outcomes of 654 ulnar nerve lesions. *J Neurosurg* 2003;98(05):993–1004
- 30 Kim DH, Cho YJ, Tiel RL, Kline DG. Outcomes of surgery in 1019 brachial plexus lesions treated at Louisiana State University Health Sciences Center. *J Neurosurg* 2003;98(05):1005–1016
- 31 Burke RE. Motor units: anatomy, physiology and functional organization. In: *Handbook of Physiology. The Nervous System. Motor Control, Sect. 1, Vol. 1*. Bethesda, MD: American Physiological Society; 1981:345–422
- 32 Al-Majed AA, Tam SL, Gordon T. Electrical stimulation accelerates and enhances expression of regeneration-associated genes in regenerating rat femoral motoneurons. *Cell Mol Neurobiol* 2004;24(03):379–402
- 33 Ahlborn P, Schachner M, Irintchev A. One hour electrical stimulation accelerates functional recovery after femoral nerve repair. *Exp Neurol* 2007;208(01):137–144
- 34 English AW, Schwartz G, Meador W, Sabatier MJ, Mulligan A. Electrical stimulation promotes peripheral axon regeneration by enhanced neuronal neurotrophin signaling. *Dev Neurobiol* 2007; 67(02):158–172
- 35 Hetzler LE, Sharma N, Tanzer L, et al. Accelerating functional recovery after rat facial nerve injury: effects of gonadal steroids and electrical stimulation. *Otolaryngol Head Neck Surg* 2008; 139(01):62–67
- 36 Lal D, Hetzler LT, Sharma N, et al. Electrical stimulation facilitates rat facial nerve recovery from a crush injury. *Otolaryngol Head Neck Surg* 2008;139(01):68–73
- 37 Asensio-Pinilla E, Udina E, Jaramillo J, Navarro X. Electrical stimulation combined with exercise increase axonal regeneration after peripheral nerve injury. *Exp Neurol* 2009;219(01): 258–265
- 38 Sharma N, Coughlin L, Porter RG, et al. Effects of electrical stimulation and gonadal steroids on rat facial nerve regenerative properties. *Restor Neurol Neurosci* 2009;27(06):633–644
- 39 Singh B, Xu QG, Franz CK, et al. Accelerated axon outgrowth, guidance, and target reinnervation across nerve transection gaps following a brief electrical stimulation paradigm. *J Neurosurg* 2012;116(03):498–512
- 40 Elzinga K, Tyreman N, Ladak A, Savaryn B, Olson J, Gordon T. Brief electrical stimulation improves nerve regeneration after delayed repair in Sprague Dawley rats. *Exp Neurol* 2015;269:142–153
- 41 Gordon T, Amirjani N, Edwards DC, Chan KM. Brief post-surgical electrical stimulation accelerates axon regeneration and muscle reinnervation without affecting the functional measures in carpal tunnel syndrome patients. *Exp Neurol* 2010;223(01): 192–202

# Outcomes of Muscle Reinnervation with Direct Nerve Implantation into the Native Motor Zone of the Target Muscle

Stanislaw Sobotka, PhD, DSc<sup>1,2</sup> Jingming Chen, MD<sup>1</sup> Themba Nyirenda, PhD<sup>1</sup> Liancai Mu, MD, PhD<sup>1</sup>

<sup>1</sup>Department of Research, Hackensack University Medical Center, Upper Airway Research Laboratory, Hackensack, New Jersey

<sup>2</sup>Department of Neurosurgery, Icahn School of Medicine at Mount Sinai, New York, New York

Address for correspondence Stanislaw Sobotka, PhD, DSc, Department of Research, Hackensack University Medical Center, 30 Prospect Ave, Hackensack, NJ 07601 (e-mail: stanislaw.sobotka@mountsinai.org).

J Reconstr Microsurg 2017;33:77–86.

## Abstract

**Background** Our recent work has demonstrated that the native motor zone (NMZ) within a given skeletal muscle is the best site for muscle reinnervation. This study was designed to explore the outcomes of direct nerve implantation (DNI) into the NMZ of denervated sternomastoid (SM) muscle in a rat model.

**Methods** The right SM muscle was experimentally denervated by transecting its innervating nerve. The proximal stump of the severed SM nerve was immediately implanted into a small muscle slit made in the NMZ of the muscle where denervated motor endplates were concentrated. The outcomes of DNI-NMZ reinnervation were evaluated 3 months after surgery. Specifically, the degree of functional recovery was examined with muscle force measurement. The extent of nerve regeneration and endplate reinnervation was assessed using histological and immunohistochemical methods.

**Results** This study showed that the mean muscle force of the treated muscles was 64% of the contralateral control. Reinnervated SM muscles weighed 71% of the weight of the control muscles. Abundant regenerated axons were identified in the NMZ of the target muscle. The mean number and area of the regenerated axons in the treated muscles was computed to be 62% and 51% of the control muscles, respectively. On average, 66% of the denervated endplates in the treated muscles were reinnervated by regenerated axons.

**Conclusion** Our results suggest that the NMZ within a muscle is an ideal site for endplate reinnervation and satisfactory functional recovery. Further studies are needed to promote the efficacy of DNI-NMZ technique for muscle reinnervation.

## Keywords

- ▶ direct nerve implantation
- ▶ nerve regeneration
- ▶ muscle force measurement

Peripheral nerve injuries (PNIs) are very common in both military<sup>1</sup> and civil<sup>2,3</sup> circumstances. Current nerve repair methods include nerve end-to-end anastomosis, end-to-side neurorrhaphy, nerve grafting, nerve transfer, muscular neurotization, tubulization techniques, and many others.<sup>4–9</sup> Unfortunately, the currently used methods result in poor

muscle reinnervation and functional recovery. Therefore, there is a great need to seek new strategies for the treatment of PNI-related muscle paralysis.

Direct nerve implantation (DNI) or muscular neurotization is commonly performed when the distal stump of the injured nerve is not available for nerve repair.<sup>8,10</sup> The proximal stump

received

May 12, 2016

accepted after revision

August 1, 2016

published online

October 13, 2016

Copyright © 2017 by Thieme Medical Publishers, Inc., 333 Seventh Avenue, New York, NY 10001, USA.  
Tel: +1(212) 584-4662.

DOI <http://dx.doi.org/10.1055/s-0036-1592362>.  
ISSN 0743-684X.

of the original nerve or a healthy but less valuable foreign motor nerve can be implanted into a denervated muscle to restore its motor function. DNI has been used for selective reinnervation of paralyzed laryngeal and facial muscles<sup>11,12</sup> as well as the extremities.<sup>8,10</sup> However, further studies are needed to determine the potential of DNI in muscle reinnervation and functional recovery.

Our recent study has demonstrated that the native motor zone (NMZ) of the target muscle is the best site for muscle reinnervation.<sup>13</sup> The concept is that the NMZ in a muscle contains numerous motor endplates which are preferentially reinnervated. Previous studies showed that after nerve injury regenerating axons preferentially grow into and reinnervate the regions of the original endplates.<sup>14–18</sup> Using DNI model, some investigators observed preferential reinnervation of the native endplates in the target muscle by abundant regenerating axons and sprouts.<sup>19,20</sup> However, little is known whether DNI-NMZ reinnervation could result in satisfactory functional recovery.

This study was designed to test our hypothesis that better functional outcome could be achieved by implanting a nerve stump into the NMZ of the target muscle. The reinnervated muscles were assessed using morphological, immunohistochemical, and electrophysiological techniques to determine the extent of muscle reinnervation and functional recovery.

## Materials and Methods

### Animals

Experiments were performed on 3-month-old female Sprague-Dawley rats (Taconic Laboratories, Cranbury, NJ) with body masses ranging from 200 to 250 g at initial operation. The experiments and procedures were ethically reviewed and approved by the Institutional Animal Care and Use Committee prior to the onset of experiments. All animals were handled in accordance with the Guide for Care and Use of Laboratory Animals published by the United States National Institutes of Health (NIH Publication no. 85–23, revised 1996). The animals were housed at a constant temperature (22°C) on a 12 hour light–dark cycle and were provided with food and water in the state of the art animal housing facilities of Hackensack University Medical Center.

### Direct Nerve Implantation-Native Motor Zone Procedures

A total of 15 animals were used to perform the DNI-NMZ procedure. The right sternomastoid (SM) muscle was experimentally denervated and reinnervated with DNI-NMZ. As SM muscle model was used in our previous muscle reinnervation studies,<sup>21–27</sup> there is a solid database regarding its innervation pattern and contractile properties available for comparison.

Surgical procedures were conducted under aseptic conditions. Animals underwent general anesthesia with a mixture of ketamine (80 mg/kg body weight) and xylazine (5 mg/kg body weight) administered intraperitoneally. A midline cervical incision was made extending from the hyoid bone to the sternum to expose the right SM muscle and its innervating nerve under an operating microscope. The right SM muscle

was denervated by transecting its innervating nerve at its entrance to the muscle. The proximal stump of the severed nerve was immediately buried into a small slit made in the NMZ of the denervated SM muscle and secured in position with an epineurial suture of 10–0 nylon (–Fig. 1). After surgery, the wound was closed.

Additional control study was run on 17 denervated rats in an identical experimental setup to that described earlier. The only difference between the surgery in the control and the DNI-NMZ groups was that in the control group after denervation rats were not subjected to the DNI-NMZ reinnervation. The right SM muscle was denervated by resecting a 5 mm segment of its innervating nerve and the cut ends of the nerve were then coagulated with a bipolar cautery to prevent nerve regeneration.

At the end of the 3-month recovery period, all experimental animals underwent postoperative evaluations to assess functional recovery, nerve regeneration, and muscle reinnervation. For each animal, contralateral intact SM served as a control.

### Maximal Tetanic Force Measurement

The degree of functional recovery of the reinnervated SM was detected using muscle force measurement as previously reported in our previous publications<sup>21,24–27</sup> and others.<sup>12,28,29</sup> Briefly, SM was exposed and dissected. The rostral tendon of the muscle was severed close to the insertion, tied with a 2–0 suture, and connected to a servomotor lever arm (model 305B Dual-Mode Lever Arm System; Aurora Scientific Inc, Aurora, Ontario, Canada). The SM nerve on each side was stimulated using a bipolar stimulating electrode.

A stimulation and recording system (National Instruments Corp, Austin, TX) controlled by user-written LabVIEW software (National Instruments Corp) was used to deliver biphasic rectangular pulses to the nerve stimulated. Isometric contraction of the SM muscle was produced with 200-millisecond trains of biphasic rectangular pulses. The duration of each phase of stimulation pulse was set at 0.2 milliseconds and the train frequency was set at 200 pulses per second. The stimulation current was gradually increased until the tetanic force reached a plateau. A break of at least 1 minute was taken before the next measurement was attempted. The maximum value of muscle force during the 200-millisecond contraction was identified, as well as initial passive tension before stimulation. The difference between the maximal active force and the preloaded passive force was used as the muscle force measurement. The force generated by the contraction of the SM muscle was transduced with the servomotor of a 305B lever system and displayed on a computer screen. At the moment of force measurement, the lever arm was stationary, and the muscle was adjusted to the optimal length for the development of maximum force. During the experiment, the rat was placed supine on a heating pad, and the core body temperature was monitored with a rectal thermistor and maintained at 36°C. The muscle and nerve examined were bathed regularly with mineral oil warmed to 35°C.

The force data were obtained and processed by an acquisition system built from a multifunction I/O National Instruments Acquisition Board (NI USB 6251; 16 bit, 1.25 Ms/s;

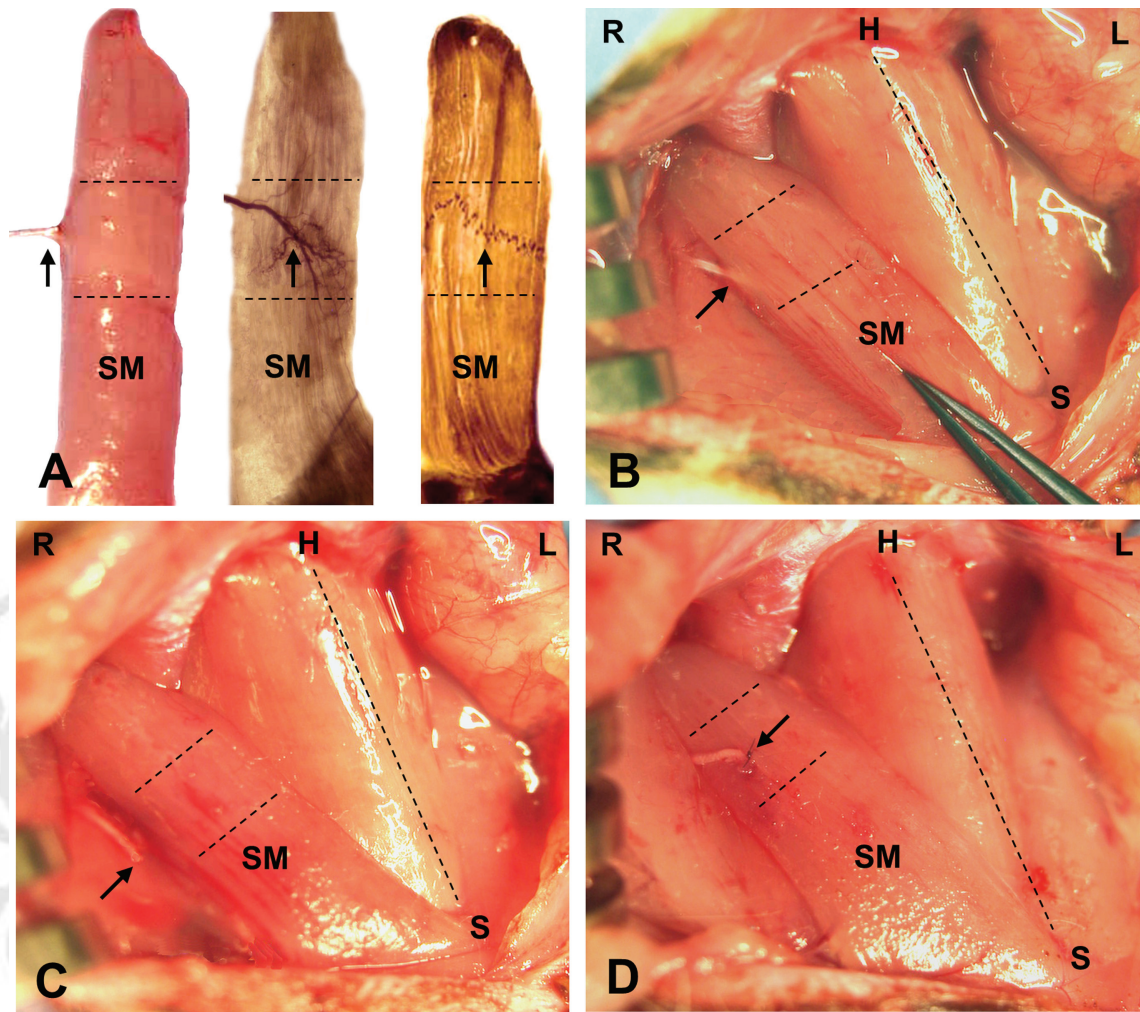


**Fig. 1** Native motor zone (NMZ) of sternomastoid (SM) muscle and surgical procedures for direct nerve implantation-native motor zone (DNI-NMZ) in the rat. (A) NMZ of the rat right SM in the middle portion of the muscle between dashed lines in fresh (left), Sihler's stained (middle), and acetylcholinesterase (right) stained muscles. Note that SM nerve enters the NMZ on the lateral margin of the muscle (arrow in the left image). The NMZ contains numerous intramuscular twigs and nerve terminals (middle image) and a motor endplate band with numerous neuromuscular junctions (right image). (B–D) Photographs from a rat during DNI-NMZ surgery, showing the entrance point (arrow) of the SM nerve into the muscle (B), transected and isolated SM nerve (C), and implantation of the proximal stump of the severed SM nerve into the NMZ of the target muscle (D). The oblique dashed line in B–D indicates the midline. Note: H, hyoid bone; L, left; R, right; S, sternum.

National Instruments) connected to a Dell laptop with a custom-written program using LabVIEW 8.2 software. The system produced stimulation pulses, which, after isolation from the ground through an optical isolation unit (Analog Stimulus Isolator model 2200; AM Systems, Inc, Carlsborg, WA), were used for the current controlled nerve stimulation. The acquisition system was also used to control muscle length and to collect a muscle force signal from the 305B Dual-Mode Lever System. Collected data were analyzed offline with DIAdem 11.0 software (National Instruments).

### Muscle Tissue Preparation

Immediately after force measurement, SM muscles on both sides in each animal were removed and weighed. Each muscle was divided into three segments: rostral, middle, and caudal. The muscle segments were frozen in melting isopentane cooled with dry ice and cut in a cryostat (Reichert-Jung 1800; Mannheim, Germany) at  $-25^{\circ}\text{C}$ . For each muscle, the

caudal and rostral segments were cut transversely ( $10\ \mu\text{m}$ ). The cross sections were stained with routine hematoxylin and eosin staining to examine muscle structure and myofiber morphology. The middle muscle segment was cut sagittally ( $60\ \mu\text{m}$ ) and immunostained to document nerve regeneration and reinnervation of the denervated endplates in the target muscle. For comparison, five right SM muscles denervated for 3 months by resecting a 5-mm segment of its innervating nerve in five additional rats were also prepared as described earlier and processed together with the experimental muscles.

### Assessments of Regenerated Axons and Reinnervated Endplates

#### Neurofilament Immunostaining

Some sagittal sections were immunostained with a monoclonal antibody against phosphorylated neurofilament (NF)

(SMI-31, Covance Research Products, Berkeley, CA) as a marker for all axons as described in our previous publications.<sup>13,30</sup> Briefly, the sections were: (1) treated in 2% bovine serum albumin for 30 minutes, (2) incubated with primary antibody SMI-31 (dilution 1:800) in PBS containing 0.03% triton at 4°C overnight, (3) incubated for 2 hours with the biotinylated secondary antibody (anti-mouse, 1:1000, Vector, Burlingame, CA), (4) treated with avidin–biotin complex method with a Vectastain ABC kit (1:1000 ABC Elite, Vector), and (5) treated with diaminobenzidine–nickel as chromogen to visualize peroxidase labeling. Control sections were stained as described except that the incubation with the primary antibody was omitted.

The stained sections were examined under a Zeiss photomicroscope (Axiophot-2; Carl Zeiss, Gottingen, Germany) and photographed using a digital camera (Spot-32; Diagnostic Instruments, Keene, NH). The intramuscular axonal density was assessed by estimating the number of the NF-immunoreactive (NF-ir) axons and the area fraction of the axons within a section area (1.0-mm<sup>2</sup>) as described in our previous publications.<sup>13,25,27</sup> For a given muscle, three sections stained for NF were selected at different spatial levels to count NF-ir axons. Areas with NF-positive staining were outlined, measured with public domain ImageJ software (v. 1.45s; NIH, Bethesda, MD).

#### Double Fluorescence Staining

Endplate reinnervation in the treated SM was detected using double fluorescence staining as described.<sup>13</sup> Briefly, some sagittal muscle sections were: (1) placed in Zamboni fixative with 5% sucrose for 20 minutes at 4°C, (2) treated with 0.1 mol/L of glycine in 1.5 T buffer for 30 minutes and dipped in 100% methanol at –20°C, (3) blocked in 1.5 T buffer containing 4% normal goat serum for 30 minutes, (4) incubated overnight at 4°C with primary antibodies (SMI-31 to detect neurofilaments and SMI-81 to label thinner axons; Covance Research Products Inc, Berkeley, CA), (5) incubated at room temperature for 2 hours both with a secondary antibody (goat anti-mouse antibody conjugated to Alexa 488) and with  $\alpha$ -bungarotoxin conjugated with Alexa 596 (Invitrogen Corporation, Carlsbad, CA), and (6) coverslipped.

The stained sections were photographed. SMI-31 and SMI-81 detected axons (green), while  $\alpha$ -bungarotoxin-labeled postsynaptic acetylcholine receptor site in the endplates (red). For each muscle sample, 50 labeled endplates were randomly selected to determine the percentages of the innervated (visible axon attachment) and noninnervated (no visible axon attachment) endplates.

#### Statistical Analysis

Muscle weights, force values, the number and the area fraction of NF-ir axons, and innervated and noninnervated endplates of the operated and unoperated SM muscles in each rat were computed. The variables of the reinnervated SM muscles were expressed as the percentages of the values of the contralateral control muscles. All data were presented as mean  $\pm$  standard deviation. The Student *t* test (paired, 2-tailed) was used to compare differences in the mean values of

the variables examined between operated and unoperated SM muscles. A difference was considered statistically significant at  $p < 0.05$ .

## Results

### Muscle Force Recovery

Muscle force data were successfully collected from both sides in 14 rats as the nerve on the operated side in one rat was damaged during muscle force recording. The degree of functional recovery of the reinnervated SM muscle was determined as compared with the force value of the contralateral control muscle in each rat. The DNI-NMZ reinnervated SM muscles produced 63.6% of the maximal tetanic tension of the contralateral control muscles (**Fig. 2**). Averaged maximal muscle force at the operated side was 0.763 N, whereas 1.200 N at the contralateral control side. The difference between these averages (0.437 N) was statistically significant ( $p = 0.0013$ ,  $t = 4.08$ ,  $df = 13$ , two-sided *t* test). The average rate (calculated between operated and control muscles) was 0.640. This rate was statistically different from 1 ( $p = 0.0022$ ,  $t = 3.80$ , two-sided single sample *t* test).

### Muscle Mass and Morphology

At the end of experiment, muscle examination showed that the mass of the DNI-NMZ reinnervated muscle was smaller than that of the contralateral control (**Fig. 3A and B**). The mean value of the wet weight of the reinnervated SM muscles (0.251 g) was smaller compared with that of the control muscles (0.352 g), but larger than that of the denervated SM muscles (0.199 g). Specifically, DNI-NMZ reinnervated SM muscles weighed 71% of the weight of contralateral control muscles (**Table 1**). The SM muscles reinnervated with the DNI-NMZ technique and studied 3 months later were greater in size than the SM muscles left with complete denervation for 3 months. The mean percent rate of wet weight of DNI-NMZ reinnervated SM muscles in relation to normal contralateral side (71%, with standard deviation [STD] = 0.11,  $n = 15$ ) was much higher than the rate of the denervated SM muscles in relation to normal contralateral side (44%, with STD = 0.20,  $n = 17$ ;  $t = 4.72$ ,  $df = 30$ ,  $p < 0.00001$ ). Man–Whitney U test confirmed strong significant difference in percentage rates between the two groups ( $U_A = 223.5$ ,  $U_B = 31.5$ ,  $p = 0.00012$ ).

Stained histological sections showed that the DNI-NMZ reinnervated muscles exhibited slight-to-moderate fiber atrophy as compared with the controls (**Fig. 3C and D**). In contrast, denervation resulted in significant myofiber atrophy as indicated by a reduction in fiber size and an increase in connective tissue (data not shown).

### Nerve Regeneration and Endplate Reinnervation

Three months after surgery, muscle sections immunostained for NF exhibited abundant axons in the NMZ of the target muscle. The regenerating axons were derived from the implanted SM nerve and supplied the denervated NMZ of the treated muscle (**Fig. 4A**). The density of the regenerated axons in the reinnervated muscles as indicated by the number

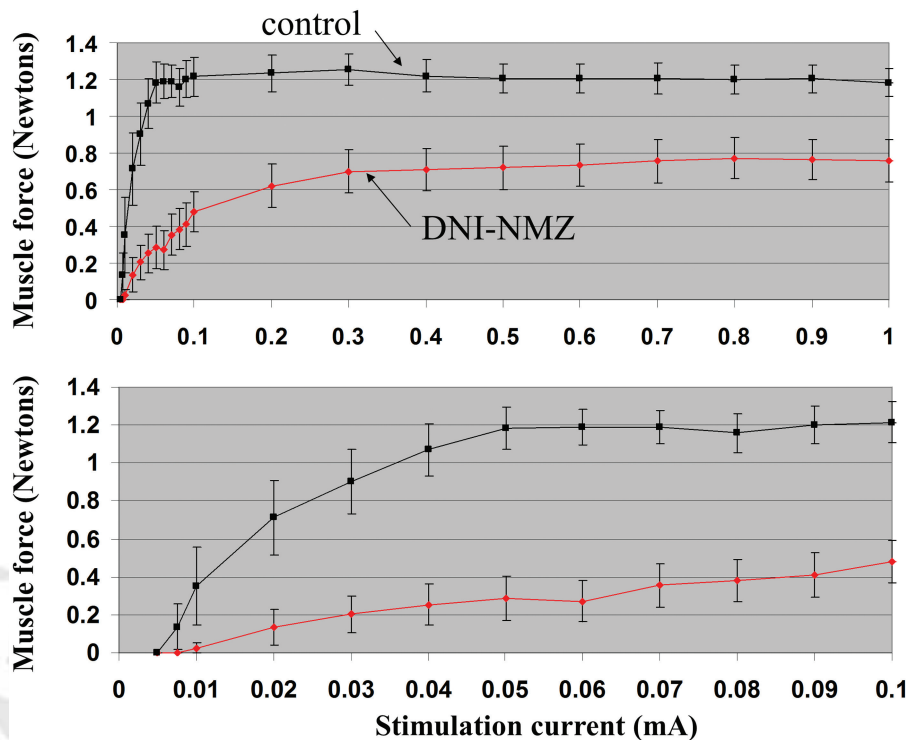


**Fig. 2** Muscle force as a function of stimulation current in operated and control sternomastoid (SM) muscles. The passive tension was set at a moderate level (0.08 N). Stimulation was made with a 0.2-second train of 0.2-millisecond-wide biphasic pulses at frequency of 200 Hz. The lower graph shows, in expanded scale, the early portion of the upper graph. Note that operated SM muscle (with DNI-NMZ label) when compared with control muscle at the opposite side (with control label) has larger stimulation threshold (0.02 vs 0.0075 mA), reach the level of maximal force with larger stimulation current (0.3 vs 0.05 mA), and has smaller maximal force. Maximal muscle force level was calculated as the average muscle force to stimulation currents from 0.6–1 mA. Average maximal muscle force level at the operated side (0.76 N) was 63.6% of muscle force at the control side (1.20 N). Vertical bars represent the standard deviation of the mean.

and the area fraction of labeled axons was summarized in ▶Table 2. The mean number and area of the NF-ir axons in the reinnervated SM muscles (▶Fig. 4A and 4A') was computed to be 62% and 51% of the contralateral control muscles (▶Fig. 4B and 4B'), respectively.

Double fluorescence staining showed the innervated and noninnervated endplates. In the treated SM, the regenerated axons were identified in the NMZ of the target muscle to innervate the denervated endplates (▶Fig. 5). On average, 66% of the denervated endplates in the treated muscles were reinnervated by regenerated axons and 34% of the endplates were unoccupied by axons. In addition, axonal sprouts and newly formed small endplates were identified in the DNI-NMZ reinnervated muscles.

## Discussion

To our knowledge, this is the first study to explore whether DNI into the NMZ of the denervated muscle could restore better motor function in a rat model. There are several key findings. First, DNI-NMZ resulted in satisfactory functional recovery as indicated by muscle force measurement. Specifically, DNI-NMZ reinnervated SM muscles produced 64% of the maximal tetanic force of the contralateral control muscles 3 months after surgery. Second, the muscle mass (71% of the control) and myofiber morphology of the DNI-NMZ reinner-

vated muscles were preserved well. Third, reinnervated muscles gained abundant regenerated axons as indicated by the mean number (62% of the control) and area (51% of the control) of the NF-ir axons in the target muscle. Finally, 66% of the denervated endplates in the treated muscles were reinnervated by regenerated axons.

DNI into the denervated muscle (neurotization) has been used in animal studies and clinical practice to reinnervate denervated muscles.<sup>8,10–12,31–36</sup> Preclinical and clinical studies have demonstrated that the outcome of DNI is associated with the chronicity of denervation,<sup>36</sup> regeneration distance,<sup>32,34,35</sup> and surgical techniques.<sup>35,37</sup> However, little is known whether DNI-NMZ reinnervation results in satisfactory functional recovery.

The NMZ is generally located in the middle region of a skeletal muscle and contains an endplate band with numerous neuromuscular junctions and their innervating nerve terminals. As endplate reinnervation is critical for motor recovery, we implanted a nerve stump into the NMZ of the target muscle to determine the outcomes of DNI-NMZ procedure. The data from this study showed that DNI-NMZ resulted in better functional recovery (64% of the control) as compared with the method reported in other studies (50%), in which DNI was not specifically performed in the NMZ of the denervated muscles.<sup>20,31,38</sup> Our encouraging results should be attributed to such a fact that DNI-NMZ procedure shortens

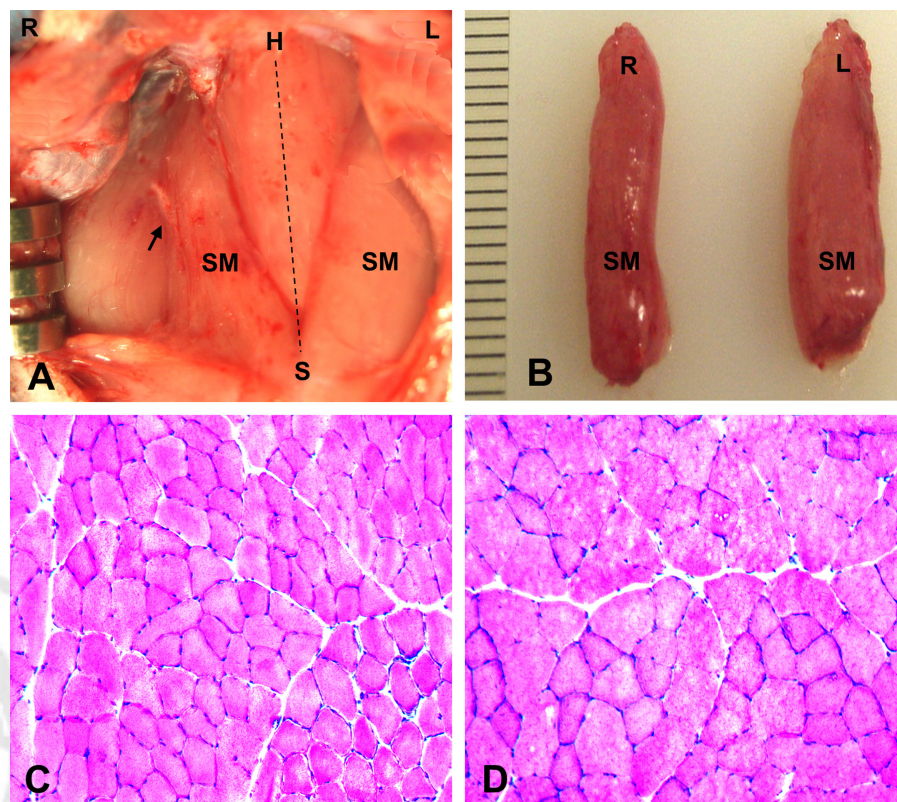


**Fig. 3** Photographs of a pair of sternomastoid (SM) muscles removed from a rat 3 months after surgery, showing the morphological difference between the reinnervated and contralateral control muscles. (A) An image taken before removal of the SM muscles, showing the implanted SM nerve (arrow). (B) Removed SM muscles from the same animal in A. Note that the mass of the right (R) operated SM muscle (0.312 g) was smaller as compared with that of the left (L) control muscle (0.390 g). (C–D) Hematoxylin and eosin -stained cross sections from the SM muscles in B. Note that the right reinnervated muscle (C) exhibited mild to moderate myofiber atrophy as compared with the control (D). Initial magnification 200 $\times$  for C and D.

**Table 1** Comparison of wet muscle weight between right operated and left control sternomastoid (SM) muscles in rats ( $n = 15$ )

Animal (No.)	Body weight (g)	Right reinnervated SM (g)	Left intact SM (g)
1	353	0.234	0.352
2	347	0.250	0.392
3	343	0.220	0.312
4	340	0.286	0.382
5	327	0.275	0.298
6	322	0.300	0.417
7	355	0.277	0.355
8	328	0.212	0.390
9	316	0.160	0.282
10	332	0.229	0.310
11	355	0.210	0.361
12	378	0.253	0.356
13	349	0.299	0.341
14	407	0.312	0.390
15	380	0.255	0.336
Average	349	0.251	0.352
Ratio, %		71	100

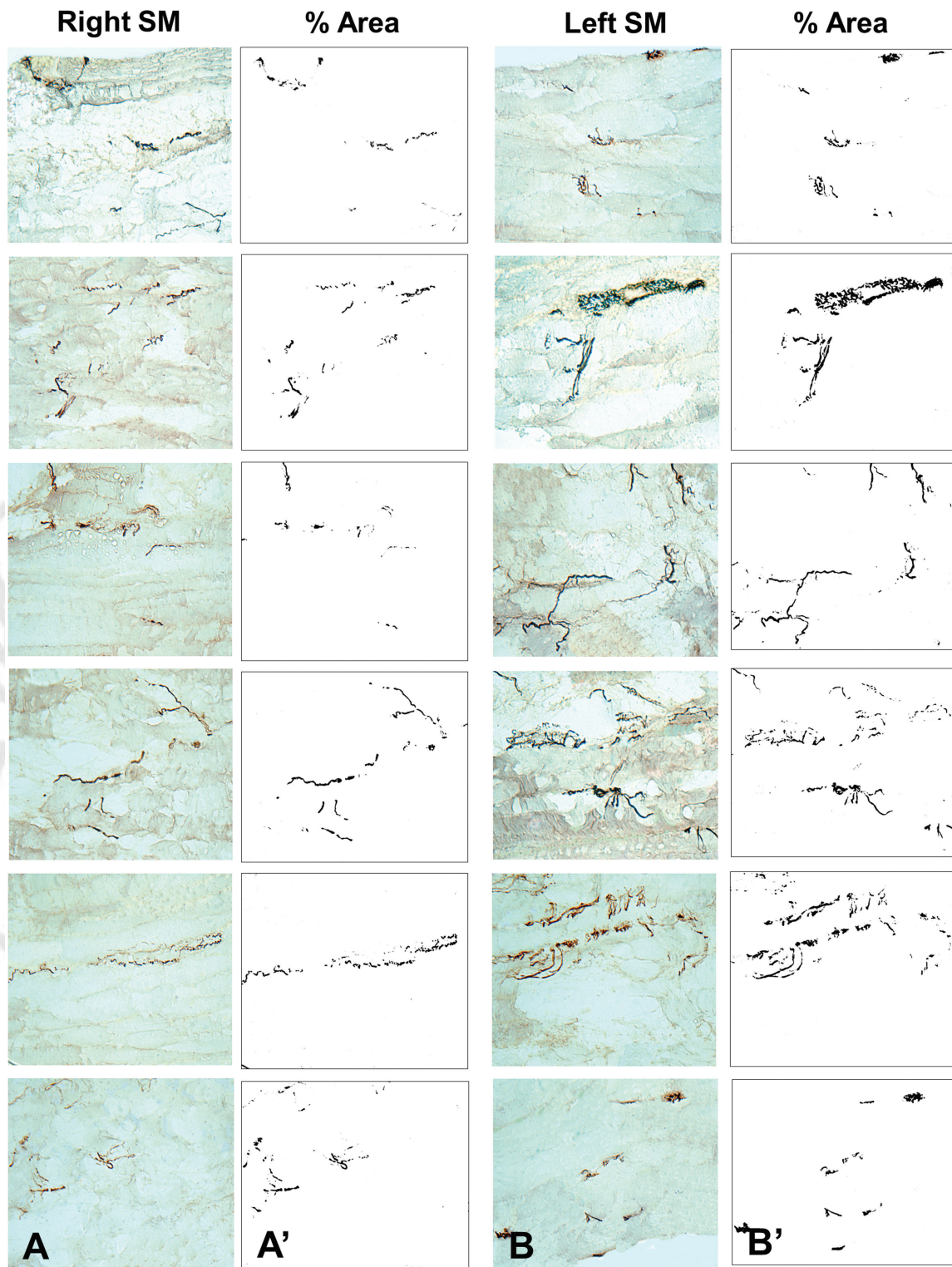


**Fig. 4** Images of sagittal sections immunostained for neurofilament (NF) from the operated and unoperated sternomastoid (SM) muscles of the rat number 15. (A) Six microscopic fields in a stained section from the right operated SM (first column), showing the NF-positive axons (dark staining) in the native motor zone of the target muscle. Magnification 200 $\times$ . (A') The images in the first column were converted to black and white (second column) by use of ImageJ software to calculate the number and percent area of staining in each section (mean axon count, 533; 56% of the control; mean area, 0.636; 43% of the control). (B-B') Images from the left unoperated SM (mean axon count, 974; mean area, 1.479). Magnification 200 $\times$ .

the distance between the nerve implantation site and the denervated endplates in the target muscle. Therefore, the regenerating axons from the implanted nerve could easily reach and reinnervate the denervated endplates in the NMZ

of the treated muscle. In contrast, if a nerve cut end is implanted into an area outside the NMZ it will take time to form new motor endplates and synapses. As reported, functional recovery may not be achieved for a long period after

**Table 2** Comparison of count and percent area of neurofilament-positive axons between right operated and left control sternomastoid (SM) muscles in rats ( $n = 15$ )

Animal (No.)	Right SM		Left SM		Ratio (R/L)	
	Count	Percent area	Count	Percent area	Count	Percent area
1	511	0.412	1640	1.336	0.312	0.308
2	668	0.430	678	0.626	0.985	0.687
3	420	0.552	1160	1.145	0.362	0.482
4	300	0.456	720	0.566	0.417	0.806
5	473	0.762	510	0.908	0.927	0.839
6	441	0.560	1074	1.358	0.411	0.412
7	312	0.370	600	1.100	0.520	0.336
8	340	0.247	649	0.931	0.524	0.265
9	624	0.623	861	1.295	0.725	0.481
10	671	0.660	752	1.303	0.892	0.507
11	499	0.640	623	1.557	0.801	0.411
12	435	0.511	814	1.496	0.534	0.342
13	319	0.509	893	1.280	0.357	0.398
14	748	0.630	751	0.716	0.996	0.880
15	533	0.636	947	1.479	0.563	0.430
Average	486	0.533	845	1.140	0.622	0.506

Abbreviations: L, left; R, right.

DNI surgery.<sup>35</sup> Studies have demonstrated that after nerve injury, functional motor recovery is primarily determined by endplate reinnervation and the absolute number of regenerated motor axons that reach target.<sup>39</sup>

Although our experiments showed the potential of DNI-NMZ in immediate muscle reinnervation, this study also has some limitations. For example, postoperative evaluations were performed at the end of 3 months after surgery. Three-month recovery period may be not enough to provide a complete picture of what occurs after DNI-NMZ. Further studies are needed to determine morphological and functional alterations at different time points after DNI-NMZ reinnervation. This information would be helpful

for better understanding the time-related changes of muscle reinnervation and functional recovery. In addition, it remains unknown if the DNI-NMZ has the potential for delayed reinnervation that is not uncommon in clinical practice. One of our ongoing studies is to determine the efficacy of DNI-NMZ for chronic muscle denervation. For this purpose, it is important to know the decreasing rate of the endplates in the completely denervated muscle and to determine the time point when all the endplates cannot be detected.

For future clinical application of this technique, our ongoing work is to promote the efficacy of DNI-NMZ reinnervation by further refining surgical procedure and accelerating

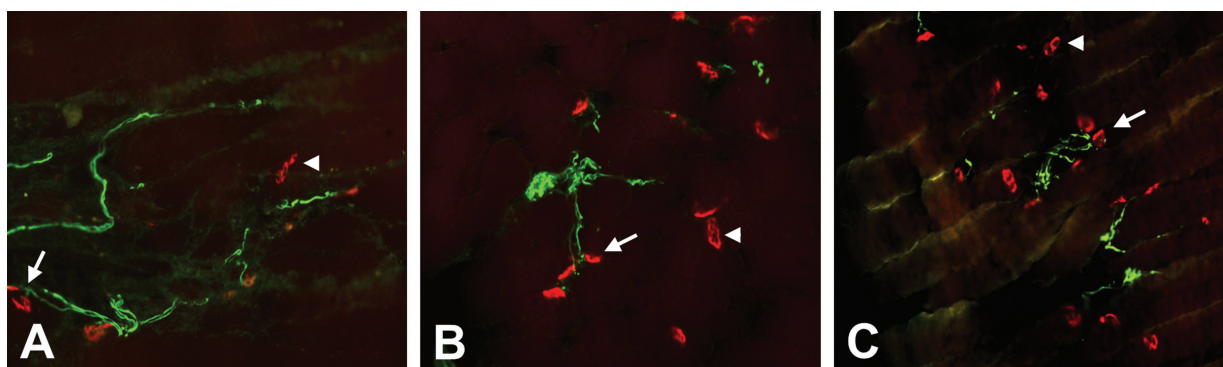


**Fig. 5** Sagittal sections immunostained with double fluorescence staining of the right sternomastoid (SM) muscle reinnervated by direct nerve implantation-native motor zone in a rat, showing reinnervated and nonreinnervated motor endplates. Note that some of the endplates were reinnervated by the regenerated axons (arrows in A–C), while others in the same muscle were unoccupied by regenerated axons (arrowheads in A–C). Original magnification 200 $\times$  for A through C.

axonal regeneration. For example, the nerve stump can be divided into two or more fascicles before implantation. Direct implantation of the divided nerve fascicles into the target muscle has shown to enhance end results.<sup>8,20</sup> This procedure can be applied to DNI-NMZ for better results. For accelerating axonal regeneration, a very brief 1-hour period of low-frequency (20 Hz) continuous electrical stimulation of the proximal nerve stump at the time of operation<sup>40,41</sup> and local administration of neurotrophic factors<sup>42</sup> could be combined with DNI-NMZ technique to enhance axonal regeneration. We believe that these approaches would promote the outcomes of the DNI-NMZ technique.

## Conclusion

In summary, DNI-NMZ technique appears to be a promising reconstructive option for muscle reinnervation. DNI-NMZ has the potential for functional motor restoration of denervated muscles in certain conditions. For optimal outcome, further studies are needed to promote the efficacy of this technique.

### Acknowledgments

The U.S. Army Medical Research Acquisition Activity, 820 Chandler Street, Fort Detrick MD 21702–5014 is the awarding and administering acquisition office.

This work was supported by the Office of the Assistant Secretary of Defense for Health Affairs under Award No. W81XWH-14-1-0442 (to Dr. Liancai Mu). Opinions, interpretations, conclusions, and recommendations are those of the authors and are not necessarily endorsed by the Department of Defense.

In conducting research using animals, the investigators adhere to the laws of the United States and regulations of the Department of Agriculture. This protocol was approved by the USAMRMC Animal Care and Use Review Office (ACURO) for the use of rats.

## References

- 1 Brininger TL, Antczak A, Breland HL. Upper extremity injuries in the U.S. military during peacetime years and wartime years. *J Hand Ther* 2008;21(2):115–122, quiz 123
- 2 Eser F, Aktekin LA, Bodur H, Atan C. Etiological factors of traumatic peripheral nerve injuries. *Neurol India* 2009;57(4):434–437
- 3 Kretschmer T, Antoniadis G, Braun V, Rath SA, Richter HP. Evaluation of iatrogenic lesions in 722 surgically treated cases of peripheral nerve trauma. *J Neurosurg* 2001;94(6):905–912
- 4 Siemionow M, Brzezicki G. Chapter 8: current techniques and concepts in peripheral nerve repair. *Int Rev Neurobiol* 2009;87:141–172
- 5 Lee SK, Wolfe SW. Peripheral nerve injury and repair. *J Am Acad Orthop Surg* 2000;8(4):243–252
- 6 Viterbo F, Amr AH, Stipp EJ, Reis FJ. End-to-side neuroorrhaphy: past, present, and future. *Plast Reconstr Surg* 2009;124(6, Suppl):e351–e358
- 7 Lundborg G, Dahlin LB, Danielsen N, et al. Nerve regeneration in silicone chambers: influence of gap length and of distal stump components. *Exp Neurol* 1982;76(2):361–375
- 8 Brunelli GA, Brunelli GR. Direct muscle neurotization. *J Reconstr Microsurg* 1993;9(2):81–90, discussion 89–90
- 9 de Medinaceli L, Prayon M, Merle M. Percentage of nerve injuries in which primary repair can be achieved by end-to-end approximation: review of 2,181 nerve lesions. *Microsurgery* 1993;14(4):244–246
- 10 Brunelli G, Brunelli LM. Direct neurotization of severely damaged denervated muscles. *Int Surg* 1980;65(6):529–531
- 11 Hall SJ, Trachy RE, Cummings CW. Facial muscle reinnervation: a comparison of neuromuscular pedicle with direct nerve implant. *Ann Otol Rhinol Laryngol* 1988;97(3 Pt 1):229–233
- 12 Goding GS Jr, Cummings CW, Bright DA. Extension of neuromuscular pedicles and direct nerve implants in the rabbit. *Arch Otolaryngol Head Neck Surg* 1989;115(2):217–223
- 13 Mu L, Sobotka S, Chen J, Nyirenda T. Reinnervation of denervated muscle by implantation of nerve-muscle-endplate band graft to the native motor zone of the target muscle. *Brain Behav* 2016. PMID: 27737470
- 14 Iwayama T. Relation of regenerating nerve terminals to original endplates. *Nature* 1969;224(5214):81–82
- 15 Bennett MR, McLachlan EM, Taylor RS. The formation of synapses in reinnervated mammalian striated muscle. *J Physiol* 1973;233(3):481–500
- 16 Sanes JR, Marshall LM, McMahan UJ. Reinnervation of muscle fiber basal lamina after removal of myofibers. Differentiation of regenerating axons at original synaptic sites. *J Cell Biol* 1978;78(1):176–198
- 17 Gorio A, Carmignoto G, Finesso M, Polato P, Nunzi MG. Muscle reinnervation—II. Sprouting, synapse formation and repression. *Neuroscience* 1983;8(3):403–416
- 18 Covault J, Cunningham JM, Sanes JR. Neurite outgrowth on cryostat sections of innervated and denervated skeletal muscle. *J Cell Biol* 1987;105(6 Pt 1):2479–2488
- 19 Guth L, Zaleski AA. Disposition of cholinesterase following implantation of nerve into innervated and denervated muscle. *Exp Neurol* 1963;7:316–326
- 20 Sakellariades HT, Sorbie C, James L. Reinnervation of denervated muscles by nerve transplantation. *Clin Orthop Relat Res* 1972;83(83):195–201
- 21 Mu L, Sobotka S, Su H. Nerve-muscle-endplate band grafting: a new technique for muscle reinnervation. *Neurosurgery* 2011;69(2, Suppl Operative):on s208–on s224, discussion on s224
- 22 Zhang X, Mu L, Su H, Sobotka S. Locations of the motor endplate band and motoneurons innervating the sternomastoid muscle in the rat. *Anat Rec (Hoboken)* 2011;294(2):295–304
- 23 Sobotka S, Mu L. Characteristics of tetanic force produced by the sternomastoid muscle of the rat. *J Biomed Biotechnol* 2010;2010:194984
- 24 Sobotka S, Mu L. Force characteristics of the rat sternomastoid muscle reinnervated with end-to-end nerve repair. *J Biomed Biotechnol* 2011;2011:173471
- 25 Sobotka S, Mu L. Force recovery and axonal regeneration of the sternomastoid muscle reinnervated with the end-to-end nerve anastomosis. *J Surg Res* 2013;182(2):e51–e59
- 26 Sobotka S, Mu L. Comparison of muscle force after immediate and delayed reinnervation using nerve-muscle-endplate band grafting. *J Surg Res* 2013;179(1):e117–e126
- 27 Sobotka S, Mu L. Muscle reinnervation with nerve-muscle-endplate band grafting technique: correlation between force recovery and axonal regeneration. *J Surg Res* 2015;195(1):144–151
- 28 Meikle D, Trachy RE, Cummings CW. Reinnervation of skeletal muscle: a comparison of nerve implantation with neuromuscular pedicle transfer in an animal model. *Ann Otol Rhinol Laryngol* 1987;96(2 Pt 1):152–157
- 29 Marie JP, Lerosey Y, Dehesdin D, Jin O, Tadié M, Andrieu-Guitrancourt J. Experimental reinnervation of a strap muscle with a few roots of the phrenic nerve in rabbits. *Ann Otol Rhinol Laryngol* 1999;108(10):1004–1011

- 30 Mu L, Chen J, Sobotka S, et al; Arizona Parkinson's Disease Consortium. Alpha-synuclein pathology in sensory nerve terminals of the upper aerodigestive tract of Parkinson's disease patients. *Dysphagia* 2015;30(4):404–417
- 31 Sorbie C, Porter TL. Reinnervation of paralysed muscles by direct motor nerve implantation. An experimental study in the dog. *J Bone Joint Surg Br* 1969;51(1):156–164
- 32 Payne SH Jr, Brushart TM. Neurotization of the rat soleus muscle: a quantitative analysis of reinnervation. *J Hand Surg Am* 1997;22(4):640–643
- 33 Park DM, Shon SK, Kim YJ. Direct muscle neurotization in rat soleus muscle. *J Reconstr Microsurg* 2000;16(5):379–383
- 34 Askar I, Sabuncuoglu BT, Yormuk E, Saray A. The fate of neurotization techniques on reinnervation after denervation of the gastrocnemius muscle: an experimental study. *J Reconstr Microsurg* 2001;17(5):347–355, discussion 355–356
- 35 Becker M, Lassner F, Fansa H, Mawrin C, Pallua N. Refinements in nerve to muscle neurotization. *Muscle Nerve* 2002;26(3):362–366
- 36 Keilhoff G, Fansa H. Successful intramuscular neurotization is dependent on the denervation period. A histomorphological study of the gracilis muscle in rats. *Muscle Nerve* 2005;31(2):221–228
- 37 Yazici I, Ayhan S, Elmas C, Temucin C, Atabay K. Motor neurotization by segmental epineurectomy and implantation: lateral muscular neurotization. *J Reconstr Microsurg* 2008;24(6):435–442
- 38 Swanson AN, Wolfe SW, Khazzam M, Feinberg J, Ehteshami J, Doty S. Comparison of neurotization versus nerve repair in an animal model of chronically denervated muscle. *J Hand Surg Am* 2008;33(7):1093–1099
- 39 Barbour J, Yee A, Kahn LC, Mackinnon SE. Supercharged end-to-side anterior interosseous to ulnar motor nerve transfer for intrinsic musculature reinnervation. *J Hand Surg Am* 2012;37(10):2150–2159
- 40 Al-Majed AA, Neumann CM, Brushart TM, Gordon T. Brief electrical stimulation promotes the speed and accuracy of motor axonal regeneration. *J Neurosci* 2000;20(7):2602–2608
- 41 Gordon T, Brushart TM, Amirjani N, Chan KM. The potential of electrical stimulation to promote functional recovery after peripheral nerve injury—comparisons between rats and humans. *Acta Neurochir Suppl (Wien)* 2007;100:3–11
- 42 Jubran M, Widenfalk J. Repair of peripheral nerve transections with fibrin sealant containing neurotrophic factors. *Exp Neurol* 2003;181(2):204–212



THIEME

# NERVE GROWTH FACTOR AND BASIC FIBROBLAST GROWTH FACTOR PROMOTE REINNERVATION BY NERVE–MUSCLE–ENDPLATE GRAFTING

LIANCAI MU, MD, PhD,<sup>1</sup> STANISLAW SOBOTKA, PhD,<sup>1,2</sup> JINGMING CHEN, MD,<sup>1</sup> and THEMBA NYIRENDA, PhD<sup>1</sup>

<sup>1</sup>Department of Biomedical Research, Hackensack University Medical Center, 40 Prospect Avenue, Hackensack, New Jersey, 07601, USA

<sup>2</sup>Department of Neurosurgery, Icahn School of Medicine at Mount Sinai, One Gustave Levy Place, New York, New York, USA

Accepted 17 June 2017

**ABSTRACT:** *Introduction:* This study was designed to test whether exogenous application of nerve growth factor (NGF) and basic fibroblast growth factor (FGF-2) to muscles reinnervated with nerve–muscle–endplate band grafting (NMEG) could promote specific outcomes. *Methods:* The right sternomastoid muscle in adult rats was experimentally denervated and immediately reinnervated by implanting an NMEG pedicle from the ipsilateral sternohyoid muscle. A fibrin sealant containing NGF and FGF-2 was focally applied to the implantation site. Maximal tetanic force, muscle weight, regenerated axons, and motor endplates were analyzed 3 months after treatment. *Results:* Mean tetanic force, wet muscle weight, and number of regenerated axons in the treated muscles were 91%, 92%, and 84% of the contralateral controls, respectively. The majority of endplates (86%) in the treated muscles were reinnervated by regenerated axons. *Discussion:* Focal administration of NGF and FGF-2 promotes efficacy of the NMEG technique.

*Muscle Nerve* 57: 449–459, 2018

**P**eripheral nerve injury (PNI) may cause muscle paralysis, which is commonly treated by nerve repair, nerve grafting, nerve transfer, direct nerve implantation, and various other techniques.<sup>1–5</sup> Despite advances in microsurgical techniques for nerve reconstruction, functional recovery is rarely complete. Considerable evidence has shown that functional motor recovery after PNI and nerve repair is determined predominantly by the absolute number of regenerated motor axons that reach the target and the time to motor endplate (MEP) reinnervation.<sup>6–8</sup>

Efforts have been made to improve functional recovery after PNI and repair by improvement of surgical techniques and by creating an optimal microenvironment for nerve regeneration. To

facilitate MEP reinnervation to treat PNI-induced muscle paralysis, we developed a surgical method called “nerve–muscle–endplate band grafting” (NMEG) for muscle reinnervation in a rat model.<sup>9</sup> The NMEG reinnervation technique is based on the concept that a paralyzed muscle can be reinnervated by transplanting an NMEG from a neighboring donor muscle. A healthy nerve branch and terminals that innervate a non-essential muscle can be transplanted to a more functionally important denervated muscle for restoring its motor function. Of course, reprogramming of the motor neurons in the central nervous system is necessary to restore normal function of the reinnervated muscle. The departure here from more conventional nerve implantation<sup>10</sup> is that tissue containing motor nerve terminals, rather than the nerve itself, is implanted. In our animal model, an NMEG pedicle containing a nerve branch and a muscle block with nerve terminals and MEPs was harvested from the sternohyoid (SH) muscle and transplanted into the ipsilateral experimentally denervated sternomastoid (SM) muscle. Our studies have demonstrated the importance of MEP reinnervation in motor recovery of the target muscle. Specifically, 3 months after implantation of the NMEG into an MEP-free area, the mean contractile force of the treated muscles was 67% of the controls.<sup>9</sup> In contrast, implantation of the NMEG into the native motor zone (NMZ) of the target muscle yielded better functional recovery (82%).<sup>11</sup> We hypothesized that the outcomes of NMEG–NMZ would be promoted by local application of neurotrophic factors to the implanted NMEG and NMZ of the target muscle to increase the rate of nerve regeneration and axon–MEP connections.

Exogenous application of neurotrophic factors, including nerve growth factor (NGF) and basic fibroblast growth factor (FGF-2), has been used locally in nerve reconstructive procedures such as nerve repair<sup>12–14</sup> and tubulization.<sup>15,16</sup> Studies have shown that use of NGF and FGF-2 improves axonal regeneration and functional recovery after PNI and nerve repair.<sup>15,17–21</sup> As reported, administration of NGF enhances nerve regeneration and motor recovery.<sup>13,14,22–28</sup> FGF-2 is a potent factor

**Abbreviations:** AChR, acetylcholine receptor; BSA, bovine serum albumin; FGF-2, basic fibroblast growth factor; H&E, hematoxylin & eosin; MEP, motor endplate; NF, neurofilament; NF-ir, neurofilament-immunoreactive; NGF, nerve growth factor; NMEG, nerve–muscle–endplate band grafting; NMZ, native motor zone; NMEG–NMZ, nerve–muscle–endplate band grafting–native motor zone; PBS, phosphate-buffered saline; PNI, peripheral nerve injury; SH, sternohyoid muscle; SM, sternomastoid muscle

**Key words:** basic fibroblast growth factor; muscle reinnervation; native motor zone; nerve growth factor; nerve–muscle–endplate grafting

**Funding:** Office of the Assistant Secretary of Defense for Health Affairs (W81XWH-14-1-0442 to L.M.).

**Disclaimer:** Opinions, interpretations, conclusions, and recommendations are those of the authors and are not necessarily endorsed by the Department of Defense.

**Correspondence to:** L. Mu; e-mail: liancai.mu@hackensackmeridian.org

© 2017 Wiley Periodicals, Inc.  
Published online 20 June 2017 in Wiley Online Library (wileyonlinelibrary.com).  
DOI 10.1002/mus.25726

that promotes axonal growth,<sup>16,17,29–31</sup> increases the number of proliferating Schwann cells and regenerating axons<sup>17,32</sup> and MEPS,<sup>33</sup> and enhances functional recovery.<sup>33</sup> The neurotrophic factors can be administered locally by direct injection into the target nerve<sup>34</sup> or muscle<sup>33</sup> or by using a surgically implanted osmotic pump for growth factor delivery,<sup>35–37</sup> according to nerve injury and repair models. Recently, local application of a fibrin sealant containing neurotrophic factors has been extensively used in PNI and repair models for the slow continual release of factors directly to the damaged and/or repaired nerve for accelerating axonal regeneration and subsequent functional recovery.<sup>13,28,38–41</sup> Some investigators<sup>13,40</sup> have used an enzyme-linked immunosorption assay to quantify *in vitro* the release characteristics of the exogenous neurotrophic factors in fibrin, and demonstrated a sustained release. The factors could be released locally *in vitro* over periods of 2 weeks<sup>13,40</sup> or 4 weeks.<sup>40</sup> Experimental studies suggested that the fibrin-based drug-delivery system for neurotrophic factor release could be a promising strategy for improving axonal regeneration and functional restoration.

The goal of this study was to investigate the effect of focal administration of fibrin sealant containing exogenous NGF and FGF-2 on outcomes of our NMEG–NMZ reinnervation technique.

## METHODS

**Animals.** Twenty-two 3-month-old female Sprague-Dawley rats (Taconic Laboratories, Cranbury, New Jersey), weighing 200–250 g, were used in this study. The proposed experiments were reviewed and approved by the institutional animal care and use committee and by the USAMRMC Animal Care and Use Review Office. All animals were handled in accordance with the *Guide for Care and Use of Laboratory Animals*, published by the National Institutes of Health (NIH Publication No. 85-23, revised 1996), and complied with the laws of the United States and regulations of the Department of Agriculture. The rats were maintained in a 22°C environment with a 12/12-hour light–dark cycle with free access to food and water.

**Surgical Procedures and Focal Administration of Exogenous Neurotrophic Factors.** Twenty-two rats were randomly assigned into reinnervation ( $n = 15$ ) and denervation ( $n = 7$ ) groups. Both groups of animals were anesthetized by an intraperitoneal injection of a mixture of ketamine (80 mg/kg) and xylazine (5 mg/kg). Under an operating microscope, the right SM muscle was denervated by resecting a 5-mm segment of its innervating nerve.

Immediately after muscle denervation, the rats in the reinnervation group underwent NMEG–NMZ surgery and neurotrophic factor therapy. The details regarding NMEG–NMZ transplantation have been described previously.<sup>11</sup> First, the NMZs in the right SM and SH muscles were outlined according to the motor point and location of intramuscular nerve terminals and MEP band (Fig. 1A–H). Second, an NMEG pedicle was obtained from the NMZ of

the right SH donor muscle. The pedicle contained a block of muscle ( $\sim 6 \times 6 \times 3$  mm), axon terminals, and an MEP band. The superficial muscle fibers on the ventral aspect of the NMEG pedicle were removed to create a denuded surface for better axonal regeneration (Fig. 1I). Third, a muscular defect, with the same dimensions as the NMEG pedicle, was made in the NMZ of the right denervated SM muscle (Fig. 1I). Fourth, a fibrin sealant (fibrinogen 90 mg/ml, thrombin 500 IU/ml, 4 mmol/L CaCl<sub>2</sub>; Baxter Healthcare Corp., Westlake Village, California), containing NGF and FGF-2, was applied locally to the SM muscle defect as combinations of neurotrophic factors yield better results than a single factor alone.<sup>35,42–44</sup> Specifically, the target SM received a single focal administration of a mixture of exogenous NGF and FGF-2. The muscular defect was covered with 0.2 ml of fibrin sealant containing recombinant rat NGF and rat FGF-2 (R&D Systems, Minneapolis, Minnesota) at a concentration of 100 ng/ml for NGF and 100 µg/ml for FGF-2. As reported, intramuscular injections of both neurotrophic factors at these concentrations resulted in better functional recovery.<sup>33</sup> Finally, the NMEG was implanted into the SM muscle defect and sutured with 4–6 10-0 nylon microsutures (Fig. 1J). After surgery, the wound was closed.

Three months after the experiments, the animals underwent postoperative outcome measurements that included functional evaluation and neuromuscular analyses. For each animal, all assessments were performed from both SM muscles, with the contralateral SM serving as a control.

**Nerve Stimulation and Force Measurement.** The degree of functional recovery of the treated muscles was assessed by measuring the maximal tetanic force, as described in our previous publications.<sup>9,11,45–49</sup> Briefly, the right treated and the left control SM muscles in each animal were exposed and dissected free from the surrounding tissues. The rostral tendon of each muscle was then divided at its insertion, tied with a 2-0 suture, and attached to a servomotor lever arm (Model 305B Dual-Mode Lever Arm System; Aurora Scientific, Inc., Aurora, Ontario, Canada). At the moment of force measurement, the lever arm was stationary, and the muscle was adjusted to the optimal length by stretching the muscle with moderate tension of 0.08 N for the development of maximum force.<sup>9,45</sup> Muscle force of the right treated SM was measured by stimulating the SH nerve branch supplying the NMEG, whereas that of the left control muscle was measured by stimulating the intact SM nerve. Each of the nerves was isolated and draped over a bipolar stimulating electrode for nerve stimulation. Trains of biphasic rectangular pulses of different current were delivered to the stimulated nerve using our stimulation and recording system, which is based on the multifunction acquisition board (National Instruments Corp., Austin, Texas) and controlled by user-written LabVIEW software (National Instruments). Isometric contraction of the SM muscle was produced with 200-ms trains of biphasic rectangular pulses. Stimuli were single pulses of 0.2-ms duration and the train frequency was set at 200 pulses/s. The stimulation current was gradually increased until the tetanic force reached a plateau. A break of at least 1 minute was taken between 2 stimulations. The maximum value of muscle force during the 200-ms contraction was identified, as well as initial passive tension before stimulation. The difference between the maximal active force and the preloaded passive force was used as the muscle force measurement. The force generated by the contraction of the SM muscle was

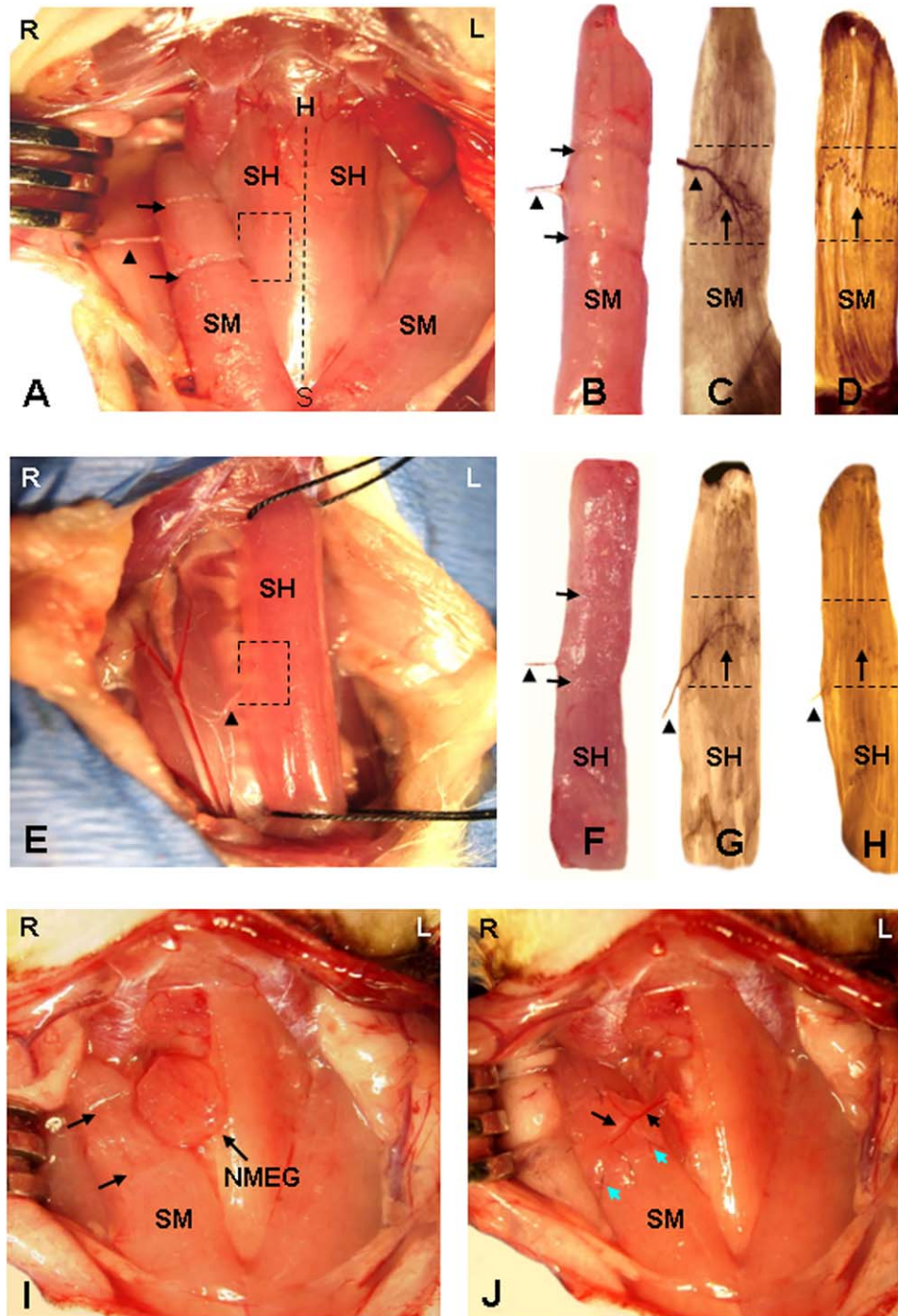


**FIGURE 1.** Native motor zone (NMZ) within the sternomastoid (SM) and sternohyoid (SH) muscles of rats and surgical procedures for nerve–muscle–endplate band grafting (NMEG). (A–D) NMZ of the right SM, as outlined during surgery [between arrows in (A)], in removed fresh muscle [between arrows in (B)], and in muscles processed with Sihler stain (C) and acetylcholinesterase stain (D). Note that a single motor nerve branch [arrowheads in (A)–(C)] enters into the middle of the muscle and that the NMZ of the muscle contains intramuscular nerve terminals [arrow in (C)] and a motor endplate (MEP) band [arrow in (D)]. H, hyoid bone; L, left, R, right; S, sternum. (E–H) NMZ of the SH muscle. Note that the right SM muscle has been removed to show the SH nerve [arrowhead in (E)]. (I–J) Surgical procedures. An NMEG pedicle was harvested from the right SH muscle (I). A muscular defect (between arrows) was made in the denervated NMZ of the right SM (I). The NMEG was embedded into the muscular defect made in the SM and sutured [green arrows in (J)]. Note that the implanted NMEG contains a nerve branch (large black arrow) and blood vessels [small black arrow in (J)].

transduced with the servomotor of a 305B lever system and displayed on a computer screen. During the experiment, body temperature was maintained at 36°C by an electric heating pad thermostatically controlled from a rectal

thermistor. The muscle and nerve examined were bathed regularly with warmed mineral oil throughout the testing.

The force data were obtained and processed by an acquisition system built from a multifunction I/O

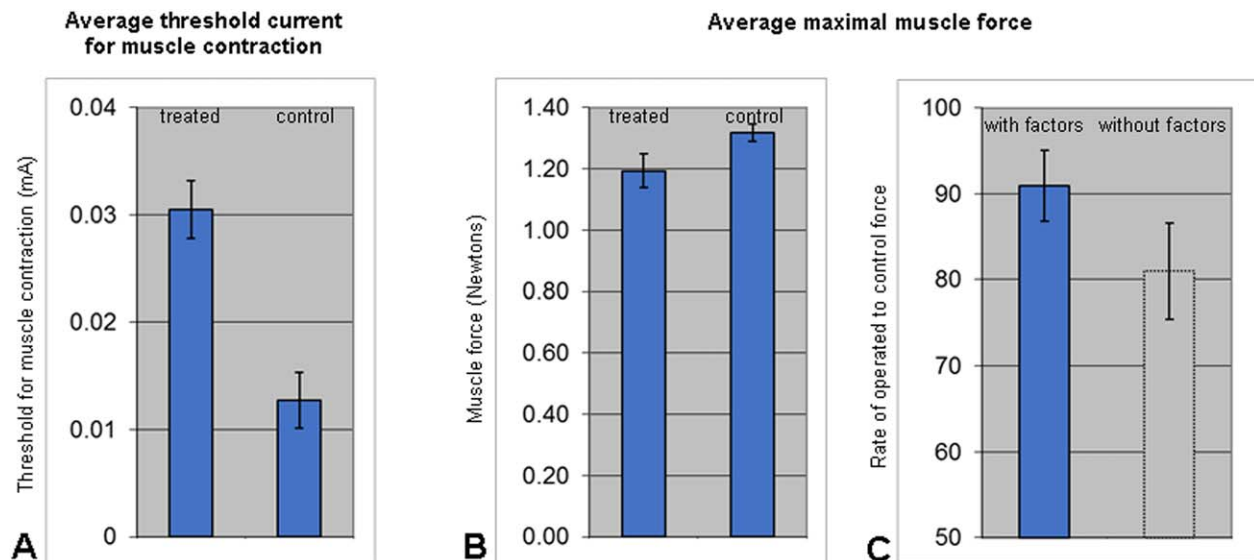


**FIGURE 2.** Muscle force from rats treated with nerve–muscle–endplate band grafting–native motor zone (NMEG–NMZ) implantation and focal administration of a mixture of exogenous NGF and FGF-2 (factors). **(A)** Comparison of current thresholds for muscle contraction between treated and control muscles. Error bars represent standard error. **(B)** Comparison of maximal muscle force between treated and control muscles. Maximal muscle force was calculated as the average force to stimulation currents from 0.6 to 1.0 mA. **(C)** Average maximal force of the SM muscles treated with NMEG–NMZ and factors was 91% of the controls (left bar). The right dotted bar illustrates average percent rate of maximal force of the SM muscles treated with NMEG–NMZ alone (82% of the control), as demonstrated in our previous study.<sup>11</sup>

acquisition board (16 bit, 1.25 ms/s; NI USB 6251; National Instruments) connected to a Dell laptop computer with a custom-written program using LabVIEW v8.2 software. The system produced stimulation pulses, which, after isolation from the ground through an optical isolation unit (Analog Stimulus Isolator Model 2200; AM Systems, Inc., Carlsborg, Washington), were used for the current-controlled nerve stimulation. The acquisition system was also used to control muscle length and to collect a muscle force signal from the 305B lever system. Collected data were analyzed offline with DIAdem v11.0 software (National Instruments). For each rat, the percentage of functional recovery of the treated SM was determined by comparing the treated muscle with the contralateral control muscle.

**Muscle Weight Measurement and Tissue Preparation.** At the end of the experiments, both SM muscles from each rat were harvested, photographed, and weighed. As a measure of the effectiveness of muscle reinnervation, wet muscle weight and myofiber morphology were examined. The wet muscle weights were reported as a ratio of the treated side to the contralateral control side. Each of the removed SM muscles was divided into 3 segments: rostral, middle, and caudal. The muscle segments were then frozen in melting isopentane cooled with dry ice and cut on a cryostat (Model 1800; Reichert-Jung, Mannheim, Germany) at  $-25^{\circ}\text{C}$ . The rostral and caudal segments were cut transversely and serial cross-sections ( $10\ \mu\text{m}$ ) were stained with routine hematoxylin and eosin (H&E) to examine muscle structure and myofiber morphology. The middle segment containing the NMZ and/or NMEG was cut sagittally ( $60\ \mu\text{m}$ ) and stained immunohistochemically to quantify regenerated axons and MEPs.

**Immunohistochemical Detection of Regenerated Axons and Innervated MEPs.** Regenerated axons and innervated MEPs were detected with immunohistochemical methods as described in what follows.

**Neurofilament Staining.** Some sagittal sections were immunostained with monoclonal antibody SMF-31 as a marker for all axons (Covance Research Products, Berkeley, California) as described elsewhere.<sup>11,50</sup> Briefly, the sections were treated in phosphate-buffered saline (PBS) containing 0.3% Triton and 2% bovine serum albumin (BSA) for 30 minutes, incubated with SMF-31 primary antibody (1:800) in PBS containing 0.03% Triton at  $4^{\circ}\text{C}$  overnight, treated for 2 hours with anti-mouse biotinylated secondary antibody (1:1,000; Vector Labs, Burlingame, California), processed with the avidin–biotin complex method using a VectaStain ABC kit (1:1,000; ABC Elite; Vector), and treated with diaminobenzidine–nickel as chromogen to visualize peroxidase labeling. Control sections were stained as described, except that the incubation with the primary antibody was omitted.

The stained sections were examined under a fluorescence microscope (Axioplan-1; Carl Zeiss, Göttingen, Germany) and photographed with a USB 3.0 digital microscope camera (Infinity 3-3URC; Lumenera Corp., Ottawa, Ontario, Canada). The extent of axonal regeneration and muscle reinnervation was evaluated by quantifying the neurofilament-immunoreactive (NF-ir) axons within the treated muscles as described in our previous publications.<sup>11,47,49</sup> The intramuscular axonal density was assessed by computing the number of the NF-ir axons and the area fraction of the axons within a section area ( $1.0\ \text{mm}^2$ ). For a given muscle, 3 stained sections at different spatial levels through the muscle were selected to count NF-ir axons. For each section, 5 microscopic fields with NF-ir axons were identified and photographed. Areas with NF-positive staining were outlined and measured with public domain ImageJ software v1.45s (National Institutes of Health, Bethesda, Maryland). For each rat, the number and the area fraction of the NF-ir axons in the treated muscle were compared with those in the contralateral control.

**Double-Fluorescence Staining.** MEPs and their innervating axons were labeled with double-fluorescence staining,

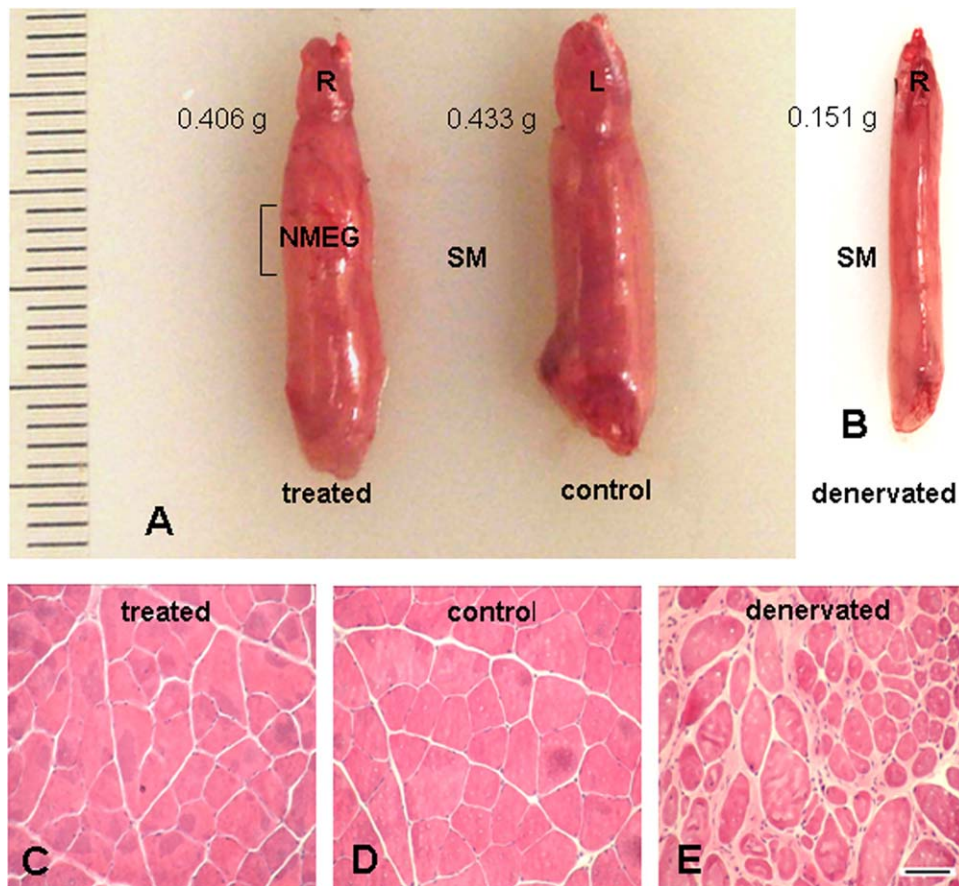


**FIGURE 3.** Gross appearance, muscle mass, and myofiber morphology of the treated, control, and denervated sternomastoid (SM) rat muscles. **(A)** A pair of SM muscles removed from a rat 3 months after nerve–muscle–endplate band grafting–native motor zone (NMEG–NMZ) implantation and focal administration of a mixture of exogenous NGF and FGF-2. Note that the mass of the right (R) treated SM muscle is close to that of the left (L) control muscle. The outlined region in the right SM is the location of the implanted NMEG. **(B)** A 3-month-denervated SM muscle. Note that the denervated SM (0.151 g) shows a more significant loss of muscle mass compared with the treated (0.406 g) and contralateral control (0.433 g) SM muscles. **(C–E)** H&E-stained cross-sections from the treated SM **(C)**, contralateral control **(D)**, and denervated **(E)** SM muscles. Note that the treated SM shows very good preservation of muscle structure and myofiber morphology with less fiber atrophy when compared with the denervated muscle. Bar = 100  $\mu\text{m}$  for **(C)–(E)**.

as described previously,<sup>11,51</sup> with some modifications. Briefly, some sagittal sections were fixed for 20 minutes in Zamboni fixative with 5% sucrose at 4°C. The fixed sections were washed extensively in 1.5 Tris buffer (pH 7.6), treated with 0.1 mol/L of glycine in 1.5 Tris buffer for 30 minutes, and dipped in 100% methanol at –20°C. The sections were blocked in 1.5 Tris buffer containing 4% normal goat serum for 30 minutes to inhibit non-specific protein binding. Axons and terminals were detected by incubating the sections overnight at 4°C with primary antibodies (SMI-31 to detect neurofilaments, and SMI-81 to detect thinner axons; 1:1,000; Covance Research Products, Inc., Berkeley, California). After washing with 1.5 Tris buffer, the sections were incubated at room temperature for 2 hours with Alexa Fluor 488 donkey anti-mouse IgG secondary antibody (1:500; Invitrogen Corp., Carlsbad, California). Postsynaptic acetylcholine receptors (AChRs) at MEPs were labeled with Alexa Fluor 596–conjugated  $\alpha$ -bungarotoxin (1:500; Invitrogen). The stained sections were rinsed in 1.5 Tris buffer and mounted with mounting medium (VectaShield; Vector Labs).

The stained axons (green) and MEPs (red) in each section were examined under a Zeiss fluorescence microscope

and photographed using the USB 3.0 digital microscope camera. For each sample, at least 100 labeled MEPs were randomly selected from stained sections to determine the percentages of the innervated (visible axon attachment) and non-innervated (no visible axon attachment) MEPs.

**Statistical Analysis.** Force values, wet muscle weights, the number and area fraction of NF-ir axons, and innervated and non-innervated MEPs of the SM muscles in each rat were determined. The variables of the treated SM muscles are expressed as a percentage of the values of the contralateral control muscles. All data are reported as mean  $\pm$  standard deviation. The Student *t*-test (paired, 2-tailed) was used to compare differences in the mean muscle force, mean muscle weight, and mean number and area fraction of NF-ir axons between treated and control SM muscles.  $P < 0.05$  was considered statistically significant.

## RESULTS

**Maximal Tetanic Muscle Force.** Muscle force data were successfully collected from both sides in 14 rats. Three months after surgery, electric stimulation of the SH nerve innervating the implanted

**Table 1.** Comparison of wet muscle weight between right treated and left control sternomastoid (SM) muscles in rats ( $n = 15$ ).

Animal No.	Body weight (g)	Right SM (g)	Left SM (g)	Ratio (R/L)
1	327	0.300	0.340	0.882
2	326	0.322	0.339	0.950
3	302	0.284	0.300	0.947
4	349	0.377	0.405	0.931
5	368	0.273	0.321	0.850
6	303	0.292	0.302	0.967
7	307	0.286	0.341	0.839
8	345	0.310	0.323	0.960
9	392	0.308	0.312	0.987
10	356	0.344	0.380	0.905
11	315	0.299	0.354	0.845
12	382	0.315	0.365	0.863
13	355	0.448	0.472	0.949
14	347	0.370	0.392	0.944
15	351	0.406	0.433	0.938
Average	342	0.329	0.359	0.917
SD	28	0.0500	0.0498	0.0490

L, left; R, right.

NMEG resulted in vigorous contractions of all treated muscles. The average threshold of nerve stimulation current that produced visible muscle contraction was 0.031 mA (standard deviation 0.010 mA, median 0.030 mA) on the treated side, but was only about one third of this value on the control side (mean 0.013 mA, standard deviation 0.009 mA, median 0.008 mA) (Fig. 2A). Increasing stimulation current was accompanied by a greater muscle force until it reached a horizontal asymptote. This saturation level was reached with higher current (0.2 mA) on the treated side than the control side (0.05 mA). The group average values of tetanic force of SM muscles from the treated (mean 1.193 N, standard deviation 0.195 N, median 1.239 N) and control (mean 1.316 N, standard deviation 0.101 N, median 1.335 N) sides are summarized in Figure 2B and C. The treated SM produced 91% of the maximal tetanic tension of the contralateral control.

**Wet Muscle Weight and Myofiber Morphology.** The size of the treated SM was similar to that of the contralateral control, but larger than that of 3-month-denervated SM (Fig. 3A and B). The mean value and standard deviation of the wet weight for the treated SM muscles and the contralateral control muscles are summarized in Table 1. The mean weight of the denervated SM muscles was  $0.138 \pm 0.062$  g. The difference in average muscle weight was relatively small between treated and control muscles, but was consistent across rats and, therefore, statistically significant ( $P < 0.00001$ ,  $t = 6.839$ , paired  $t$ -test). The average ratio of treated to control muscles (0.92) was substantially larger than

the average ratio (0.38) of denervated to control muscles in rats that had SM muscle denervation without treatment ( $P < 0.00001$ ,  $t = 14.226$ , unpaired  $t$ -test). H&E-stained cross-sections showed that myofiber morphology of the treated SM (Fig. 3C) was close to that of the contralateral control (Fig. 3D) and better than that of the denervated muscle (Fig. 3E). Remarkable fiber atrophy was found in the denervated muscles.

**Regenerated Axons and Innervated MEPS.** NF staining showed that NF-ir axons were confined to the NMZ of the treated and contralateral control SM muscles. The treated SM exhibited extensive axonal regeneration. By counting NF-ir axons (green) per field at  $200\times$  magnification, we observed that, in the treated SM, the regenerating axons from the implanted NMEG supplied the denervated NMZ and reached the most distal portion of the muscle (Fig. 4). Table 2 shows the mean number and area fraction of the NF-ir axons for each muscle in each animal. The mean number of the NF-ir axons in the treated muscles was 84% of the control. Regenerated axons in the treated muscles were more abundant than those in the muscles reinnervated by NMEG–NMZ surgery alone (77% of the control;  $P = 0.049$ ,  $t = 2.05$ , unpaired  $t$ -test).<sup>11</sup>

The muscle sections immunostained with double-fluorescence staining showed the innervated and non-innervated MEPS. In the treated SM muscles, the regenerating axons grew across the NMZ to innervate the denervated MEPS (Fig. 5A–C). The majority of the denervated MEPS (86%) in the treated muscles were reinnervated by regenerating axons. In the treated muscles, innervated and non-innervated MEPS (Fig. 5A–E), small, newly formed MEPS (Fig. 5F and G), and axonal sprouts (Fig. 5H and I) were identified. Terminal axons within the innervated MEPS were visualized (Fig. 5J and K). In 3-month-denervated muscles, denervated MEPS were still present. However, only a few fragments and/or accumulations of decomposed axons (arrows) and non-innervated MEPS (no visible axon attachment) were observed (Fig. 5L).

## DISCUSSION

In this study we have demonstrated that NMEG–NMZ and NGF/FGF-2 co-treated muscles exhibited better muscle reinnervation and functional recovery when compared with those treated only with NMEG–NMZ microsurgery.<sup>11</sup> Our findings indicate that focal application of exogenous NGF and FGF-2 promotes reinnervation by NMEG.

Poor motor recovery after PNI and nerve repair is closely related to insufficient axonal regeneration and reinnervation of the denervated MEPS in

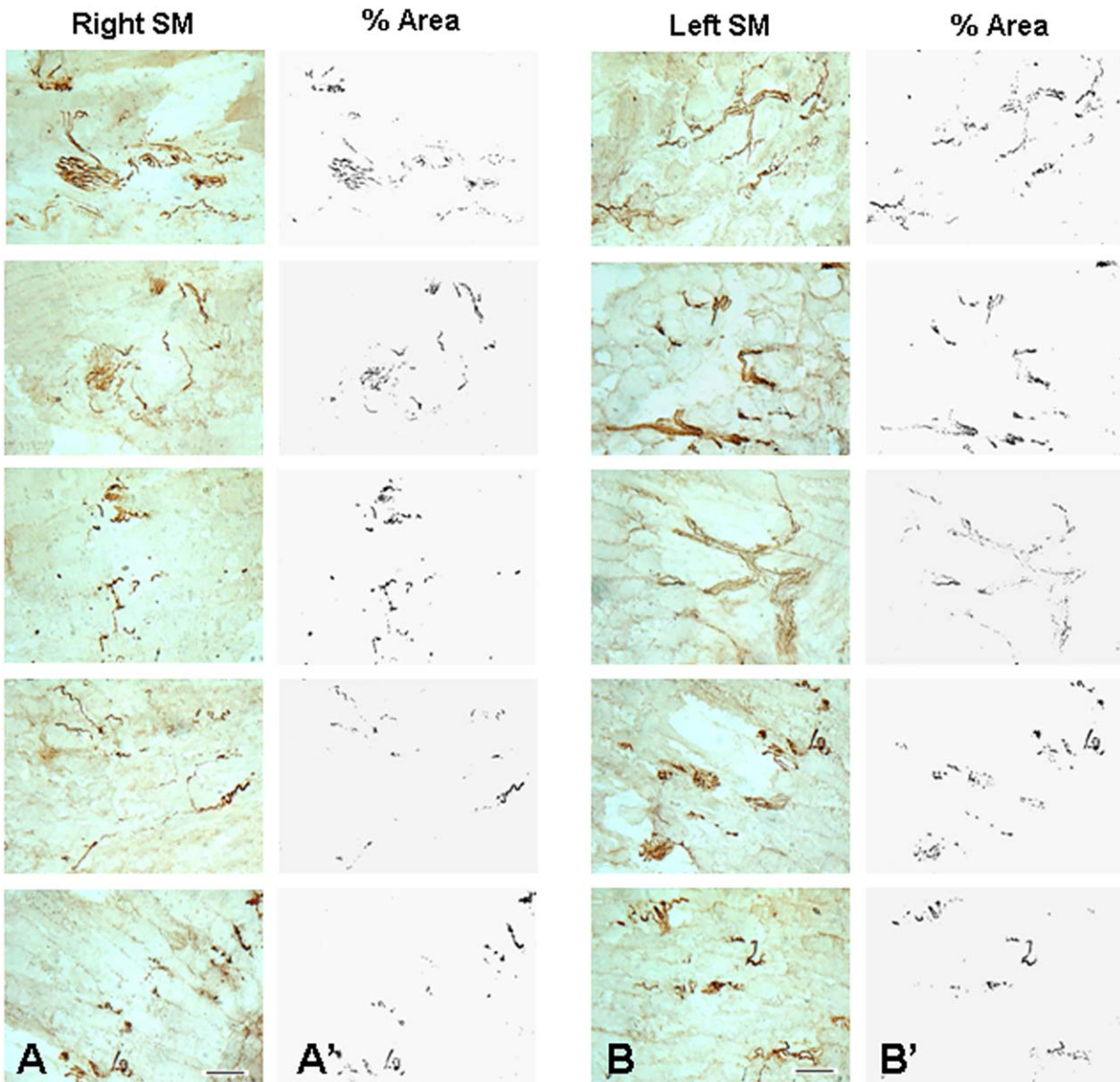


**FIGURE 4.** Photomicrographs of the immunostained sagittal sections from right treated (**A**) and left control (**B**) sternomastoid (SM) rat muscles. The sections were immunostained with antibody against neurofilament (NF). Images were taken from 5 microscopic fields in each section. Note that the nerve fascicles and axons (darkly stained threads and dots) in the right treated SM are distributed throughout the thickness of the muscle. Bar = 100  $\mu\text{m}$  for (**A**) and (**B**). (**A'**, **B'**) Images (**A**) and (**B**) were opened using ImageJ software and converted to 8-bit (binary) images, color thresholded, and particle analyzed for nerve morphometry. The density of the axons was evaluated by calculating the number and percent area of the NF-positive axons in each section. For this animal (rat no. 13), as compared with the left control SM (mean axon count 902, mean area 0.899), the right SM shows very good muscle reinnervation, as indicated by the mean axon count (779, 86.4% of control) and mean area (0.824, 91.7% of the control).

the target muscle.<sup>7</sup> One of the critical reasons for the impaired target reinnervation could be degradation of MEPs during prolonged denervation. Our studies have documented that the NMZ of the target muscle is the best site to design microsurgical procedures such as NMEG–NMZ<sup>11</sup> and/or direct nerve implantation into the NMZ<sup>52</sup> for muscle reinnervation. The regenerating axons from the implanted nerve or NMEG pedicle could easily reach and reinnervate the denervated MEPs in the NMZ of the target muscle. We have shown that the NMEG–NMZ technique resulted in better

functional recovery (82% of the control)<sup>11</sup> when compared with our originally designed NMEG procedure (67% of the control).<sup>9</sup> The suboptimal functional outcome of our original NMEG procedure could be due, at least in part, to the fact that the NMEG pedicle was implanted into an aneural region in the target muscle. In this case, regenerating axons from the implanted NMEG pedicle may need more time to reach the most distal muscle fibers and form new MEPs. The potential advantages of NMEG–NMZ technique over the original NMEG procedure include reduced nerve

**Table 2.** Comparison of count and percent area of neurofilament-immunoreactive axons between right treated and left control sternomastoid (SM) muscles in rats ( $n = 15$ ).

Animal no.	Right SM		Left SM		Ratio (R/L)	
	Count	%Area	Count	%Area	Count	%Area
1	683	0.738	896	1.056	0.762	0.699
2	866	0.605	995	0.803	0.870	0.753
3	926	0.801	1,033	0.982	0.896	0.816
4	901	0.674	1,128	0.874	0.799	0.771
5	587	0.509	898	0.786	0.654	0.648
6	955	1.200	1,074	0.996	0.889	1.205
7	493	0.605	723	0.862	0.682	0.702
8	889	0.826	834	0.974	1.066	0.848
9	510	0.721	670	0.865	0.761	0.834
10	809	1.002	876	1.033	0.924	0.970
11	917	0.801	1,056	0.796	0.868	1.006
12	558	0.725	801	0.854	0.697	0.849
13	779	0.824	902	0.899	0.864	0.917
14	882	0.879	997	1.120	0.885	0.785
15	970	0.934	993	0.982	0.977	0.951
Average	782	0.790	925	0.925	0.840	0.850
SD	170	0.17	131	0.10	0.11	0.14

L, left; R, right.

regeneration distances and rapid axon–MEP connections. The re-established functional synapses could avoid muscle atrophy and achieve optimal functional recovery.

Innervation that occurs at the NMZ contains numerous intramuscular nerve terminals and MEPs.<sup>11,52</sup> The MEP is a highly specialized structure that initiates action potential propagation required for excitation/contraction coupling to generate force for movement and maintain myofiber properties.<sup>53–55</sup> Existing evidence favors the view that MEP regions of mammalian muscle fibers are preferentially reinnervated as a consequence of some special property of the muscle fiber at this site. After nerve injury<sup>56–60</sup> and/or direct nerve implantation,<sup>61,62</sup> regenerating axons and sprouts preferentially grow into the sites of the original MEPs and form synapses. The synaptic basal lamina at the MEP contains molecules that direct the formation of synaptic specializations on regenerating axon terminals and myofibers.<sup>63</sup> Some other chemotropic substance released from the MEPs may attract the regenerating axons in the vicinity. Hence, the reinnervation of the denervated MEPs in the NMZ of a target muscle must occur as a consequence of some property of the muscle fiber at this site that favors synapse formation.

In a crushed nerve, regenerating axons can grow along pre-existing pathways and form MEPs on the same fibers that they originally innervated.<sup>64</sup> When the proximal nerve stump is not available, the target denervated muscle may be reinnervated by transplantation of a foreign motor nerve. Motor axons from the transplanted foreign

nerve could make ectopic synapses with the muscle fiber. If the axons of the foreign nerve approach the endplate zone of the target muscle, these axons avoid making ectopic synapses in a zone, the so-called “refractory zone” (~1 mm), around the original endplates.<sup>65,66</sup> Instead, these axons make synaptic contact at the original endplates. This refractory zone may be explained by Schwann cell growth from the old endplates. Regenerating axons would tend to follow these processes to the original endplate zone and make synapses. Axonal sprouts could locate denervated MEPs, the preferred site for synapse formation.<sup>67,68</sup> Some chemotropic substances released from the MEPs may exert an attraction on the regenerating axons.

Successful restoration of muscle function after microsurgery is highly dependent on the absolute number of nerve fibers that enter the denervated muscle, the rate at which they grow distally, and the number of functional synapses they establish with the muscle. The optimal outcomes of this study should be attributed to the potential advantage of the NMEG–NMZ technique and the additive effects of NGF and FGF-2 on nerve regeneration. Specifically, NMEG–NMZ microsurgery creates an ideal condition that physically facilitates axon–MEP connections. The regenerating axons derived from the implanted NMEG could rapidly contact the denervated MEPs and form functional synapses in the target muscle. A transplanted NMEG provides an abundant source of nerve terminals and has sufficient pedicle–recipient muscle interfaces, which provide enough space for axonal regeneration. The axons

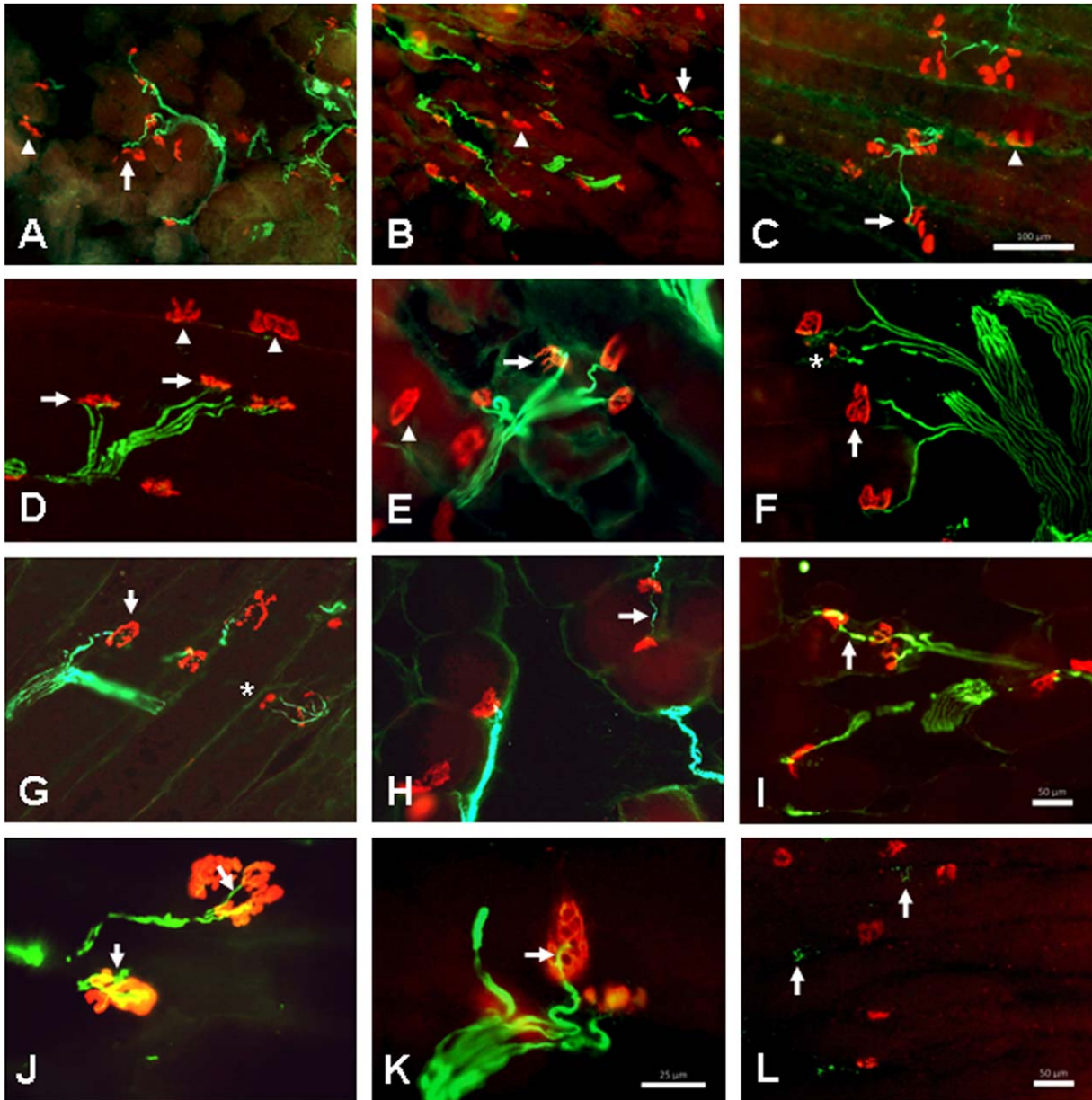


**FIGURE 5.** Double-immunofluorescence labeling of sagittal sections from right treated sternomastoid (SM) rat muscle (**A–K**) and from a denervated SM muscle (**L**). The immunostained sections show labeled axons (green) and motor endplates (MEPs, red). (**A–C**) Low-power view of the stained sections, showing the distribution of the MEPs and axons within the muscle. Note that the majority of the MEPs in the treated SM muscle were reinnervated by regenerated axons (arrows). The non-innervated MEPs are indicated by the arrowheads. Bar = 100  $\mu\text{m}$  for (**A**)–(**C**). (**D–I**) High-power view of the stained sections, showing innervated (arrows) and non-innervated (arrowheads) MEPs (**D**, **E**), small, newly formed MEPs [asterisks in (**F**) and (**G**)], and ultraterminal sprouts [arrows in (**H**) and (**I**)]. Bar = 50  $\mu\text{m}$  for (**D**)–(**I**). (**J**, **K**) Higher power view of stained MEPs, showing terminal axons [arrows in (**J**) and (**K**)] and acetylcholine receptors at MEPs. Bar = 25  $\mu\text{m}$  for (**J**) and (**K**). (**L**) An immunostained section from a rat SM muscle denervated for 3 months. Note that only a few fragments and/or accumulations of neurofilament-immunoreactive decomposed nerve fibers (arrows) and non-innervated MEPs (no visible axon attachment) can be seen. Bar = 50  $\mu\text{m}$ .

could start to regenerate at multiple points in the implanted NMEG and grow across the pedicle–recipient muscle interfaces to reach the recipient muscle fibers. In this study, application of NGF and FGF-2 to the NMEG–NMZ-reinnervated muscles provided trophic support and a biologically permissive environment to accelerate the processes of axonal regeneration and muscle reinnervation. The beneficial effects of NGF and

FGF-2 on axonal regeneration and functional recovery observed in our study are in line with previous reports.<sup>13,15,17–21,26,29,32,33</sup>

In many peripheral nerve regeneration studies, a number of exogenous neurotrophic factors have been extensively investigated.<sup>69</sup> Due to their relatively short half-life *in vivo*,<sup>70,71</sup> the growth factors were administered weekly for several weeks after microsurgery for muscle reinnervation.<sup>27</sup>

Therefore, effort was focused on the delivery of growth factors over a more prolonged time period,<sup>72,73</sup> such as the local use of a fibrin sealant containing neurotrophic factors.<sup>13,14,28,38–40</sup> Several different neurotrophic factors have already been tested in clinical trials for the treatment of peripheral nerve disease, with variable results. Clinical uses for NGF have been proposed for Parkinson and Alzheimer diseases,<sup>74</sup> and other neurotrophic factors have also been advocated, such as ciliary neurotrophic factor to treat amyotrophic lateral sclerosis.<sup>75</sup> Increasing evidence suggests that, in the future, application of exogenous neurotrophic factors may become a valuable therapeutic tool to accelerate motor nerve regeneration and reduce muscle atrophy. Our findings may provide a rationale to consider surgical and biological solutions to improve nerve regeneration and MEP reinnervation. This combination may prove useful as a strategy to treat PNI-related muscle paralysis.

The authors thank the anonymous reviewers for their constructive comments on this manuscript.

## REFERENCES

- Wiberg M, Terenghi G. Will it be possible to produce peripheral nerves? *Surg Technol Int* 2003;11:303–310.
- Ichihara S, Inada Y, Nakamura T. Artificial nerve tubes and their application for repair of peripheral nerve injury: an update of current concepts. *Injury* 2008;39(suppl 4):S29–39.
- Lee SK, Wolfe SW. Peripheral nerve injury and repair. *J Am Acad Orthop Surg* 2000;8:243–252.
- Mykатыn TM, Mackinnon SE. A review of research endeavors to optimize peripheral nerve reconstruction. *Neurol Res* 2004;26:124–138.
- Siemionow M, Brzezicki G. Chapter 8: Current techniques and concepts in peripheral nerve repair. *Int Rev Neurobiol* 2009;87:141–172.
- Payne SH, Brushart TM. Neurotization of the rat soleus muscle: a quantitative analysis of reinnervation. *J Hand Surg Am* 1997;22:640–643.
- Ma CHE, Omura T, Cobos EJ, Latremoliere A, Ghasemlou N, Brenner GJ, et al. Accelerating axonal growth promotes motor recovery after peripheral nerve injury in mice. *J Clin Invest* 2011;121:4332–4347.
- Barbour J, Yee A, Kahn LC, Mackinnon SE. Supercharged end-to-side anterior interosseous to ulnar motor nerve transfer for intrinsic musculature reinnervation. *J Hand Surg Am* 2012;37:2150–2159.
- Mu L, Sobotka S, Su H. Nerve-muscle-endplate band grafting: a new technique for muscle reinnervation. *Neurosurgery* 2011;69(suppl 2):208–224.
- Jansen JK, Lomo T, Nicolaysen K, Westgaard RH. Hyperinnervation of skeletal muscle fibers: dependence on muscle activity. *Science* 1973;181:559–561.
- Mu L, Sobotka S, Chen J, Nyirenda T. Reinnervation of denervated muscle by implantation of nerve-muscle-endplate band graft to the native motor zone of the target muscle. *Brain Behav* 2017;7:e00668.
- McCallister WV, Tang P, Smith J, Trumble TE. Axonal regeneration stimulated by the combination of nerve growth factor and ciliary neurotrophic factor in an end-to-side model. *J Hand Surg* 2001;26A:478–488.
- Zeng L, Worsg A, Redl H, Schlag G. Peripheral nerve repair with nerve growth factor and fibrin matrix. *Eur J Plast Surg* 1994;17:228–232.
- Jubran M, Widenfalk J. Repair of peripheral nerve transections with fibrin sealant containing neurotrophic factors. *Exp Neurol* 2003;181:204–212.
- Wang S, Cai Q, Hou J, Bei J, Zhang T, Yang J, et al. Acceleration effect of basic fibroblast growth factor on the regeneration of peripheral nerve through a 15-mm gap. *J Biomed Mater Res A* 2003;66:522–531.
- Danielsen N, Pettman B, Vahlsing HL, Manthorpe M, Varon S. Fibroblast growth factor effects on peripheral nerve regeneration in a silicone chamber model. *J Neurosci Res* 1988;20:320–330.
- Grothe C, Ninkovic G. The role of basic fibroblast growth factor in peripheral nerve regeneration. *Anat Embryol (Berl)* 2001;204:171–177.
- Heumann R. Regulation of the synthesis of nerve growth factor. *J Exp Biol* 1987;132:133–150.
- Thoenen H, Bandtlow C, Heumann R, Lindholm D, Meyer M, Rohrer H. Nerve growth factor: cellular localization and regulation of synthesis. *Cell Mol Neurobiol* 1988;8:35–40.
- Raivich G, Kreutzberg GW. Peripheral nerve regeneration: role of growth factors and their receptors. *Int J Dev Neurosci* 1993;11:311–324.
- Campanot RB. NGF and the local control of nerve terminal growth. *J Neurobiol* 1994;25:599–611.
- Saika T, Senba E, Noguchi K, Sato M, Yoshida S, Kubo T, et al. Effects of nerve crush and transection on mRNA levels for nerve growth factor receptor in the rat facial motoneurons. *Brain Res Mol Brain Res* 1991;9:157–160.
- He C, Chen Z, Chen Z. Enhancement of motor nerve regeneration by nerve growth factor. *Microsurgery* 1992;13:151–154.
- Derby A, Engleman VW, Friedrich GE, Neises G, Rapp SR, Roufa DG. Nerve growth factor facilitates regeneration across nerve gaps: morphological and behavioral studies in rat sciatic nerve. *Exp Neurol* 1993;119:176–191.
- Chen ZW, Wang MS. Effects of nerve growth factor on crushed sciatic nerve regeneration in rats. *Microsurgery* 1995;16:547–551.
- Pu LL, Syed SA, Reid M, Patwa H, Goldstein JM, Forman DL, et al. Effects of nerve growth factor on nerve regeneration through a vein graft across a gap. *Plast Reconstr Surg* 1999;104:1379–1385.
- Menderes A, Yilmaz M, Vayvada H, Ozer E, Barutcu A. Effects of nerve growth factor on the neurotization of denervated muscles. *Ann Plast Surg* 2002;48:415–422.
- Lee AC, Yu VM, Lowe JB, Brenner MJ, Hunter DA, Mackinnon SE, et al. Controlled release of nerve growth factor enhances sciatic nerve regeneration. *Exp Neurol* 2003;184:295–303.
- Grothe C, Haastert K, Jungnickel J. Physiological function and putative therapeutic impact of the FGF-2 system in peripheral nerve regeneration—lessons from in vivo studies in mice and rats. *Brain Res Rev* 2006;51:293–299.
- Aebischer P, Salessiotis AN, Winn SR. Basic fibroblast growth factor released from synthetic guidance channels facilitates peripheral nerve regeneration across long nerve gaps. *J Neurosci Res* 1989;23:282–289.
- Fujimoto E, Mizoguchi A, Hanada K, Yajima M, Ide C. Basic fibroblast growth factor promotes extension of regenerating axons of peripheral nerve. In vivo experiments using a Schwann cell basal lamina tube model. *J Neurocytol* 1997;26:511–528.
- Jungnickel J, Haase K, Konitzer J, Timmer M, Grothe C. Faster nerve regeneration after sciatic nerve injury in mice over-expressing basic fibroblast growth factor. *J Neurobiol* 2006;66:940–948.
- Iwata Y, Ozaki N, Hirata H, Sugiura Y, Horri E, Nakao E, et al. Fibroblast growth factor-2 enhances functional recovery of reinnervated muscle. *Muscle Nerve* 2006;34:623–630.
- Casella GTB, Almeida VW, Grumbles RM, Liu Y, Thomas CK. Neurotrophic factors improve muscle reinnervation from embryonic neurons. *Muscle Nerve* 2010;42:788–797.
- Lewin SL, Utley DS, Cheng ET, Verity AN, Terris DJ. Simultaneous treatment with BDNF and CNTF after peripheral nerve transection and repair enhances rate of functional recovery compared with BDNF treatment alone. *Laryngoscope* 1997;107:992–999.
- Mohiuddin L, Delcroix JD, Fernyhough P, Tomlinson DR. Focally administered nerve growth factor suppresses molecular regenerative responses of axotomized peripheral afferents in rats. *Neuroscience* 1999;91:265–271.
- McCallister WV, McCallister EL, Dubois B, Trumble TE. Regeneration along intact nerves using nerve growth factor and ciliary neurotrophic factor. *J Reconstr Microsurg* 2004;20:473–481.
- Cheng H, Fraidakis M, Blomback B, Lapchak P, Hoffer B, Olson L. Characterization of a fibrin glue-GDNF slow-release preparation. *Cell Transplant* 1998;7:53–61.
- Yin Q, Kemp CJ, Yu LG, Wagstaff SC, Frostick SP. Neurotrophin-4 delivered by fibrin glue promotes peripheral nerve regeneration. *Muscle Nerve* 2001;24:345–351.
- Tajdaran K, Gordon T, Wood MD, Shoichet MS, Borschel GH. A glia cell line—derived neurotrophic factor delivery system enhances nerve regeneration across acellular nerve allografts. *Acta Biomater* 2016;29:62–70.
- Wood MD, Gordon T, Kemp SWP, Liu EH, Kim H, Shoichet MS, et al. Functional motor recovery is improved due to local placement of GDNF microspheres after delayed nerve repair. *Biotechnol Bioeng* 2013;110:1272–1281.
- Mitsumoto H, Ikeda K, Klinkosz B, Cedarbaum JM, Wong V, Lindsay RM. Arrest of motor neuron disease in wobbler mice cotreated with CNTF and BDNF. *Science* 1994;265:1107–1110.
- Hanson Jr MG, Shen S, Wiemelt AP, McMorris FA, Barres BA. Cyclic AMP elevation is sufficient to promote the survival of spinal motor neurons in vitro. *J Neurosci* 1998;18:7361–7371.
- Ho PR, Coan GM, Cheng ET, Niell C, Tarn DM, Zhou H, et al. Repair with collagen tubules linked with brain-derived neurotrophic

- factor and ciliary neurotrophic factor in a rat sciatic nerve injury model. *Arch Otolaryngol Head Neck Surg* 1998;124:761–766.
45. Sobotka S, Mu L. Characteristics of tetanic force produced by the sternomastoid muscle of the rat. *J Biomed Biotechnol* 2010;2010:194984.
  46. Sobotka S, Mu L. Force characteristics of the rat sternomastoid muscle reinnervated with end-to-end nerve repair. *J Biomed Biotechnol* 2011;2011:173471.
  47. Sobotka S, Mu L. Force recovery and axonal regeneration of the sternomastoid muscle reinnervated with the end-to-end nerve anastomosis. *J Surg Res* 2013;182:e51–59.
  48. Sobotka S, Mu L. Comparison of muscle force after immediate and delayed reinnervation using nerve-muscle-endplate band grafting. *J Surg Res* 2013;179:e117–126.
  49. Sobotka S, Mu L. Muscle reinnervation with nerve-muscle-endplate band grafting technique: Correlation between force recovery and axonal regeneration. *J Surg Res* 2015;195:144–151.
  50. Mu L, Chen J, Sobotka S, Nyirenda T, Benson B, Gupta F, et al. Alpha-synuclein pathology in sensory nerve terminals of the upper aerodigestive tract of Parkinson's disease patients. *Dysphagia* 2015;30:404–417.
  51. Grumbles RM, Sesodia S, Wood PM, Thomas CK. Neurotrophic factors improve motoneuron survival and function of muscle reinnervated by embryonic neurons. *J Neuropathol Exp Neurol* 2009;68:736–746.
  52. Sobotka S, Chen J, Nyirenda T, Mu L. Outcomes of muscle reinnervation with direct nerve implantation into the native motor zone of the target muscle. *J Reconstr Microsurg* 2017;33:77–86.
  53. Sanes JR, Lichtman JW. Development of the vertebrate neuromuscular junction. *Ann Rev Neurosci* 1999;22:389–442.
  54. Bassel-Duby R, Olson EN. Signaling pathways in skeletal muscle remodeling. *Ann Rev Biochem* 2006;75:19–37.
  55. Wu H, Xiong WC, Mei L. To build a synapse: signaling pathways in neuromuscular junction assembly. *Development* 2010;137:1017–1033.
  56. Iwayama T. Relation of regenerating nerve terminals to original endplates. *Nature* 1969;224:81–82.
  57. Bennett MR, McLachlan EM, Taylor RS. The formation of synapses in reinnervated mammalian striated muscle. *J Physiol Lond* 1973;233:481–500.
  58. Sanes JR, Marshall LM, McMahan UJ. Reinnervation of muscle fiber basal lamina after removal of myofibers. Differentiation of regenerating axons at original synaptic sites. *J Cell Biol* 1978;78:176–198.
  59. Gorio A, Carmignoto G, Finesso M, Polato P, Nunzi MG. Muscle reinnervation. II. Sprouting, synapse formation, and repression. *Neuroscience* 1983;8:403–416.
  60. Covault J, Cunningham JM, Sanes JR. Neurite outgrowth on cryostat sections of innervated and denervated skeletal muscle. *J Cell Biol* 1987;105:2479–2488.
  61. Guth L, Zalewski AA. Disposition of cholinesterase following implantation of nerve into innervated and denervated muscle. *Exp Neurol* 1963;7:316–326.
  62. Sakellarides HT, Sorbie C, James L. Reinnervation of denervated muscles by nerve transplantation. *Clin Orthop Relat Res* 1972;83:195–201.
  63. McMahan UJ, Wallace BG. Molecules in basal lamina that direct the formation of synaptic specializations at neuromuscular junctions. *Dev Neurosci* 1989;11:227–247.
  64. Nguyen QT, Sanes JR, Lichtman JW. Pre-existing pathways promote precise projection patterns. *Nat Neurosci* 2002;5:861–867.
  65. Lomo T, Pockett S, Sommerschild H. Control of number and distribution of synapses during ectopic synapse formation in adult rat soleus muscles. *Neuroscience* 1988;24:673–686.
  66. Lomo T. What controls the position, number, size and distribution of neuromuscular junctions on rat muscle fibers? *J Neurocytol* 2003;32:835–848.
  67. Son YJ, Thompson WJ. Schwann cell processes guide regeneration of peripheral axons. *Neuron* 1995;14:125–132.
  68. Son YJ, Thompson WJ. Nerve sprouting in muscle is induced and guided by processes extended by Schwann cells. *Neuron* 1995;14:133–141.
  69. Terenghi G. Peripheral nerve regeneration and neurotrophic factors. *J Anat* 1999;194:1–14.
  70. Whalen GF, Shing Y, Folkman J. The fate of intravenously administered bFGF and the effect of heparin. *Growth Factors* 1989;1:157–164.
  71. Nimni ME. Polypeptide growth factors: targeted delivery systems. *Biomaterials* 1997;18:1201–1225.
  72. Jeon O, Ryu SH, Chung JH, Kim BS. Control of basic fibroblast growth factor release from fibrin gel with heparin and concentrations of fibrinogen and thrombin. *J Control Release* 2005;105:249–259.
  73. Lee JS, Go DH, Bae JW, Lee SJ, Park KD. Heparin conjugated polymeric micelle for long-term delivery of basic fibroblast growth factor. *J Control Release* 2007;117:204–209.
  74. Olson L, Backman L, Ebendal T, Eriksdotter-Jonhagen M, Hoffer B, Humpel C, et al. Role of growth factors in degeneration and regeneration in the central nervous system; clinical experience with NGF in Parkinson's and Alzheimer's diseases. *J Neurol* 1994;242(suppl 1):S12–15.
  75. Penn RD, Kroin JS, York MM, Cedarbaum JM. Intrathecal ciliary neurotrophic factor delivery for treatment of amyotrophic lateral sclerosis (phase I trial). *Neurosurgery* 1997;40:94–99.

# Immunohistochemical Detection of Motor Endplates in the Long-Term Denervated Muscle

Liancai Mu, MD, PhD<sup>1</sup> Jingming Chen, MD<sup>1</sup> Jing Li, BS<sup>1</sup> Themba Nyirenda, PhD<sup>1</sup>  
Mary Fowkes, MD, PhD<sup>2</sup> Stanislaw Sobotka, PhD, DSc<sup>1,3</sup>

<sup>1</sup>Department of Biomedical Research, Hackensack University Medical Center, Hackensack, New Jersey

<sup>2</sup>Department of Pathology, Icahn School of Medicine at Mount Sinai, New York, New York

<sup>3</sup>Department of Neurosurgery, Icahn School of Medicine at Mount Sinai, New York, New York

Address for correspondence Liancai Mu, MD, PhD, Department of Biomedical Research, Hackensack University Medical Center, Hackensack, NJ 07601 (e-mail: Liancai.Mu@hackensackmeridian.org).

J Reconstr Microsurg 2018;34:348–358.

## Abstract

**Background** We have demonstrated that the native motor zone (NMZ) within a muscle is an ideal target for performing nerve-muscle-endplate band grafting (NMEG) to restore motor function of a denervated muscle. This study was designed to determine spatiotemporal alterations of the myofibers, motor endplates (MEPs), and axons in the NMZ of long-term denervated muscles for exploring if NMEG-NMZ technique would have the potential for delayed reinnervation.

**Methods** Sternomastoid (SM) muscles of adult female Sprague-Dawley rats ( $n = 21$ ) were experimentally denervated and denervation-induced changes in muscle weight, myofiber size, MEPs, and intramuscular nerve axons were evaluated histomorphometrically and immunohistochemically at the end of 3, 6, and 9 months after denervation. The values obtained from the ipsilateral normal side served as control.

**Results** The denervated SM muscles exhibited a progressive reduction in muscle weight (38%, 31%, and 19% of the control) and fiber diameter (52%, 40%, and 28% of the control) for 3-, 6-, and 9-month denervation, respectively. The denervated MEPs were still detectable even 9 months after denervation. The mean number of the denervated MEPs was 79%, 65%, and 43% of the control in the 3-, 6-, and 9-month denervated SM, respectively. Degenerated axons in the denervated muscles became fragmented.

**Conclusions** Persistence of MEPs in the long-term denervated SM suggests that some surgeries targeting the MEPs such as NMEG-NMZ technique should be effective for delayed reinnervation. However, more work is needed to develop strategies for preservation of muscle mass and MEPs after denervation.

## Keywords

- ▶ denervation
- ▶ peripheral nerve injury
- ▶ motor endplate
- ▶ acetylcholine receptor
- ▶ muscle atrophy
- ▶ native motor zone

Peripheral nerve injury (PNI) results in muscle denervation characterized by deleterious changes including progressive myofiber atrophy, loss of muscle mass, and functional impairment. These denervation-induced morphological and functional changes can be reversed by reinnervation. However, functional recovery is frequently poor following PNI and nerve repair, especially in cases with chronic denervation or delayed nerve reconstruction.<sup>1,2</sup>

The poor functional recovery after PNI and nerve repair is closely associated with insufficient axonal regeneration and reinnervation of the denervated motor endplates (MEPs) in the target muscle.<sup>3–6</sup> Recent studies by Dr. Gordon's laboratory have demonstrated that chronic distal nerve stump denervation, induced by delayed nerve repair or prolonged

received

September 1, 2017

accepted after revision

December 23, 2017

published online

March 6, 2018

Copyright © 2018 by Thieme Medical Publishers, Inc., 333 Seventh Avenue, New York, NY 10001, USA.  
Tel: +1(212) 584-4662.

DOI <https://doi.org/10.1055/s-0038-1627463>.  
ISSN 0743-684X.

regeneration distance, is the key factor leading to reduced axonal regeneration and subsequently poor functional outcome.<sup>1,2,7-10</sup>

Our recent studies highlight the importance of native motor zone (NMZ) of the target muscle in reinnervation surgeries. We developed a novel microsurgical method called "nerve-muscle-endplate band grafting (NMEG)" for muscle reinnervation.<sup>11</sup> The idea is that a paralyzed muscle could be reinnervated by transplanting an NMEG from a neighboring donor muscle. A healthy nerve branch and terminals that innervate an expendable muscle can be transplanted to a more functionally important denervated muscle for restoring its motor function. In our animal experiments, a NMEG pedicle containing a nerve branch and a muscle block with nerve terminals and MEPs was harvested from the sternohyoid (SH) muscle and transplanted into the ipsilateral experimentally denervated sternomastoid (SM) muscle. In a rat immediate reinnervation model, we recently demonstrated that implantation of the NMEG into the NMZ of the target muscle, which lies in the midregion of the muscle, yielded better functional recovery (82% of the control)<sup>12</sup> 3 months after surgery when compared with implantation of the NMEG into an aneural region in the target muscle (67%).<sup>11</sup> Our studies have documented that the NMZ of the target muscle is the best site to design some microsurgical procedures such as NMEG-NMZ<sup>12</sup> and/or direct nerve implantation (DNI) into the NMZ<sup>13</sup> for muscle reinnervation. The satisfactory outcomes of NMEG-NMZ and DNI-NMZ reinnervation procedures should be attributed to such a fact that both techniques could reduce nerve regeneration distances and favor rapid axon-MEP connections. The regenerating axons from the implanted nerve or NMEG pedicle could easily reach and reinnervate the denervated MEPs in the NMZ of the target muscle. The re-established functional synapses could avoid muscle atrophy and restore motor function.

Although NMEG-NMZ or DNI-NMZ has the potential for immediate muscle reinnervation, it remains unknown if such techniques are effective for the restoration of motor function of long-term denervated muscles. In the clinical setting, some patients suffer from PNI-induced muscle denervation for years. It has been reported that prolonged delay in the reinnervation of skeletal muscle leads to poor functional recovery because reinnervation is incomplete.<sup>1,14</sup> The incomplete restoration of long-term denervated muscle is related to a failure of regenerating nerves to reach all of the atrophic muscle fibers and establish mature muscle-nerve contacts.<sup>1,15</sup> Time to reinnervation is one of the most important determinants of functional outcome because muscle fibers progressively undergo an irreversible degeneration process, if reinnervation does not occur.<sup>16-18</sup> The degree of functional restoration of the target muscle following reinnervation procedures is inversely related to the denervation time: that is, the longer the muscle denervation, the poorer the functional outcome following reinnervation surgeries. It is, therefore, important to directly determine if MEPs are preserved in the chronically denervated muscles. However, neuromuscular alterations induced by long-term denerva-

tion of the SM muscle have yet to be determined. The time-course of morphological changes and progression of post-denervation atrophy of the muscle have never been determined. It is necessary to determine the presence or absence of the MEPs in the long-term denervated muscle because the presence of a greater number of preserved MEPs in the target muscle is important for more efficient and successful reinnervation.

The purpose of this study was to investigate the effect of prolonged denervation on the degradation of the existing junctional acetylcholine receptors (AChRs) at MEPs of the rat SM muscle. Specifically, we sought to determine whether or not the MEPs can be detected after prolonged periods of denervation for providing the baseline for future application of the NMEG-NMZ reinnervation technique to treat PNI-induced chronic muscle paralysis. The information about the morphological and histochemical alterations in myofibers and MEPs at different time points following denervation can help to design effective surgical procedures and other therapeutic strategies to delay or prevent myofiber atrophy and MEP degradation following PNI. We hope to gain greater insight into the potential treatment of chronic muscle paralysis by NMEG-NMZ and other therapies.

## Materials and Methods

### Animals

Twenty-one three-month-old female Sprague-Dawley rats (Taconic Laboratories, Cranbury, NJ) weighing from 200 to 250 g were used. All protocols for animal procedures were approved by the Institutional Animal Care and Use Committee prior to the onset of experiments. All animals were handled in accordance with the Guide for Care and Use of Laboratory Animals published by the US National Institutes of Health (NIH publication no. 85-23, revised 1996). The rats were housed at a constant temperature (22°C) on a 12 hours light/dark cycle and were given food and water as desired.

### Muscle Denervation

The 21 rats were randomly allocated into three groups each comprising 7 animals on the basis of the observation period after SM nerve resection. The animals in the 3 groups were euthanized with an overdose of ketamine and xylazine 3 months, 6 months, or 9 months after SM denervation. For each animal, all the assessments were performed from both SM muscles and the contralateral SM served as a control.

For muscle denervation, the animals were anesthetized with intraperitoneal ketamine (80 mg/kg) and xylazine (5 mg/kg). Under a surgical microscope (Olympus America Inc., Center Valley, PA), a vertical midline skin incision was made to expose the right SM muscle and its innervating nerve. A 5-mm segment of the nerve was resected to denervate the muscle. Both nerve ends were coagulated with a bipolar cautery to avoid nerve regeneration. After completion of muscle denervation, the wound was closed.

Denervation of the SM muscles was prolonged for periods of 3, 6, and 9 months. At the end of each denervation period,

muscle weight, fiber size, and MEPs were measured and compared between denervated and contralateral control SM muscles.

### Muscle Weight Measurement and Tissue

#### Preparation

At the end of the experiment 3, 6, and 9 months after denervation, both SM muscles for each rat were harvested, photographed, and weighed. Wet muscle weights directly indicating that the degree of denervation was reported as a ratio of the denervated to the contralateral control side. Each of the removed SM muscles was divided into three segments: rostral, middle, and caudal. The muscle segments were frozen by immersion in melting isopentane cooled to  $-65^{\circ}\text{C}$  with dry ice and cut on a cryostat (Reichert-Jung 1800; Mannheim, Germany) at  $-25^{\circ}\text{C}$ . The rostral and caudal segments were cut transversely ( $10\ \mu\text{m}$ ) and stained histologically and immunohistochemically to examine denervated and atrophic myofibers. The middle segment containing the NMZ was cut sagittally ( $60\ \mu\text{m}$ ) and immunostained to detect and quantify MEPs and axons.

### Identification of Denervated and Atrophic Myofibers

#### Immunofluorescent Labeling of Neural Cell Adhesion Molecule

Immunohistochemical labeling for neural cell adhesion molecule (N-CAM), a molecular marker of muscle fiber denervation, was used to detect denervated myofibers. N-CAM is a developmental molecule, is present on the surface of embryonic myotubes, declines in level as development proceeds, nearly disappears in the adult muscle, reappears when adult muscles are denervated, and is lost after reinnervation.<sup>19–21</sup> N-CAM immunoreactivity on muscle fiber membranes in cross-sections provides a sensitive means of detecting denervated fibers in the denervated muscles.<sup>20,22,23</sup> In this study, tissue sections from the rat SM muscles were immunostained by using the method as described previously,<sup>23</sup> with some modifications. Briefly, some cross-sections were (1) fixed with methanol for 20 minutes at  $-20^{\circ}\text{C}$ , (2) blocked with 5% goat serum (Sigma, St. Louis, MO) in phosphate-buffered saline (PBS) for 30 minutes, (3) incubated with a primary monoclonal rabbit antirat N-CAM antibody (Chemicon, Temecula, CA) for 2 hours, and (4) incubated with a secondary CY3-conjugated goat antirabbit immunoglobulin G (IgG) (Jackson ImmunoResearch laboratories, West Grove, PA) at room temperature (RT) for 1 hour. The sections were washed extensively in PBS between steps. Control sections were stained without the incubation with the primary antibody. The stained sections were mounted with Vectashield mounting medium (Vector Laboratories, Burlingame, CA) and kept in dark at  $4^{\circ}\text{C}$ .

The immunostained sections were examined under a Zeiss fluorescence microscope (Axioplan-1; Carl Zeiss, Gottingen, Germany) and photographed using a USB 3.0 digital microscope camera (Infinity 3–3URC, Lumenera Corp., Ottawa, Canada).

### Fiber Diameter Measurement

Some cross-sections were immunostained with a monoclonal antibody NOQ7–5–4D against type I myosin heavy chain for fiber diameter measurement as this staining outlines fiber contour clearly. The avidin–biotin complex method was used as described in our previous publication.<sup>24</sup> In brief, the sections were fixed in 4% paraformaldehyde for 10 minutes and treated in 2% bovine serum albumin with 0.1% Triton X-100 for 20 minutes to block nonspecific binding. The sections were incubated with NOQ7–5–4D primary antibody (1:1,000; Sigma) for 1 hour at RT. The sections were then incubated for 1 hour with an antimouse IgG (ATCC, Rockville, MD). The incubated sections were processed with avidin–biotin complex reagent (Vector Laboratories) for 1 hour at RT. The sections were processed for 10 minutes at RT with 3,3'-diaminobenzidine substrate kit (SK-4100; Vector Laboratories) to visualize peroxidase labeling. The stained sections were dehydrated in ethanol, cleared in xylene, and mounted with Permount (Fisher Scientific, Fair Lawn, NJ).

Three stained sections were randomly selected from a given muscle and photographed. Images were taken at  $\times 200$  from four microscopic fields at four quadrants of each section. The photographed images were imported into an image-processing program (ImageJ v. 1.45s; NIH, Bethesda, MD) to measure fiber diameter. In each muscle, at least 100 myofibers were randomly selected to measure the least fiber diameter (the maximum diameter across the least aspect of the muscle fiber) using a previously described method.<sup>25</sup> Atrophic changes in the SM muscle were evaluated by comparing the mean fiber diameters between the denervated and control sides.

### Immunohistochemical Detection of MEPs and Axons

Triple fluorescence labeling was performed on some sagittal sections from the NMZ (middle segment) of the denervated and contralateral SM muscles in each rat to detect MEPs and intramuscular nerve axons, as described previously,<sup>12,26,27</sup> with some modifications. Briefly, the sections were fixed in Zamboni fixative with 5% sucrose for 20 minutes at  $4^{\circ}\text{C}$ . After washed extensively in 1.5T buffer (0.05 M Tris, pH 7.6 and 1.5% NaCl), the sections were rinsed for 30 minutes with 0.1 mol/L of glycine in 1.5T buffer and immersed for 20 minutes in 100% methanol at  $-20^{\circ}\text{C}$ . After blocked for 30 minutes in 1.5T buffer containing 4% normal goat serum, the sections were incubated overnight at  $4^{\circ}\text{C}$  with primary monoclonal antibodies (SMI-31 to detect neurofilaments, 1:1,000, Biolegend, San Diego, CA; and SVP-38 to reveal the presynaptic nerve terminals, 1:1,000, Sigma, St. Louis, MO). The sections were then incubated at RT for 2 hours both with Alexa Fluor 488 goat antimouse IgG secondary antibody (1:500; Invitrogen Corp., Carlsbad, CA) to label axons and with Alexa Fluor 596–conjugated  $\alpha$ -bungarotoxin (1:500; Invitrogen) to visualize postsynaptic AChRs at MEPs. Control sections were stained without the incubation with the primary antibody. The sections were washed several times with 1.5T buffer with 0.05% Tween-20 between steps. The stained sections were mounted with Vectashield mounting medium (Vector Laboratories) and kept in dark at  $4^{\circ}\text{C}$ .

The immunostained sections showing axons and terminals (green) and postsynaptic AChRs at the MEPs (red) were examined and photographed. Three stained sections at different spatial levels were selected and photographed to examine MEP and axon profiles. The stained MEPs in the SM muscles on both sides were counted and denervated/control (D/C) ratio for each animal was computed.

### Statistical Analysis

Wet muscle weights, fiber diameters, and MEP counts of the SM muscles in each rat were computed. All data were reported as mean  $\pm$  standard deviation. The variables of the denervated SM muscles were expressed as the percentages of the values of the contralateral control muscles. Average rates in three studied groups were compared with one-way analysis of variance (ANOVA) for independent samples. Post-hoc analysis was made with Tukey honest significant difference (HSD) test. Difference with  $p < 0.05$  was treated as statistically significant. SAS v. 9.4 software was used in statistical analyses.

## Results

### Muscle Mass and Wet Weight

Denervation of the SM resulted in significant reductions in muscle mass. The size of the denervated SM was smaller than that of the contralateral control (**Fig. 1A**). The muscle weights of the denervated and control SM muscles and D/C ratio for each animal, as well as mean value and standard deviation of the wet weight for each group are summarized in **Table 1**. The mass values of the denervated muscles were inferior to those of the controls. The presence of muscle atrophy was confirmed postmortem by the reduced weight

of the denervated muscles which dropped to 38%, 31%, and 19% of the control muscles after 3-, 6-, and 9-month denervation, respectively. The average muscle weight was significantly smaller in denervated than in control muscles ( $t = 19.7$ ,  $df = 20$ ,  $p < 0.00001$ ). Statistical analysis (one-way ANOVA) of the averaged rates of SM muscle weight (denervated to control) in these three groups indicated a strong trend toward decreasing rate with denervation time, but did not show statistical significant differences between these three groups ( $F = 3.25$ ,  $df = 2/18$ ,  $p = 0.0627$ ).

Note that the analysis was performed on assumption of normality holds; however, when sample sizes are less than 10 (such as 7), the Shapiro–Wilk test of normality has little power to detect deviations from normality. In fact, the Kruskal–Wallis test reported a statistically significant difference between these groups ( $p = 0.0422$ ). The box plots illustrating the distribution of data in 3-month, 6-month, and 9-month groups are shown in **Fig. 2**. Clearly, the reduction in the muscle mass is associated with denervation time.

Average body weights of all three groups (341 g, 324 g, and 366 g) were not statistically different ( $F = 1.57$ ,  $df = 2/18$ ,  $p = 0.235$ ).

### Denervated and Atrophic Myofibers

Muscle fibers after SM denervation underwent progressive atrophy (**Fig. 1B**). Long-term denervated muscles exhibited increased connective tissue with small atrophic muscle fibers. Most of the atrophic fibers were angular in shape.

Mean fiber diameters of the denervated and control muscles were summarized in **Fig. 3**. The fiber diameters of the denervated muscles were reduced versus those of the controls. Specifically, the mean fiber diameters were reduced

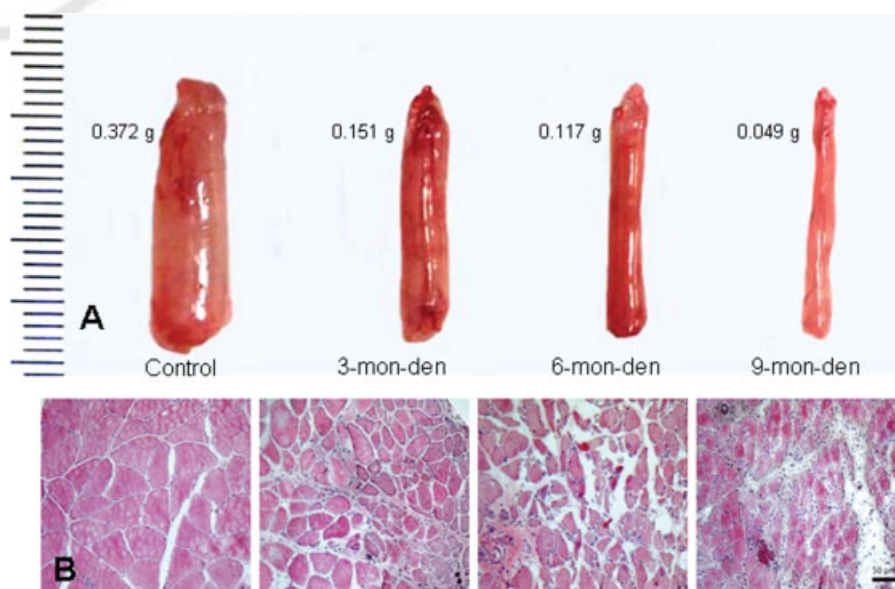


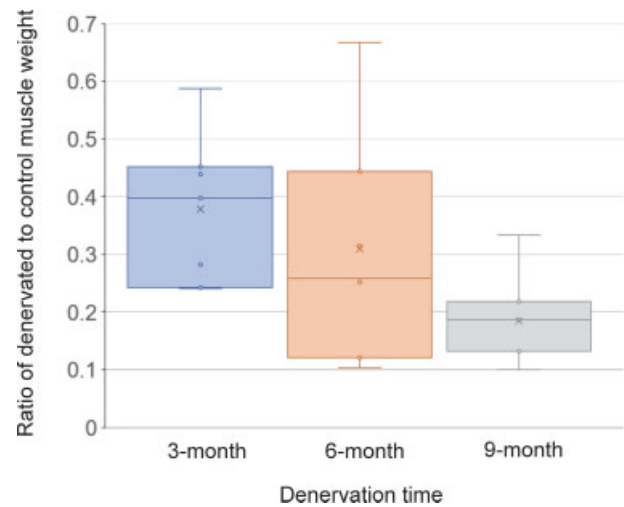
**Fig. 1** Comparison of muscle mass and myofiber morphology between control and denervated sternomastoid (SM) muscles in the rat. (A) Photographs of the removed control SM and denervated SM muscles, showing a progressive decline in muscle mass with denervation time. (B) Hematoxylin and eosin-stained cross-sections from the control and denervated SM muscles, showing a progressive reduction in fiber size of the denervated SM. 3-mon-den, 3-month denervation; 6-mon-den, 6-month denervation; 9-mon-den, 9-month denervation.

**Table 1** Wet muscle weights of 3-month-, 6-month-, and 9-month-denervated and control sternomastoid (SM) muscles in rats ( $n = 21$ )

Animal (No.)	Body weight (g)	Denervated SM (g)	Control SM (g)	Ratio D/C
<b>3-month DEN</b>				
1	259	0.150	0.342	0.439
2	370	0.151	0.335	0.451
3	353	0.075	0.311	0.241
4	324	0.101	0.357	0.283
5	319	0.075	0.309	0.243
6	379	0.164	0.413	0.397
7	386	0.250	0.425	0.588
Average	341.4	0.138	0.356	0.377
SD	44.6	0.062	0.046	0.129
<b>6-month DEN</b>				
1	296	0.258	0.386	0.668
2	390	0.117	0.372	0.315
3	378	0.039	0.380	0.103
4	282	0.075	0.298	0.252
5	304	0.047	0.390	0.121
6	296	0.166	0.374	0.444
7	324	0.101	0.391	0.258
Average	324.3	0.115	0.370	0.309
SD	42.8	0.077	0.033	0.196
<b>9-month DEN</b>				
1	323	0.082	0.376	0.218
2	330	0.138	0.415	0.333
3	300	0.066	0.353	0.187
4	394	0.049	0.371	0.132
5	398	0.037	0.369	0.100
6	412	0.052	0.382	0.136
7	408	0.073	0.378	0.193
Average	366.4	0.071	0.378	0.186
SD	46.9	0.033	0.019	0.077

Abbreviations: DEN, denervation; D/C, denervated/control; SD, standard deviation.

to 52%, 40%, and 28% of the control for 3-, 6-, and 9-month denervation groups, respectively. Statistical analysis (one-way ANOVA) of the rates (denervated to control) of the muscle fiber diameter showed strong statistical significant difference between these three groups ( $F = 17.7$ ,  $df = 2/13$ ,  $p = 0.000196$ ). Post-hoc testing (Tukey HSD test) shows statistical difference between means of each pair of three groups. Average of 3-month denervation group is signifi-

**Fig. 2** Box plots showing the distribution of sternomastoid (SM) muscle weight ratios (denervated to control) in 3-month, 6-month, and 9-month denervation groups. Median ratio is the largest in 3-month group (0.40) and decreases with length of denervation time to 0.26 in 6-month group and finally to 0.19 in the 9-month group.

cantly larger than average of 9-month denervation group ( $p < 0.01$ ). Also average of 3-month denervation group is significantly larger than that of 6-month denervation group ( $p < 0.05$ ) and average of 6-month denervation group is significantly larger than that of 9-month denervation group ( $p < 0.01$ ).

Denervated and atrophied myofibers in the SM were immunopositive for N-CAM protein. N-CAM was expressed around muscle fibers and/or muscle fibers displayed sarco-plasmic expression (►Fig. 4). The N-CAM-positive fibers were very few in the control muscle (►Fig. 4A). However, the majority of the myofibers in the long-term denervated muscles were labeled positively for N-CAM protein. Most of the N-CAM-positive fibers in the SM muscles were atrophied (►Fig. 4B–D).

#### Motor Endplates and Intramuscular Nerve Axons

NMZ in the rat SM muscle contains intramuscular nerve terminals (►Fig. 5A) and a MEP band with numerous neuromuscular junctions (►Fig. 5B, C) as documented in our previous studies.<sup>12</sup> The MEP band in the rat SM muscle was also visualized in the muscle sections immunostained with triple fluorescence staining (►Fig. 6A–D). In the control muscle, the axons were confined in the NMZ (►Fig. 6A) to innervate the MEPs (►Fig. 6A<sup>1</sup>, A<sup>2</sup>). A typical MEP had an elaborate, complex distribution of AChRs with a pretzel-like appearance (►Fig. 6A<sup>2</sup>), as described previously.<sup>28</sup> In contrast, noninnervated MEPs (no visible axon attachment) were identified in all the denervated SM muscles. The mean number of the denervated MEPs was 79%, 65%, and 43% of the control in the 3-, 6-, and 9-month denervated SM, respectively (►Table 2). Statistical analysis (one-way ANOVA) of the rates (denervated to control) of MEP counts showed strong statistical significant difference between these three groups ( $F = 30.2$ ,  $df = 2/18$ ,  $p < 0.0001$ ). Post-hoc testing (Tukey HSD test) shows statistical difference

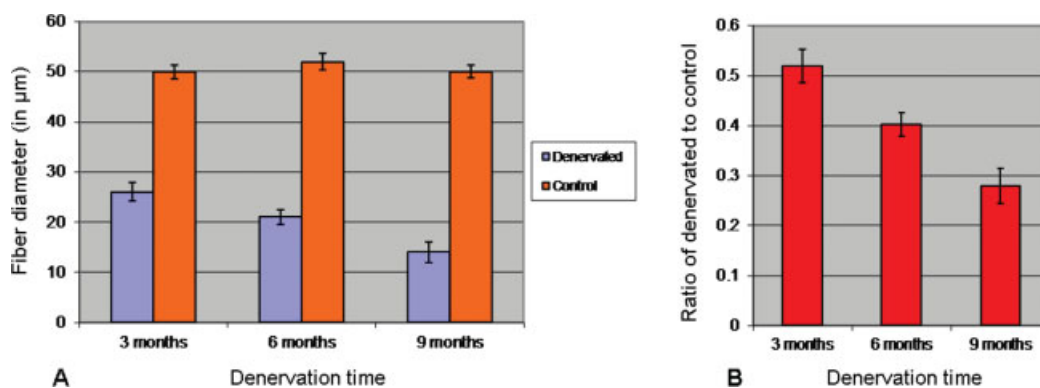


**Fig. 3** Comparison of myofiber diameters of the sternomastoid (SM) muscles between denervated and control sides and among denervation groups. (A) Distribution of mean fiber diameters of the denervated and control SM muscles. (B) Ratio of the mean fiber size of the denervated to control muscles. Note that the fiber diameters of the denervated muscles are reduced progressively with denervation time. Vertical bars represent standard error.

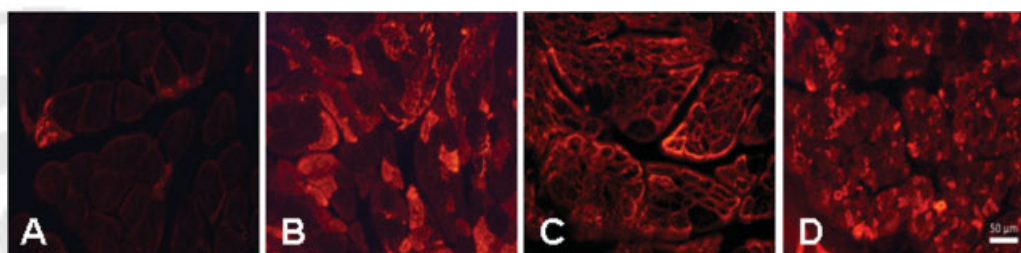


**Fig. 4** Immunofluorescent photomicrographs of cross-sections of the rat sternomastoid (SM) muscles on the normal and denervated sides. The sections were processed with neural cell adhesion molecule (N-CAM) immunostaining to label denervated muscle fibers in the muscles studied. (A) Normal SM. (B) SM muscle denervated for 3 months. (C) SM muscle denervated for 6 months. (D) SM muscle denervated for 9 months. Note that most of the N-CAM-positive fibers (bright staining) in the denervated SM were atrophied. Scale bar = 50 μm for (A) through (D).

between means of each pair of three groups. Average of 3-month denervation group is significantly larger than average of 6-month ( $p < 0.05$ ) and 9-month ( $p < 0.01$ ) denervation groups. Also average of 6-month group is significantly larger than that of 9-month group ( $p < 0.05$ ).

In the stained muscle sections, fragments and/or accumulations of axonal debris were identified (► **Fig. 6B–D**<sup>2</sup>). The long-term denervated muscles, especially 9-month-denervated muscles (► **Fig. 6D–D**<sup>2</sup>), showed the presence of small, shrunken and distorted MEPs. Some of the denervated MEPs displayed broken and fragmented forms, and thin lengthened shapes.

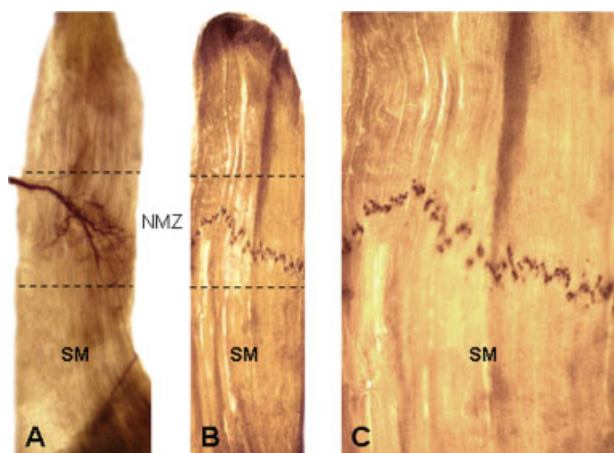


**Fig. 5** Native motor zone (NMZ) of the rat sternomastoid (SM) muscle visualized by Sihler's whole mount nerve staining (A) and acetylcholinesterase staining (B, C). Note that the NMZ in the SM muscle is located in the middle portion of the muscle (outlined region in [A] and [B]) and contains a single nerve branch with numerous intramuscular nerve terminals (A) and a motor endplate band (B, C) with numerous neuromuscular junctions (black dots).

## Discussion

In this study, we investigated neuromuscular alterations induced by long-term denervation and demonstrated that complete SM denervation in the rat resulted in progressive reduction in muscle mass and myofiber size. We found that normal axons almost disappeared and replaced by accumulations of axonal debris 3 months after denervation. In contrast, MEP band was readily recognizable at all-time points. Some denervated MEPs still remained certain characteristics such as a typical pretzel-like structure after the prolonged period of denervation. These findings suggest that some surgeries targeting the MEPs such as NMEG-NMZ and DNI-NMZ techniques should be effective for delayed reinnervation.

Denervation has been widely used in reinnervation and nerve regeneration studies. Our findings are in agreement with those observed by previous investigators,<sup>29,30</sup> who reported that muscle denervation is followed by the

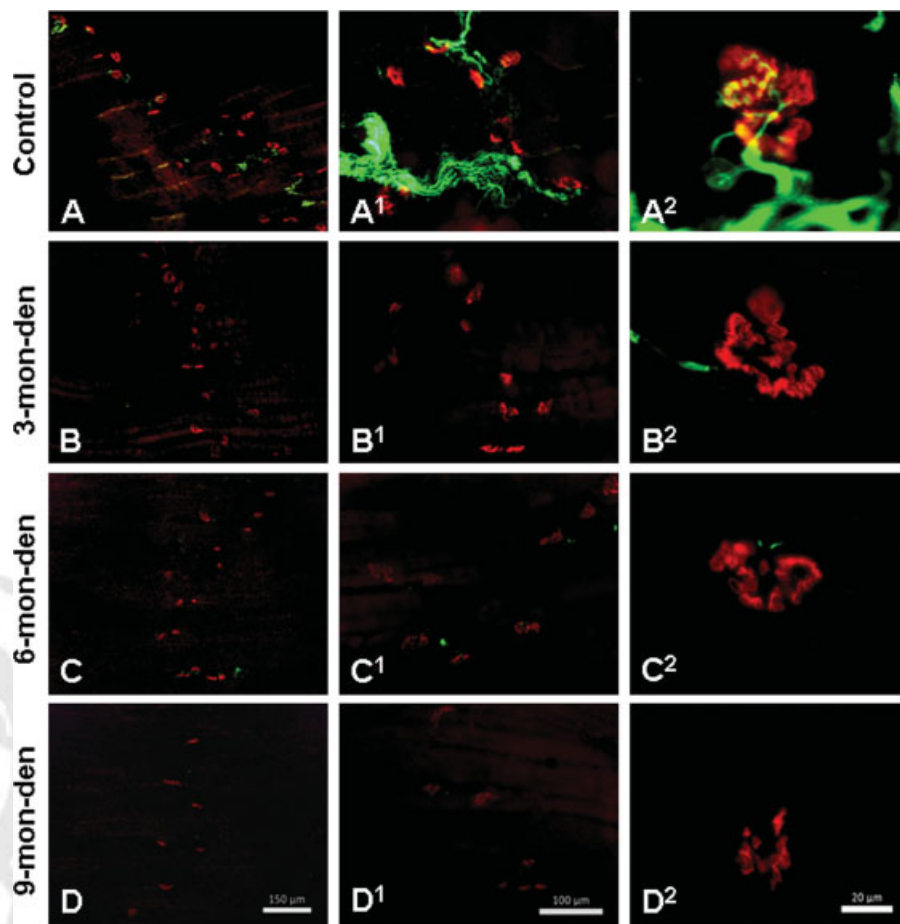


**Fig. 6** Immunofluorescence labeling of sagittal sections from normal (A–A<sup>2</sup>) and denervated (B–D<sup>2</sup>) rat sternomastoid (SM) muscles. The immunostained sections show labeled axons and terminals (green) and motor endplates (MEPs, red). The low-magnification images (left column) show the MEP band, whereas the high-magnification images (middle and right columns) show alterations in acetylcholine receptor clusters in the denervated SM muscles. 3-mon-den, 3-month denervation; 6-mon-den, 6-month denervation; 9-mon-den, 9-month denervation.

progressive muscle atrophy and a loss of muscle mass. However, there is no consensus regarding denervation-induced MEP alterations, as increase, decrease, and no change in the MEP area have been reported.<sup>31–34</sup> The number of junctional AChRs was shown to increase in the first week<sup>35</sup> and to decrease at later times.<sup>34,36</sup> In agreement with other investigators,<sup>37</sup> we observed that a decrease in presynaptic nerve terminals preceded the decrease in the postsynaptic AChRs. When the nerve supply to muscle is interrupted, the MEP degenerates although the MEP itself may remain unaltered for relatively long periods.<sup>38</sup> This study showed that MEPs were detected in 9-month-denervated SM muscle. These findings support the notion that postsynaptic AChRs of the vertebrate MEPs are remarkably stable in that they persist for long periods following denervation.<sup>39–41</sup>

The MEP is the primary connection between lower motor neurons and its target skeletal muscle fiber. Communication between these two structures is vital for muscle contraction and movement, which is essential for maintaining myofiber properties.<sup>42–44</sup> It is known that each of the mammalian skeletal muscle fibers usually has one MEP which is located mid-way between its origin and insertion, thereby forming a narrow band in the middle of the muscle. MEP regions of

mammalian muscle fibers are preferentially reinnervated as a consequence of some special property of the muscle fiber at this site. After nerve injury and/or DNI,<sup>45–51</sup> regenerating axons and sprouts have been identified to preferentially grow into the sites of the original MEPs and form synapses. Synaptic basal lamina at the MEP contains molecules that direct the formation of synaptic specializations on regenerating axon terminals and myofibers.<sup>52</sup> Some other chemotropic substance released from the MEPs may attract the regenerating axons in the vicinity. Hence, reinnervation of the denervated MEPs in the NMZ of a target muscle must occur as a consequence of some property of the muscle fiber at this site which favors synapse formation.

The MEP band is a potential site for clinical and experimental manipulations since MEP is the physiological interface between the motoneuron and the muscle fiber. The NMZ in a muscle contains a MEP band with numerous neuromuscular junctions and their innervating axons. We have demonstrated that the NMZ within a given muscle is an ideal site for muscle reinnervation. Using an immediate reinnervation model, we have documented that NMEG-NMZ resulted in optimal functional recovery.<sup>12</sup> However, it remains unknown if this technique has the potential for

**Table 2** Motor endplate counts for the 3-month-, 6-month-, and 9-month-denervated and control sternomastoid (SM) muscles in rats ( $n = 21$ )

Animal (No.)	Denervated SM	Control SM	Ratio D/C
<b>3-month DEN</b>			
1	81	115	0.704
2	76	104	0.730
3	72	93	0.774
4	87	110	0.790
5	69	87	0.793
6	109	121	0.900
7	98	118	0.830
Average	84.6	106.9	0.789
SD	14.5	12.9	0.064
<b>6-month DEN</b>			
1	68	101	0.673
2	71	115	0.617
3	39	88	0.443
4	94	128	0.734
5	63	98	0.643
6	78	104	0.750
7	52	79	0.658
Average	66.4	101.9	0.645
SD	17.7	16.3	0.101
<b>9-month DEN</b>			
1	58	123	0.471
2	65	108	0.601
3	47	99	0.474
4	40	112	0.357
5	38	104	0.365
6	43	111	0.387
7	46	128	0.359
Average	48.1	112.1	0.431
SD	9.9	10.2	0.091

Abbreviations: DEN, denervation; D/C, denervated/control; SD, standard deviation.

reinnervation of the long-term denervated muscles. The results from this study would be helpful for determining the proper timing for the reinnervation of denervated muscles by NMEG-NMZ, DNI-NMZ, and/or other procedures that target MEPs. Our results suggest that the muscles denervated even for 6 months should have a good chance to be successfully reinnervated by NMEG-NMZ technique based on the preserved muscle mass and the reasonable number of the preserved original MEPs in these denervated muscles.

Denervation-induced neuromuscular alterations cause impairment of muscle functional properties that represent

major impediments to successful surgical interventions.<sup>53</sup> Previous studies showed that the muscle experienced irreversible muscle atrophy and weakness after 6 month of denervation.<sup>1,54</sup> For optimal outcome of NMEG-NMZ and other reinnervation techniques in the treatment of long-term denervated muscle, additional approaches should be considered to maintain muscle mass and original MEPs before irreversible structural or functional impairments occur. Without significant restoration of muscle mass and MEPs, delayed reinnervation of denervated muscle may produce limited effect on muscle function. Further research is needed to identify viable therapeutic targets to delay and/or prevent deterioration of the denervated muscle following PNI. When immediate nerve reconstruction is not possible, sensory protection may offer an option to avoid irreversible muscle atrophy and loss of opportunity for successful delayed reinnervation. Sensory protection provides a temporal protective effect on the denervated muscle before nerve repair and reinnervation procedures can be performed. Sensory protection techniques have been investigated in animal models<sup>55-62</sup> and applied to humans.<sup>63</sup> A donor sensory nerve can be coapted to the distal motor nerve stump or directly implanted into the denervated muscle (neurotization) for the maintenance of muscle bulk. The donor sensory nerve is thought to provide trophic support to denervated muscle, thereby retarding and preventing irreversible denervation atrophy and preserving muscle volume and myofiber structures, and improving muscle function following denervation.<sup>55-64</sup> In the sensory protected muscle, an increased number of MEPs has been also observed.<sup>62</sup>

More work is needed to reveal specific therapeutic strategies for preventing MEP degradation following PNI. Preservation of the original MEPs in the denervated muscle is important for precise contact, synaptic differentiation, and maintenance of reestablished neural connections,<sup>47,65</sup> and for successful reinnervation by NMEG-NMZ<sup>12</sup> and DNI-NMZ.<sup>13</sup> The benefit of surgery and successful functional rehabilitation is related to the time delay following onset of denervation and surgery. This study showed that the morphometric changes in muscle mass, fiber size, and MEPs were more pronounced in the 9-month-denervated muscles as compared with those in the 3- and 6-month-denervated muscles. Neurotrophic factors, which have neuroprotective and regenerative properties, have been intensely studied for their therapeutic potential in both the preclinical and clinical setting. There is growing evidence suggesting that some neurotrophic factors such as nerve growth factor, basic fibroblast growth factor, glial cell line-derived neurotrophic factor, brain-derived neurotrophic factor, and ciliary neurotrophic factor are intimately involved in the maturation, maintenance and reinnervation of the MEPs and the recovery of motor function after denervation.<sup>66-72</sup> Therefore, local administration of these neurotrophic factors to the MEP zone in the target muscle may serve as a therapeutic option for preserving the denervated MEPs in the chronically denervated muscle. Preservation of MEPs for a longer period of time could enlarge the

therapeutic time-window for NMEG-NMZ and promote functional recovery of the muscles with delayed reinnervation. Indeed, the outcomes of NMEG-NMZ technique can be further improved by a combination of NMEG-NMZ surgery with other supplementary therapies to obtain a synergistic effect.<sup>27,73</sup>

## Conclusion

The results from this study allow us to make the following conclusions.

First, prolonged denervation resulted in a progressive reduction of muscle mass and myofiber size. Fiber atrophy was more pronounced in the 9-month-denervated muscle than that in the 3- and 6-month-denervated muscles. As muscle atrophy is one of the main factors for hampering successful recovery from muscle denervation, it is necessary for the development of strategies to rescue muscle from atrophy. In the absence of alternative primary treatments, sensory protection would provide temporary trophic support to prevent denervation atrophy, thereby preserving muscle volume for delayed reinnervation.

Second, normal axons almost disappeared and replaced by fragmented or accumulated axonal debris 3 months after denervation. In contrast, MEPs were still detectable in the 9-month-denervated muscles, suggesting that MEPs are more stable when compared with nerve axons after denervation.

Finally, further research should focus on the protection of MEPs in the long-term denervated muscle. Therapeutic strategies aimed at preserving MEPs would be the most effective for successful functional recovery of the delayed reinnervated muscle by NMEG-NMZ and/or DNI-NMZ techniques. One therapeutic strategy is the direct delivery of exogenous neurotrophic factors to the MEP zone in the denervated muscle, which could delay or prevent myofiber atrophy and degradation of MEPs following PNI. Maintenance of original MEPs in the long-term denervated muscle could facilitate rapid axon-MEP connections, thereby improving functional outcomes of NMEG-NMZ, DNI-NMZ, and/or other nerve repair procedures.

### Conflict of Interest

None.

### Acknowledgments

This work was supported by the Office of the Assistant Secretary of Defense for Health Affairs under Award No. W81XWH-14-1-0442 (to Dr. Liancai Mu). The U.S. Army Medical Research Acquisition Activity, 820 Chandler Street, Fort Detrick MD 21702-5014 is the awarding and administering acquisition office. Opinions, interpretations, conclusions, and recommendations are those of the authors and are not necessarily endorsed by the Department of Defense. In conducting research using animals, the investigators adhere to the laws of the United States and regulations of the Department of Agriculture. This protocol was approved by the USAMRMC Animal Care and Use Review Office (ACURO) for the use of rats.

## References

- 1 Fu SY, Gordon T. Contributing factors to poor functional recovery after delayed nerve repair: prolonged denervation. *J Neurosci* 1995;15(5 Pt 2):3886-3895
- 2 Gordon T, Tyreman N, Raji MA. The basis for diminished functional recovery after delayed peripheral nerve repair. *J Neurosci* 2011;31(14):5325-5334
- 3 Payne SH Jr, Brushart TM. Neurotization of the rat soleus muscle: a quantitative analysis of reinnervation. *J Hand Surg Am* 1997;22(04):640-643
- 4 Park DM, Shon SK, Kim YJ. Direct muscle neurotization in rat soleus muscle. *J Reconstr Microsurg* 2000;16(05):379-383
- 5 Ma CH, Omura T, Cobos EJ, et al. Accelerating axonal growth promotes motor recovery after peripheral nerve injury in mice. *J Clin Invest* 2011;121(11):4332-4347
- 6 Barbour J, Yee A, Kahn LC, Mackinnon SE. Supercharged end-to-side anterior interosseous to ulnar motor nerve transfer for intrinsic musculature reinnervation. *J Hand Surg Am* 2012;37(10):2150-2159
- 7 Midha R, Munro CA, Chan S, Nitising A, Xu QG, Gordon T. Regeneration into protected and chronically denervated peripheral nerve stumps. *Neurosurgery* 2005;57(06):1289-1299, discussion 1289-1299
- 8 Sulaiman OA, Gordon T. Role of chronic Schwann cell denervation in poor functional recovery after nerve injuries and experimental strategies to combat it. *Neurosurgery* 2009;65(4, Suppl):A105-A114
- 9 Sulaiman OA, Midha R, Munro CA, Matsuyama T, Al-Majed A, Gordon T. Chronic Schwann cell denervation and the presence of a sensory nerve reduce motor axonal regeneration. *Exp Neurol* 2002;176(02):342-354
- 10 Sulaiman OA, Gordon T. Effects of short- and long-term Schwann cell denervation on peripheral nerve regeneration, myelination, and size. *Glia* 2000;32(03):234-246
- 11 Mu L, Sobotka S, Su H. Nerve-muscle-endplate band grafting: a new technique for muscle reinnervation. *Neurosurgery* 2011;69(2, Suppl Operative):ons208-ons224, discussion ons224
- 12 Mu L, Sobotka S, Chen J, Nyirenda T. Reinnervation of denervated muscle by implantation of nerve-muscle-endplate band graft to the native motor zone of the target muscle. *Brain Behav* 2017;7(06):e00668
- 13 Sobotka S, Chen J, Nyirenda T, Mu L. Outcomes of muscle reinnervation with direct nerve implantation into the native motor zone of the target muscle. *J Reconstr Microsurg* 2017;33(02):77-86
- 14 Finkelstein DI, Dooley PC, Luff AR. Recovery of muscle after different periods of denervation and treatments. *Muscle Nerve* 1993;16(07):769-777
- 15 Irintchev A, Draguhn A, Wernig A. Reinnervation and recovery of mouse soleus muscle after long-term denervation. *Neuroscience* 1990;39(01):231-243
- 16 Hall ZW, Sanes JR. Synaptic structure and development: the neuromuscular junction. *Cell* 1993;72(Suppl):99-121
- 17 Battiston B, Geuna S, Ferrero M, Tos P. Nerve repair by means of tubulization: literature review and personal clinical experience comparing biological and synthetic conduits for sensory nerve repair. *Microsurgery* 2005;25(04):258-267
- 18 Keilhoff G, Fansa H. Successful intramuscular neurotization is dependent on the denervation period. A histomorphological study of the gracilis muscle in rats. *Muscle Nerve* 2005;31(02):221-228
- 19 Covault J, Sanes JR. Neural cell adhesion molecule (N-CAM) accumulates in denervated and paralyzed skeletal muscles. *Proc Natl Acad Sci U S A* 1985;82(13):4544-4548
- 20 Sanes JR, Schachner M, Covault J. Expression of several adhesive macromolecules (N-CAM, L1, J1, NILE, uvomorulin, laminin, fibronectin, and a heparan sulfate proteoglycan) in embryonic, adult, and denervated adult skeletal muscle. *J Cell Biol* 1986;102(02):420-431

- 21 Cashman NR, Covault J, Wollman RL, Sanes JR. Neural cell adhesion molecule in normal, denervated, and myopathic human muscle. *Ann Neurol* 1987;21(05):481–489
- 22 Müller-Felber W, Küllmer K, Fischer P, et al. Fibre type specific expression of Leu19-antigen and N-CAM in skeletal muscle in various stages after experimental denervation. *Virchows Arch A Pathol Anat Histopathol* 1993;422(04):277–283
- 23 Kalliainen LK, Jejurikar SS, Liang LW, Urbanchek MG, Kuzon WM Jr. A specific force deficit exists in skeletal muscle after partial denervation. *Muscle Nerve* 2002;25(01):31–38
- 24 Mu L, Sobotka S, Chen J, et al; Arizona Parkinson's Disease Consortium. Altered pharyngeal muscles in Parkinson disease. *J Neuropathol Exp Neurol* 2012;71(06):520–530
- 25 Dubowitz V. *Muscle Biopsy. A Practical Approach*. 2nd ed. London: Bailliere Tindall; 1985
- 26 Grumbles RM, Sesodia S, Wood PM, Thomas CK. Neurotrophic factors improve motoneuron survival and function of muscle reinnervated by embryonic neurons. *J Neuropathol Exp Neurol* 2009;68(07):736–746
- 27 Mu L, Sobotka S, Chen J, Nyirenda T. Nerve growth factor and basic fibroblast growth factor promote reinnervation by nerve-muscle-endplate grafting. *Muscle Nerve* 2017. doi: 10.1002/mus.25726
- 28 Marques MJ, Conchello JA, Lichtman JW. From plaque to pretzel: fold formation and acetylcholine receptor loss at the developing neuromuscular junction. *J Neurosci* 2000;20(10):3663–3675
- 29 Grossman EJ, Roy RR, Talmadge RJ, Zhong H, Edgerton VR. Effects of inactivity on myosin heavy chain composition and size of rat soleus fibers. *Muscle Nerve* 1998;21(03):375–389
- 30 Schmalbruch H, al-Amood WS, Lewis DM. Morphology of long-term denervated rat soleus muscle and the effect of chronic electrical stimulation. *J Physiol* 1991;441:233–241
- 31 Csillik B, Nemcsók J, Chase B, Csillik AE, Knyihár-Csillik E. Intra-terminal spreading and extrajunctional expression of nicotinic acetylcholine receptors in denervated rat skeletal muscle. *Exp Brain Res* 1999;125(04):426–434
- 32 Prakash YS, Zhan WZ, Miyata H, Sieck GC. Adaptations of diaphragm neuromuscular junction following inactivity. *Acta Anat (Basel)* 1995;154(02):147–161
- 33 Marques MJ, Mendes ZT, Minatel E, Santo Neto H. Acetylcholine receptors and nerve terminal distribution at the neuromuscular junction of long-term regenerated muscle fibers. *J Neurocytol* 2005;34(06):387–396
- 34 Frank E, Gautvik K, Sommerschild H. Cholinergic receptors at denervated mammalian motor end-plates. *Acta Physiol Scand* 1975;95(01):66–76
- 35 Szabo M, Salpeter EE, Randall W, Salpeter MM. Transients in acetylcholine receptor site density and degradation during reinnervation of mouse sternomastoid muscle. *J Neurochem* 2003;84(01):180–188
- 36 Fumagalli G, Balbi S, Cangiano A, Lomo T. Regulation of turnover and number of acetylcholine receptors at neuromuscular junctions. *Neuron* 1990;4(04):563–569
- 37 Kumai Y, Ito T, Matsukawa A, Yumoto E. Effects of denervation on neuromuscular junctions in the thyroarytenoid muscle. *Laryngoscope* 2005;115(10):1869–1872
- 38 Birks R, Katz B, Miledi R. Physiological and structural changes at the amphibian myoneural junction, in the course of nerve degeneration. *J Physiol* 1960;150:145–168
- 39 Frank E, Gautvik K, Sommerschild H. Persistence of junctional acetylcholine receptors following denervation. *Cold Spring Harb Symp Quant Biol* 1976;40:275–281
- 40 Sanes JR, Marshall LM, McMahan UJ. Reinnervation of skeletal muscle: restoration of the normal synaptic pattern. In: Jewett DL, McCarrroll HR, eds. *Nerve Repair: Its Clinical and Experimental Basis*. St. Louis (MO): Mosby; 1980
- 41 Steinbach JH. Neuromuscular junctions and alpha-bungarotoxin-binding sites in denervated and contralateral cat skeletal muscles. *J Physiol* 1981;313:513–528
- 42 Sanes JR, Lichtman JW. Development of the vertebrate neuromuscular junction. *Annu Rev Neurosci* 1999;22:389–442
- 43 Bassel-Duby R, Olson EN. Signaling pathways in skeletal muscle remodeling. *Annu Rev Biochem* 2006;75:19–37
- 44 Wu H, Xiong WC, Mei L. To build a synapse: signaling pathways in neuromuscular junction assembly. *Development* 2010;137(07):1017–1033
- 45 Iwayama T. Relation of regenerating nerve terminals to original endplates. *Nature* 1969;224(5214):81–82
- 46 Bennett MR, McLachlan EM, Taylor RS. The formation of synapses in reinnervated mammalian striated muscle. *J Physiol* 1973;233(03):481–500
- 47 Sanes JR, Marshall LM, McMahan UJ. Reinnervation of muscle fiber basal lamina after removal of myofibers. Differentiation of regenerating axons at original synaptic sites. *J Cell Biol* 1978;78(01):176–198
- 48 Gorio A, Carmignoto G, Finesso M, Polato P, Nunzi MG. Muscle reinnervation—II. Sprouting, synapse formation and repression. *Neuroscience* 1983;8(03):403–416
- 49 Covault J, Cunningham JM, Sanes JR. Neurite outgrowth on cryostat sections of innervated and denervated skeletal muscle. *J Cell Biol* 1987;105(6 Pt 1):2479–2488
- 50 Guth L, Zalewski AA. Disposition of cholinesterase following implantation of nerve into innervated and denervated muscle. *Exp Neurol* 1963;7:316–326
- 51 Sakellarides HT, Sorbie C, James L. Reinnervation of denervated muscles by nerve transplantation. *Clin Orthop Relat Res* 1972;83:195–201
- 52 McMahan UJ, Wallace BG. Molecules in basal lamina that direct the formation of synaptic specializations at neuromuscular junctions. *Dev Neurosci* 1989;11(4-5):227–247
- 53 Schwarting S, Schröder M, Stennert E, Goebel HH. Morphology of denervated human facial muscles. *ORL J Otorhinolaryngol Relat Spec* 1984;46(05):248–256
- 54 Gutmann E, Young JZ. The re-innervation of muscle after various periods of atrophy. *J Anat* 1944;78(Pt 1-2):15–43
- 55 Hynes NM, Bain JR, Thoma A, Veltri K, Maguire JA. Preservation of denervated muscle by sensory protection in rats. *J Reconstr Microsurg* 1997;13(05):337–343
- 56 Bain JR, Veltri KL, Chamberlain D, Fahnestock M. Improved functional recovery of denervated skeletal muscle after temporary sensory nerve innervation. *Neuroscience* 2001;103(02):503–510
- 57 Beck-Broichsitter BE, Becker ST, Lamia A, Fregnan F, Geuna S, Sinis N. Sensoric protection after median nerve injury: babysitter-procedure prevents muscular atrophy and improves neuronal recovery. *Biomed Res Int* 2014;2014:724197, 7 pages
- 58 Wang H, Gu Y, Xu J, Shen L, Li J. Comparative study of different surgical procedures using sensory nerves or neurons for delaying atrophy of denervated skeletal muscle. *J Hand Surg Am* 2001;26(02):326–331
- 59 Noordin S, Ahmed M, Rehman R, Ahmad T, Hashmi P. Neuronal regeneration in denervated muscle following sensory and muscular neurotization. *Acta Orthop* 2008;79(01):126–133
- 60 Veltri K, Kwicien JM, Minet W, Fahnestock M, Bain JR. Contribution of the distal nerve sheath to nerve and muscle preservation following denervation and sensory protection. *J Reconstr Microsurg* 2005;21(01):57–70, discussion 71–74
- 61 Hosseinian MA, Shirian S, Loron AG, Ebrahimi AA, Hayatolah1 GH. Distal sensory to distal motor nerve anastomosis can protect lower extremity muscle atrophy in a murine model. *Eur J Plast Surg* 2017. doi: 10.1007/s00238-017-1313-z
- 62 Papakonstantinou KC, Kamin E, Terzis JK. Muscle preservation by prolonged sensory protection. *J Reconstr Microsurg* 2002;18(03):173–182, discussion 183–184

- 63 Bain JR, Hason Y, Veltri K, Fahnestock M, Quartly C. Clinical application of sensory protection of denervated muscle. *J Neurosurg* 2008;109(05):955–961
- 64 Nghiem BT, Sando IC, Hu Y, Urbancheck MG, Cederna PS. Sensory protection to enhance functional recovery following proximal nerve injuries: current trends. *Plast Aesthet Res* 2015;2:202–207
- 65 Bader D. Reinnervation of motor endplate-containing and motor endplate-less muscle grafts. *Dev Biol* 1980;77(02):315–327
- 66 Grosheva M, Nohroudi K, Schwarz A, et al. Comparison of trophic factors' expression between paralyzed and recovering muscles after facial nerve injury. A quantitative analysis in time course. *Exp Neurol* 2016;279:137–148
- 67 Fox MA, Sanes JR, Borza DB, et al. Distinct target-derived signals organize formation, maturation, and maintenance of motor nerve terminals. *Cell* 2007;129(01):179–193
- 68 Sakuma K, Yamaguchi A. The recent understanding of the neurotrophin's role in skeletal muscle adaptation. *J Biomed Biotechnol* 2011;2011:201696
- 69 Zahavi EE, Ionescu A, Gluska S, Gradus T, Ben-Yaakov K, Perlson E. A compartmentalized microfluidic neuromuscular co-culture system reveals spatial aspects of GDNF functions. *J Cell Sci* 2015;128(06):1241–1252
- 70 Wang J, Sun J, Tang Y, et al. Basic fibroblast growth factor attenuates the degeneration of injured spinal cord motor endplates. *Neural Regen Res* 2013;8(24):2213–2224
- 71 Yang LX, Nelson PG. Glia cell line-derived neurotrophic factor regulates the distribution of acetylcholine receptors in mouse primary skeletal muscle cells. *Neuroscience* 2004;128(03):497–509
- 72 Suzuki M, McHugh J, Tork C, et al. Direct muscle delivery of GDNF with human mesenchymal stem cells improves motor neuron survival and function in a rat model of familial ALS. *Mol Ther* 2008;16(12):2002–2010
- 73 Sobotka S, Chen J, Nyirenda T, Mu L. Intraoperative 1-hour electrical nerve stimulation enhances outcomes of nerve-muscle-endplate band grafting technique for muscle reinnervation. *J Reconstr Microsurg* 2017;33(08):533–543



THIEME